Dissertation

zur Erlangung des Doktorgrades

der Fakultät für Chemie und Pharmazie der

Ludwigs-Maximilians-Universität München

Novel formulation approaches for ballistic intradermal vaccination

Cihad Anamur

aus Neuwied, Deutschland

2015

Erklärung:

Diese Dissertation wurde im Sinne des § 7 der Promotionsordnung vom 28. November 2011 von Herrn Prof. Dr. Gerhard Winter betreut.

Eidesstattliche Versicherung

Diese Dissertation wurde eigenständig und ohne unerlaubte Hilfe erarbeitet.

München, 10.10.2015

(Cihad Anamur)

Dissertation eingereicht am :

1. Gutachter	Prof. Dr. Gerhard Winter
2. Gutachter	Prof. Dr. Wolfgang Frieß
Mündliche Prüfung am:	26.10.2015

Für meine Familie

Acknowledgments

The present thesis was prepared between February 2011 and November 2014 at the Department of Pharmacy, Pharmaceutical Technology and Biopharmaceutics at the Ludwigs-Maximilians-University (LMU) in Munich under the supervision of Prof. Dr. Gerhard Winter.

First, I want to express my deepest gratitude to my supervisor Prof. Dr. Gerhard Winter for offering me the possibility to become a member of his research group and for supervising the present thesis. In particular I would like to thank him for his dedicated scientific guidance and outstanding, trustful and professional advice throughout the project. I want to highlight his ambition to support my scientific as well as my personal development.

My sincere thanks also go to Dr. Julia Engert. Without her precious support it would not be possible to conduct this research.

I also want to express my deepest gratitude to Dr. Peter Lell and Christian Fellner from Pyroglobe GmbH. This dissertation could not have been completed without the great support that I have received from them. I profited in many ways from the outstanding scientific and creative expertise. I will really miss the intensive time we spent together in scientific ant personal manner.

I further want to thank Dr. Stefan Henke, Dr. Jörg Bender, Dr. Heiko Spilgies and Rolf Pracht from IIS Innovative Injektions-Systeme GmbH Co.KG for their support and valuable scientific discussion during the route of the project.

I want to thank Prof. Wolfgang Frieß for interesting discussions as well as the scientific and personal input over the last years and especially for his effort in organizing scientific and social events together with Prof. Gerhard Winter. Thereby, an excellent personal and working atmosphere was created.

My tremendous gratitude is expressed to all my companions from the research groups from Prof. Gerhard Winter and Prof. Wolfgang Frieß. I very much enjoyed the scientific and personal support from each of you: Dr. Gerhard Simon, Dr. Ahmed Besheer, Dr. Madlen Hubert, Dr. Alexandra Mösslang, Alice Hirschmann, Imke

Leitner, Ayla Tekbudag, Dr. Angelika Freitag, Dr. Yibin Deng, Dr. Sarah Claus, Dr. Julia Kasper, Dr. Eva Maria Ruberg, Dr. Mathäus Noga, Dr. Elisabeth Härtel, Dr. Sarah Zölls, Dr. Markus Hofer, Dr. Gerhard Sax, Dr. Kerstin Höger, Dr. Tim Menzen, Dr. Roman Mathäs, Dr. Marie-Paule Even, Sebastian Hertl, Madeleine Witting, Kay Strüver, Ilona Konrad, Moritz Vollrath, Robert Liebner, Angela Schoch, Randy Wanner, Christian Neuhofer , Elisa Agostini, Matthias Lucke, Philipp Matthias, Ellen Köpf, Ben Werner, Verena Saller, Christoph Korpus, Stefanie Funke and Kerstin Hoffman.

In particular, special thanks to Elsa Etzl, who welcomed me warmly in our lab and Laura Engelke, who created an excellent atmosphere and fun during the last two years.

I want to thank Dr. Raimund Geidobler for the indispensable scientific support and sporting challenges beside the lab. I really met a friend in you.

Words cannot express how grateful I am to Michaela Wimmer who was always there to support me.

My deepest gratitude goes to my parents and my brother and sister for all the support they gave me over all the years.

Table of contents

Table of contents ..... **VII**

List of abbreviations ..... **X**

1. Chapter - General introduction **1**

1.1 Introduction 2

1.1.1 General introduction “vaccination” 2

1.1.2 Influenza and the development of influenza vaccine 4

1.1.3 Intradermal route versus intramuscularly injection 8

1.1.4 Skin as vaccine administration site 10

1.1.5 Intradermal vaccination with focus on epidermal powder immunization 11

1.2 Objectives of this thesis 14

1.3 References 15

2. Chapter - Stability of collapse lyophilized influenza vaccine formulations **19**

2.1 Abstract 20

2.2 Introduction 21

2.3 Material and Methods 23

2.3.1 Materials 23

2.3.2 Methods 23

2.4 Results 33

2.4.1 Hemagglutinin quantification using RP-HPLC 33

2.4.2 Light obscuration measurements 34

2.4.3 Turbidity measurements 35

2.4.4 Sodium dodecyl sulfate-Polyacrylamide gel electrophoresis (SDS-Page) 36

2.4.5 Westernblot analysis 37

2.4.6 Hemagglutination inhibition assay (HAI) 38

2.4.7 Determination of the residual moisture content 40

2.4.8 Scanning electron microscopy (SEM) 41

2.4.9 Determination of the specific surface area (SSA) 42

2.5 Discussion 43

2.6 Conclusion 46

2.7 Acknowledgments 47

2.8 References 48

3. Chapter - Stability of lyophilized influenza vaccine under long-term storage conditions and in presence of oily components **51**

3.1 Introduction 52

3.2 Material and Methods 54

3.2.1 Materials 54

3.2.2 Methods 54
3.3 Results 57
3.3.1 Hemagglutinin (HA) quantification using RP-HPLC 57
3.3.2 Light obscuration measurements 58
3.3.3 Turbidity measurements 61
3.3.4 Sodium dodecyl sulfate-Polyacrylamide gel electrophoresis (SDS-Page) 63
3.3.5 Westernblot analysis 64
3.3.6 Hemagglutination inhibition assay (HAI) 65
3.3.7 Determination of the residual moisture content 66
3.3.8 Determination of vaccine stability in presence of oily components (AS03, oily components of AS03, and paraffin) using HAI 67
3.3.9 Determination of vaccine stability in presence of oily components (AS03, oily components of AS03, and paraffin) using RP-HPLC 68
3.4 Discussion 72
3.5 Conclusion 75
3.6 References 76
4. Chapter – Intradermal administration of particles 78
4.1 Introduction 79
4.2 Material and Methods 81
4.2.1 Materials 81
4.2.2 Methods 82
4.3 Results 91
4.3.1 Determination of particle velocity (in cooperation with Dr. P. Lell, C. Fellner, Pyroglobe, Hettenshausen, Germany) 91
4.3.2 Scanning electron microscopy (SEM) 93
4.3.3 Microscopic examination of skin slices 95
4.3.4 Determination of penetrated particle count in pig skin and skin model using MFI 99
4.4 Discussion 101
4.4.1 Device and particle velocity 101
4.4.2 Application of particles to skin 102
4.5 Conclusion 104
4.6 Appendix 105
4.7 References 107
5. Chapter – Device development 109
5.1 Guiding principles of device design 110
5.2 Development of the combustor 112
5.3 Composition and development of combustion chamber filling 113
5.4 Choice of material and design of the membranes 115

5.5 Design of support plate 117
5.6 Choice of the gas-generator 118
5.7 Conclusion 119
5.8 References 120
6. Chapter – Proof of concept of intradermal ballistic vaccination in an animal model 121
6.1 Introduction 122
6.2 Material and Methods 124
6.2.1 Materials 124
6.2.2 Methods 125
6.3 Results 136
6.3.1 RP-HPLC – Comparison of antigen concentration 136
6.3.2 Administration sites after intradermal powder immunization 137
6.3.3 Histological characterization of administration site 149
6.3.4 Determination of endotoxin content in samples 151
6.3.5 Blood samples and IgG immune response determined using ELISA 152
6.4 Discussion 156
6.5 Conclusion 158
6.6 Attachments 160
6.7 References 165
7. Chapter - Final summary of the thesis 166
7.1 Basis of the thesis 167
7.2 Final summary and outlook 174
7.3 References 175

List of abbreviations

CAIV	Cold-adapted influenza vaccine
APC	Antigen presenting cells
AUC	Area under the curve
BCG	Bacillus Calmette-Guérin
BMI	Body mass index
cST	Centi Stokes
CTL	Cytotoxic immune lymphocyte
DC	Dendritic cells
EPI	Epidermal powder immunization
FITC	Fluorescein isothiocyanate
FNU	Formazine Nephelometric Unit
H1N1	Influenza virus hemagglutinin sub-type 1; neuraminidase sub-type 1
HA	Hemagglutinin
HAI	Hemagglutination inhibition assay
HE stain	Hematoxylin and eosin stained
HPLC	High performance liquid chromatography
i.d.	Intra dermal
i.m	Intra muscular
IgA	Immunoglobulin A
IgG	Immunoglobulin G
kDa	Kilo Dalton
LAIV	Live attenuated influenza vaccine
LC	Langerhans cells
M1, M2	Matrix protein
MFI	Micro-flow-Imaging
mRNA	Messenger RNA
NA	Neuraminidase
NP	Nuleoprotein
Ph. Eur.	Pharmacopoea Europaea
RP	Reversed phase
RT	Retention time
SC	Stratum corneum

SDS PAGE	Sodium dodecyl sulphate polyacrylamide gel electrophoresis
SEM	Scanning electron microscopy
SSA	Specific surface area
ssRNA	Single stranded RNA (Ribonucleic acid)
TFF	Tangential flow filtration
T_g	Glass transition temperature
Th	T-helper cells
T_{reg}	Regulatory T-lymphocytes
WHO	World Health Organization

1. Chapter - General introduction

1.1 Introduction

1.1.1 General introduction “vaccination”

The human race has always been threatened by diseases. In order to protect humans against infections and epidemics vaccination as deliberate attempt has become more and more the focus of scientific development. Since the time of Edward Jenner (1749-1823), the “father of modern vaccination”, several major diseases could be controlled using vaccination such as diphtheria, tetanus, rubella or smallpox [1-3]. Moreover, in the case of smallpox, vaccination was carried out until the late 1970s with the success of eradication. During the last two centuries, vaccination has demonstrated a huge impact on human and animal health and has significantly reduced morbidity and mortality. Nonetheless, it was a long way from Jenner´s development of large scale vaccination using the direct arm-to-arm-transmission of the “lymph” from people who are afflicted to modern vaccines (e.g.: DNA or sub-unit vaccines) [4]. The risks of transmissions of other diseases along the direct inoculation process did not end until the 1890s when glycerin preservation of the vaccine solution (lymph from infected animals) was introduced by Robert Koch. Around the same time Louis Pasteur perceived that an attenuated (weakened) form of the microbe (virus) could provide immunity with minimized risk of infection. The Pasteur concept of attenuation offered the possibility to make vaccines cultivatable and standardly reproducible [5]. The next major step was the introduction of “killed vaccines”, which used e.g. heat or chemical treatment to destroy the microorganism, at the end of the 19th century. This concept was also applied for bacterial toxins to produce the so called “toxoids” which were used to induce immunity against diseases such as diphtheria and tetanus. Despite the developments of the vaccine modifications, the vaccine production was still rudimentary and focused on immunization and collection of “lymph” from animals for human immunization. The vaccine production substantially improved after the introduction of the chorioallantoic membrane of fertile hen´s egg as a growing medium for vaccine strains [6]. The next significant development of vaccine production exceeded after the usage of cell cultures in the second half of the 20th century while the last important introduction process of improving vaccine efficacy and safety was established using the technology of recombinant vaccine production [7,

8]. During the last two decades several recombinant vaccines were licensed such as high-potency zoster vaccine, quadrivalent human papilloma virus and cold-adapted influenza vaccine (CAIV) [9].

Vaccine-mediated protection is a complex reaction. The efficacy of vaccines is primarily demonstrated via evidence of antigen-specific antibody titer [10]. It should be kept in mind that the immunity is not only a result of the peak of vaccine-mediated antibodies, it is also important that a long-term protection is induced [11-13]. This persisting protection can be generated by circulating specific antibodies and/or memory cells which are capable of a rapid immune response after a subsequent exposure to the same or comparable antigen. The efficacy of the immunity depends on a precise interaction between different immune cells such as B cells and T cells. The antibodies with high binding affinities to specific pathogens are produced in B-lymphocytes while T-lymphocytes (CTL) (CD8+) limit the spreading of the infection within the host by killing infected cells or secreting antimicrobial cytokines [14, 15].

The balance and the moderation of the immune cells is provided by T-helper-lymphocytes (Th) (CD4+). This group of immune cells is further divided into two subpopulations Th1 and Th2 which are regulated by regulatory T cells (T_{reg}) [16]. Moreover, the activation of specific vaccine-mediated (antigen-mediated) B and/or T lymphocyte response is mainly induced by antigen presenting cells (APC) such as monocytes, macrophages, dendritic cells (DCs) or Langerhans cells (LCs). They can start maturation after being activated by antigen exposition while they migrate to the draining lymph nodes to induce a cascade of immune cells (e.g. B and T cells) [17]. Generally, T and B-cells are activated after direct pathogen exposure (vaccination) or contact with antigen presenting APCs while Th1 and Th2 moderate the immune response and support the differentiation of the immature T and B cells to effector cells (CTL or B plasma cells) [12].

In order to demonstrate the efficacy of a vaccine and/or vaccination route it is not enough to detect involved immune cells and secreted mediators (cytokines) but a formal demonstration of vaccine-mediated protection is mandatory [18, 19]. Therefore, studies of titer changes, appearance of clinical symptoms, and hospitalization have been documented to show a successful vaccination technology.

The goal of vaccination is to induce a sufficient number of memory cells after priming (first contact with antigen) which reactivate, proliferate and differentiate rapidly after being exposed to the same antigen again. Furthermore, these maturated cells display

and secrete e.g. antibodies with significantly higher affinity to the antigen compared to avidity after priming. The vaccination should make the immune system capable to reactivate memory cells and to induce rapid antibody secretion over a threshold faster than the incubation time of the pathogen to protect the host sufficiently.

1.1.2 Influenza and the development of influenza vaccine

The influenza virus belongs to the family of orthomyxoviridae. Influenza is classified in three genera; A, B and C, depending on the type specific nucleoprotein (NP). Usually, influenza A and B cause the human influenza disease which is characterized by fever, cough, body aches etc. The characteristic of the virus is a single stranded RNA (ssRNA) with a helical symmetry, divided in eight RNA fragments (seven for influenza C) with a negative polarity (Figure 1.1.1). Each RNA fragment encodes at least one of the virus proteins. The genomic fragments are closely associated with the nucleoprotein to form a helical structure. Moreover, every genomic fragment possesses its own duplicating proteins (PB1, PB2 and PA) which amplify the viral RNA within the host cell. The RNA replicas are also utilized as mRNA to modify the host protein production into viral related protein production. An envelope, which originates from the host`s cytoplasmic membrane, surrounds the RNA fragments while viral proteins and new viruses are assembled. The viral envelope is associated with membrane proteins, such as hemagglutinin (HA), neuraminidase (NA), matrix protein (M1) and an ionic channel protein (M2). Due to their importance for viral life history strategy HA and NA are examined in detail. The ratio of HA to NA on the envelope is 8:1 to 10:1 [13, 15]. The trimeric hemagglutinin can mediate the attachment to a host cell sialic acid residue and initiate the virus fusion with the host cell. At present, 17 subtypes of hemagglutinin are known for the influenza A virus. On the contrary, the tetrameric neuraminidase promotes the release of the virus from the host cell-membrane and the distribution of self-assembled virus duplicates (virions) by cleavage between sialic acid residue and glycosaccharide. Moreover, NA is able to cleave the mucus proteins secreted inside the host´s respiratory tract, which leads to a formation of small droplets [16, 17]. The droplets form a delivery system to transport influenza viruses to the airways of the next host when the influenza disease carrying individual

sneezes or coughs. Currently, nine subtypes of neuraminidase are known for the influenza A virus. Both membrane proteins (HA and NA) can constantly change due to the viral structure and RNA organization. This continuous antigenic evolution of the influenza virus is based on two mechanisms: the antigenic drift and antigenic shift [12, 15].

High mutation rates and accumulations of point mutations in the eight RNA fragments (seven for influenza C) caused by the virus' own multiplying proteins (PB1, PB2 and PA) during the amplification create an astonishing high genomic alteration of the surface antigens HA and NA. Small genomic differences, called as antigenic drift, can lead to slightly changed viral proteins. These randomly occurring mutations in proteins (e.g.: HA and NA) can cause a circumvention of the host`s immune response. Moreover, sufficient alteration of the antigenic proteins can initiate a reinfection and can lead to a coexistence of subpopulations of several influenza viruses in the host at the same time. In response to the selection pressure to evade human (host) immunity, obvious changes in the genetic composition of the influenza virus occur every two to eight years. Alterations (point mutation) can lead to reduced antibody binding affinity to a known influenza strain. Influenza B is showing relatively little antigenic drift, whereas influenza A strains are demonstrating a high flexibility in genomic composition [15, 18, 19]. The impact of the antigenic drift to human health varies from season to season. Typically, 5-15% of the worldwide population is infected by seasonal influenza epidemics either asymptomatically or with clinical illness [4-6, 20]. Moreover, influenza A virus is capable of infecting mammalian as well as avian hosts depending on the subtype of hemagglutinin. This broad range of hosts enables the virus to mix up homologous RNA fragments if two or more influenza viruses of different strains infect the same host cell. This exchange of RNA fragments, the basis for genetic re-assortments and antigenic shift, can result in new viruses that have never been present in circulation, yet [4, 15]. The antigenic shift, resulting from double (triple etc.) infections, is capable to emerge a deadly influenza disease such as the 1918 Spain flu which caused over 50 million deaths worldwide, the Hong Kong Flu 1968 with over 34000 deaths in USA or the most recent one, the swine flu in 2009 with over 18500 deaths [21-24]. However, the antigenic shift has happened rarely up to the present, and approximately three times in a century [25, 26].

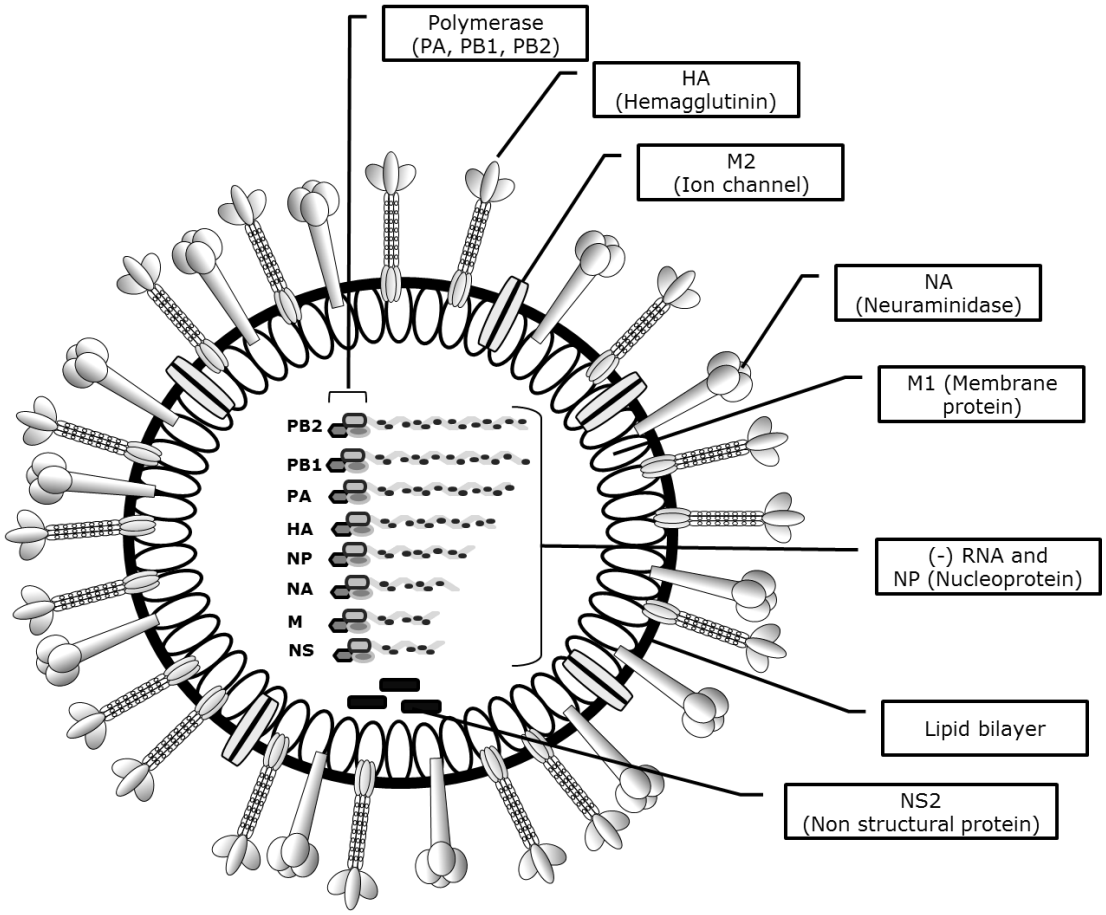

Figure 1.1.1: Structure of influenza A particle. Types of membrane protein: hemagglutinin (HA), neuraminidase (NA) and ionic channel (M2-protein). Within the virus envelope are located eight single stranded (-)-RNA segments, whereas every segment contains an individual protein complex.

In the early 1930s the influenza virus was firstly isolated in pigs and few years later it was shown in humans that the swine influenza virus had caused the influenza pandemic in 1918 [20-22]. Shortly after the discovery of the virus, two vaccines were introduced from embryonated eggs, one live attenuated and the other with killed whole viruses [23-25]. Today, influenza vaccines are mainly composed of the subunit hemagglutinin (HA). The production of live attenuated influenza viruses in embryonated eggs could result in rapid virus mutations and a revirulence of the strain within the host [26, 27]. This drawback was overcome after the development of new technologies such as reverse genetics and cold-adaption which demonstrated improved safety and long-term immunity. The cold adaption allows the virus to grow in cooler body parts (e.g.: nasal passage with approximately 32°C) but limited the amplification in warmer internal organs (37°C) [28, 29]. The cold adaption is a concept of co-infection of cell cultures with wild and attenuated strains which results in reassortants

("mixing of gens") due to the segmental genomes of the virus. Reassortants have also been used for vaccines with killed (inactivated) viruses (sub-unit vaccines, purified protein or polysaccharide) [9]. This concept may be improved by new technologies (e.g.: phage display, reverse genetics, and recombinant vaccines) to simplify the annual influenza sub-unit vaccine development and production [30].

Inactivated (seasonal) influenza vaccine induces rapid local and systemic immune response in up to 90% of the tested patients (developing a hemagglutination inhibition titer (HAI) above 40) within two weeks after immunization [31]. Nonetheless, several studies have demonstrated the necessity of a second (boost) injection of inactivated unadjuvanted influenza vaccine to provoke a sufficient immunogenicity in unprimed patients, particularly in children.

The inactivated influenza vaccines which are inoculated and amplified in embryonated eggs are primarily purified using centrifugation and chromatographic steps to reduce residual egg material [6]. Subsequently, the virus envelopes which are important for the virus reactogenicity and infectivity, are disrupted to assure viral inactivation using detergents such as tri-N-butyl phosphate, Triton X-100 or Triton N101 [32]. The envelope disruptions lead to a mixture of antigenic proteins in the inactivated influenza vaccine. Beside hemagglutinin the main immunogenic protein, neuraminidase, nucleoprotein or matrix proteins are included in varying amounts in the vaccine. A further purification step can be implemented to provide an influenza vaccine consisting of only HA. Over the last decades, inactivated influenza virus vaccine has been administered by intramuscular, oral, intranasal, subcutaneous or intradermal routes. The most reproducible immune responses and lowest occurrence of adverse reactions have been associated with intramuscular application route [33].

However, recent studies demonstrated that intradermal routes using a prefilled liquid-jet based device require fewer antigens (of the inactivated influenza vaccine) than intramuscular injection to induce a comparable immunogenicity but resulted in more but mild irritations at the application side [17, 34].

An alternative approach to inactivated influenza virus vaccine is an administration of live attenuated influenza vaccine (LAIV). While the reassortant virus strain for vaccine production should contain the genes for the surface antigens (HA and NA), it must also demonstrate a minor virus reactogenicity and infectivity to prevent significant illnesses [35]. Several methods have been used to prepare attenuated influenza strains such as host-range, temperatures-sensitive, and cold-adaption.

However, host-range strains could not be reliably attenuated and demonstrated a reversion of virulence and were not further investigated. Cold-adaption of virus strains at successively lower temperature (25°C) led to reduced virus replication capabilities and additional virus attenuation at higher temperatures (39°C) [36].

Growing at successively lower temperature (25°C) of cold-adapted virus strains led to reduced virus replication. Reassortant influenza virus strains are generated by coinfection of the wild-type virus and the cold-adapted virus in a host cell (e.g. mammalian cell lineage). In contrast to the inactivated influenza vaccine LAIVs are sprayed directly into the nose using a syringe to provide an environment of approximately 30-33°C for attenuated virus amplification. The capability of virus amplification and the resulting point mutations can provide a higher cross- protection against drifted influenza strains and a long-term persistence of immunity also may occur compared to inactivated influenza vaccines [37, 38]. Analysis of the genetic sequences revealed that none of the changes occurred at positions that refer to virus attenuation or antigenicity which promises a high vaccine safety [39]. Furthermore, the nasal immunization strategy can provoke an additional mucosal IgA protection beside the serum IgG protection. This supplementary protection can also be induced using the intradermal vaccination route.

An emerging influenza pandemic will create a surge of a rapid and global vaccination, and new immunization strategies will be needed to optimize the protection of unprimed persons, particularly when a certain vaccine may be limited.

1.1.3 Intradermal route versus intramuscularly injection

The way of vaccine administration can have considerable impact on efficacy of the procedure, compliance, and safety. Currently licensed vaccines are administered via one of five main routes: the majority of the vaccines is applied intramuscularly (hepatitis A and B, diphtheria, or tetanus); subcutaneously applied vaccines are measles, mumps, or rubella; intradermal route is used for BCG and rabies; intranasal administration site is utilized for live attenuated influenza vaccine (LAIV), and poliomyelitis and cholera are applied orally [40].

It should be kept in mind that the route of vaccine administration can also control the efficacy and class of immune response (moderation of cellular and/or humoral immunity).

While administering vaccines intramuscularly several aspects should be considered such as injection site (e.g. gluteal, quadriceps or deltaoid muscle), needle size based on volume, muscle size, overlying subcutaneous tissue and desired deposition depths [41]. However, to avoid any nerve injuries (e.g. sciatic nerve at the gluteal region) and severe pain, health-care worker should pay strict attention to the administration instructions. In order to reduce the pain and discomfort, several methods were described associated with intramuscular injections such as pre-treatment with topical local anaesthetics (e.g. lidocaine) or topical refrigerant spray [42].

In contrast, the intradermal vaccine administration would circumvent some of the intramuscular drawbacks (detailed description in **Chapters 1.1.4** and **1.1.5**) such as improving patient compliance, easy handling and elicited immune response. Moreover, intensive training of health-care personnel is redundant due to easy accessibility of the administration site and a lack of free nerve ending and blood vessels in the targeted area (epidermis) of the immunocompetent cells.

Despite all the indisputable benefits for patients, the intradermal vaccination offers further significant advantages such as dose sparing.

Conventionally, the inactivated influenza vaccine (subunit-vaccine) is administered intramuscularly (i.m.) to protect the host against influenza and its severe complications. Influenza vaccines are currently supplied in multi-dose vials which are typically overfilled to accommodate the dead space in needle and syringe. A conversion to prefilled single-dose syringe can reduce the waste of vaccine significantly [43-45]. As the next step of dose sparing would be a direct targeting of immunocompetent cells to minimize a vaccine waste in the tissue. Intradermal influenza vaccination demonstrated equivalent or even superior immune response after vaccination using needle and syringe and also promises a substantial dose reduction which is useful when vaccines are scarce [46].

1.1.4 Skin as vaccine administration site

The intradermal injection of tuberculin by Charles Mantoux in 1910 formed the basis for intradermal vaccination which is still used today for rabies and Bacillus Calmette-Guérin (BCG) [47]. The most impressive achievement of intradermal vaccination is the program launched from the World Health Organization (WHO) which eradicated the smallpox in the 1980 by applying a small amount of the potent vaccine with a bifurcated needle into skin [48, 49].

The skin excels as a target tissue due to easy accessibility and high immunogenicity. It is the least invasive route and demonstrated less unanticipated serious adverse effects than other administration routes (e.g. paralysis after nasal administration, abscesses after intramuscular injections). Additionally, a high number of dendritic cells and Langerhans cells, which form a synergistic network throughout the different skin layers, lead to an improved immune response. These cells can activate antigen-specific B and T-cells in the draining lymph nodes after antigen exposure [50, 51].

The skin comprises of three major layers such as epidermis, dermis and hypodermis (subcutis).

The epidermis is approximately 150-200 µm thick and consists of 90% of keratinocytes and some Langerhans cells (LCs) and melanocytes are also located in this tissue [52]. The outermost layer of the epidermis is the stratum corneum (SC) which is only 10-20 µm thick in humans and consists of 10-20 layers of corneocytes. These cells are terminally differentiated keratinocytes which derived from the basal lamina and differentiate during the 30 day lasting migration towards the skin surface (stratum corneum). Despite the low layer thickness, SC serves as an effective physical and chemical barrier.

While the Langerhans cells populate the epidermal layer of the skin, they form a tight network as a first line of immunological defence to rapidly detect intruding pathogens which breach through the stratum corneum (SC). After a pathogen exposure LCs scavenge the antigen and start maturating and migrating to the lymph nodes. While cells leave the network, continuous proliferations of LCs replenish the ranks to ensure a tight functioning network [53].

The dermis is located below the basal lamina which is comprised of collagen, elastin, and reticular fibres. This 1.5–3 mm thick flexible and elastic layer consists of a dense network of capillary blood and lymphatic vessels. While fibroblast are the dominant

cells type, the endothelial cells play a significant role in the inflammatory process by secreting different kinds of cytokines e.g. to induce vasodilation and vasomotion and/or converting leukocytes and trafficking of APCs. Furthermore, heterogenic populations of dendritic cells (DCs) are located in this layer. The composition of the cutaneous DC population changes depending on the type and degree of inflammation. New blood-derived DCs can migrate into the tissue while others leave towards the draining lymph nodes to present the pathogens. Performing this continuous turnover, a rapid immunogenic response and permanent adaption to the inflammation can be ensured [53]. The subcutaneous tissue is a loose connective tissue where the larger blood vessels are located to supply the capillaries in the dermis. In order to address the APCs located in the lower layers (epidermis and dermis) the vaccine administration has to disrupt or bypass the SC [54, 55].

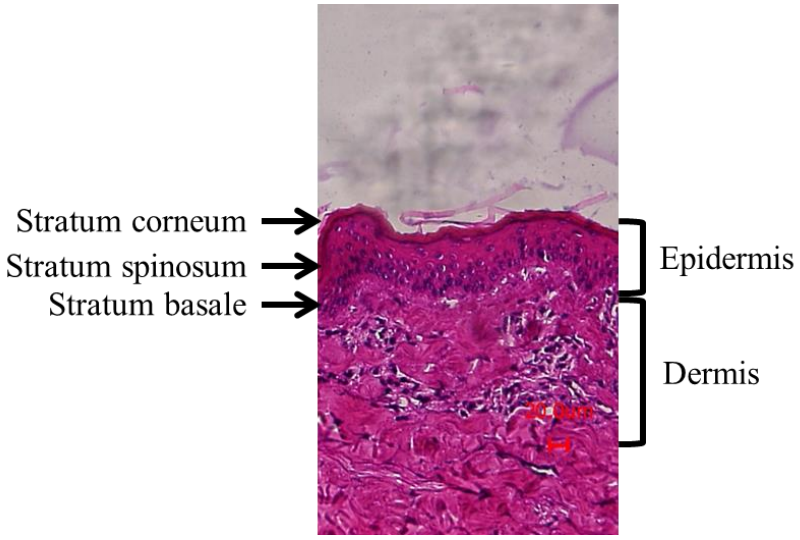

Figure 1.1.2: Microscopical image of hematoxylin and eosin stained pig skin

1.1.5 Intradermal vaccination with focus on epidermal powder immunization

New concepts of intradermal vaccine administration are currently under investigation to improve the patient compliance and reduce vaccine dosage at the same time, compared to intramuscular injections [56].

Several methods are currently in the scientific focus such as microneedles, tattoo vaccination, or epidermal powder immunization. Generally, needles are used not only to deposit vaccines intradermally, it is also the main route to deliver vaccine intramuscularly, subcutaneously except few jet-based injectors [57]. However, the administration of liquid vaccines using conventional needles and syringes holds the risk of pain, discomfort, needle-stick injuries and thereby the transmission of blood-borne diseases.

In contrast, penetration of the skin using microneedles is a huge scientific area which resulted in manifold designs and conception of microneedles [58]. While solid microneedles often form a basis for simple skin piercing or coating, hollow or biodegradable microneedles are more complex in preparation. Dissolving (biodegradable) microneedles prepared from e.g. carboxymethylcellulose, polyvinyl alcohol are pressed into the skin (manually or using a device) and subsequently dissolve within few minutes to administer the incorporated vaccine. The amount of delivered vaccine can differ while a certain vaccine volume can be directly injected using the hollow microneedles. Another approach is using a high-frequency oscillating needle for tattoo vaccination to deliver (DNA-) vaccines instead of tattoo ink into the skin. The promising methods highly depend on the deposited DNA concentration to elicit a sufficient immune response [59, 60].

Epidermal powder immunization excels as a needle-free application. In contrast to the liquid-based vaccine delivery, the EPI deposits dried particles into the skin at supersonic speed. Using this concept, the administered volume can be drastically reduced (100 to 500-fold) while the vaccine stability can also be improved [61, 62].

The dry state may offer a superior long-term stability of the vaccine in comparison to liquid formulations.

In contrast to PowderJect® which used helium gas to blow the spray-dried vaccine particles into the skin, the concept of ballistic intradermal vaccination uses a pyrotechnical activator as energy source to administer collapse freeze-dried particles to the APCs in the epidermis [62-64]. Using such a powerful energy source to accelerate the vaccine particles, the device should be designed to canalize the generated pressure towards the vaccine particles and contain the blast within the combustor due to safety reasons. Energy transfer and safety could be improved using a suitable filling material in the combustor surrounding the pyrotechnical activator compared to air-filling. Furthermore, the device should resist the mechanical stress

and the supersonic acceleration, which could be provided by an optimal choice of materials. Beside the properties of the device, the design of the particles could also have an impact to skin penetration. Particle characteristics such as size, density, shape and morphology have a great influence on the penetration depth of the particles. The new concept of collapse freeze-drying can provide lyophilized particles with an increased (high) rigidity of the particles [65, 66].

Furthermore, particle surface structure and particle porosity can also prevent fragmentation of the particles during acceleration and penetration through the mechanical barrier (stratum corneum).

The usage of sugars (carbohydrates) as excipients to stabilize the vaccine during the preparation process implicates a rather low density of the particles (700–1200 kg/m^3) but also promises a fast dissolving and a broad distribution of the vaccine within the tissue. However, to achieve appropriate momentum to deposit the low density vaccine particles into the skin and prevent inducing pain sizes of 20–70 mm were needed [66].

1.2 Objectives of this thesis

This work will outline the manufacturing of a collapse freeze-dried vaccine used as a vehicle for a new pyrotechnical device for epidermal powder immunization.
As a proof of concept, a liquid model vaccine (influenza vaccine) should be stabilized using collapse freeze-drying process. In order to provide particles for epidermal powder immunization, particles in a range of 20 µm to 80 µm should be prepared to avoid pain and bleeding during the application. A characterization and monitoring should be conducted to determine any part of the manufacturing process and storage conditions of the lyophilizates and the particles (2-8°C, 25°C and 40°C) over a time period of 12 months (**Chapter 2** and **3**).

In preliminary tests (not published work of Elsa Etzl) particles with velocities below 400 m/s could not breach the mechanical barrier of the skin. In order to determine the velocity requirements to penetrate the skin visualization methods of particle velocity and skin penetration should be established. A pyrotechnical energy source was anticipated to generate sufficient particle velocity for epidermal powder administration. Investigations of safety and particle acceleration were to be performed to develop a new pyrotechnical device (**Chapter 4** and **5**).

As proof of concept, a successful immunization using the collapse freeze-dried vaccine and the new pyrotechnical device should demonstrated in an animal model. The vaccine particles should breach the mechanical barrier of the skin (stratum corneum) to deliver the vaccine to the immunocompetent cells located in the epidermis. Pigs as laboratory animals should be assessed to provide a proper skin model for epidermal powder immunization of humans in the future. The administration side, histological changes of the tissue after vaccination and induction of immune response should be monitored to demonstrate the successful realization of the concept (**Chapter 6**).

1.3 References

1. Plotkin, S.A., *Vaccines: past, present and future.* Nature medicine, 2005. **11**: p. S5-S11.

2. Plotkin, S.L. and S.A. Plotkin, *A short history of vaccination.* Vaccines, 2004. **5**: p. 1-16.

3. Stern, A.M. and H. Markel, *The history of vaccines and immunization: familiar patterns, new challenges.* Health Affairs, 2005. **24**(3): p. 611-621.

4. Abraham, E.G., et al., *Analysis of the Plasmodium and Anopheles transcriptional repertoire during ookinete development and midgut invasion.* J Biol Chem, 2004. **279**(7): p. 5573-80.

5. Hilleman, M.R., *Vaccines in historic evolution and perspective: a narrative of vaccine discoveries.* Vaccine, 2000. **18**(15): p. 1436-1447.

6. Hardy, C.T., et al., *Egg Fluids and Cells of the Chorioallantoic Membrane of Embryonated Chicken Eggs Can Select Different Variants of Influenza A (H3N2) Viruses.* Virology, 1995. **211**(1): p. 302-306.

7. Halperin, S.A., A.C. Nestruck, and B.J. Eastwood, *Safety and immunogenicity of a new influenza vaccine grown in mammalian cell culture.* Vaccine, 1998. **16**(13): p. 1331-1335.

8. Audsley, J.M. and G.A. Tannock, *Cell-based influenza vaccines: progress to date.* Drugs, 2008. **68**(11): p. 1483-1491.

9. Beyer, W., et al., *Cold-adapted live influenza vaccine versus inactivated vaccine: systemic vaccine reactions, local and systemic antibody response, and vaccine efficacy: a meta-analysis.* Vaccine, 2002. **20**(9): p. 1340-1353.

10. Levine, M.M. and M.B. Sztein, *Vaccine development strategies for improving immunization: the role of modern immunology.* Nature immunology, 2004. **5**(5): p. 460-464.

11. Pashine, A., N.M. Valiante, and J.B. Ulmer, *Targeting the innate immune response with improved vaccine adjuvants.* Nat Med, 2005. **11**(4 Suppl): p. S63-8.

12. Mackay, I. and I.M. Roitt, *The immune system.* N Engl J Med, 2000. **343**(1): p. 37-49.

13. Mackay, I. and I. Roitt, *The immune system: second of two parts.* New England Journal of Medicine, 2000. **343**(2): p. 108-117.

14. Mackay, I.R., et al., *The Immune System.* New England Journal of Medicine, 2000. **343**(2): p. 108-117.

15. von Andrian, U.H. and T.R. Mempel, *Homing and cellular traffic in lymph nodes.* Nat Rev Immunol, 2003. **3**(11): p. 867-878.

16. von Andrian, U.H. and C.R. Mackay, *T-cell function and migration. Two sides of the same coin.* N Engl J Med, 2000. **343**(14): p. 1020-34.

17. Bloom, D.E., D. Canning, and M. Weston, *The value of vaccination.* World Economics, 2005. **6**(3): p. 15-39.

18. Osterholm, M.T., et al., *Efficacy and effectiveness of influenza vaccines: a systematic review and meta-analysis.* The Lancet Infectious Diseases, 2012. **12**(1): p. 36-44.

19. Belshe, R., *Translational research on vaccines: influenza as an example.* Clinical Pharmacology & Therapeutics, 2007. **82**(6): p. 745-749.

20. Koopmann, H., *Die pathologische Anatomie der Influenza 1918/19.* Virchows Archiv, 1920. **228**(1): p. 319-344.

21. Johnson, N.P. and J. Mueller, *Updating the accounts: global mortality of the 1918-1920" Spanish" influenza pandemic.* Bulletin of the History of Medicine, 2002. **76**(1): p. 105-115.

22. Grist, N., *Pandemic influenza 1918.* British medical journal, 1979. **2**(6205): p. 1632.

23. Carrat, F. and A. Flahault, *Influenza vaccine: The challenge of antigenic drift.* Vaccine, 2007. **25**(39–40): p. 6852-6862.

24. Potter, C.W., *A history of influenza.* Journal of Applied Microbiology, 2001. **91**(4): p. 572-579.

25. Wood, J.M., *Selection of influenza vaccine strains and developing pandemic vaccines.* Vaccine, 2002. **20, Supplement 5**(0): p. B40-B44.

26. Cox, N.J. and K. Subbarao, *Global epidemiology of influenza: past and present.* Annual Review of Medicine, 2000. **51**(1): p. 407-421.

27. Cox, R.J., K.A. Brokstad, and P. Ogra, *Influenza Virus: Immunity and Vaccination Strategies. Comparison of the Immune Response to Inactivated and Live, Attenuated Influenza Vaccines.* Scandinavian Journal of Immunology, 2004. **59**(1): p. 1-15.

28. Kemble, G. and H. Greenberg, *Novel generations of influenza vaccines.* Vaccine, 2003. **21**(16): p. 1789-1795.

29. Nevel, A. and C. Layton, *Influenza Vaccine Manufacturing.* 2005.

30. Palese, P., *Making better influenza virus vaccines?* Emerging infectious diseases, 2006. **12**(1): p. 61.

31. Layne, S.R., *Human influenza surveillance: the demand to expand.* Emerging Infectious Diseases, 2006. **12**(4): p. 562-568.

32. Szymczakiewicz-Multanowska, A., et al., *Safety and Immunogenicity of a Novel Influenza Subunit Vaccine Produced in Mammalian Cell Culture.* Journal of Infectious Diseases, 2009. **200**(6): p. 841-848.

33. Amorij, J.-P., et al., *Needle-free influenza vaccination.* The Lancet Infectious Diseases, 2010. **10**(10): p. 699-711.

34. Shefer, A., et al., *Improving immunization coverage rates: an evidence-based review of the literature.* Epidemiologic Reviews, 1999. **21**(1): p. 96.

35. Belshe, R.B., *Current status of live attenuated influenza virus vaccine in the US.* Virus Research, 2004. **103**(1–2): p. 177-185.

36. Bardiya, N. and J.H. Bae, *Influenza vaccines: recent advances in production technologies.* Applied Microbiology and Biotechnology, 2005. **67**(3): p. 299-305.

37. Zambon, M.C. and J.S. Ellis, *Molecular methods for diagnosis of influenza*. 2001, Elsevier. p. 267-273.

38. De Jong, J.C., et al., *Influenza virus: a master of metamorphosis.* Journal of Infection, 2000. **40**(3): p. 218-228.

39. Ellis, J.S. and M.C. Zambon, *Molecular diagnosis of influenza.* Reviews in Medical Virology, 2002. **12**(6): p. 375-389.

40. Lambert, P.H. and P.E. Laurent, *Intradermal vaccine delivery: Will new delivery systems transform vaccine administration?* Vaccine, 2008. **26**(26): p. 3197-3208.

41. Rahman, F., et al., *Cellular and humoral immune responses induced by intradermal or intramuscular vaccination with the major hepatitis B surface antigen.* Hepatology, 2000. **31**(2): p. 521-527.

42. Nicoll, L.H. and A. Hesby, *Intramuscular injection: an integrative research review and guideline for evidence-based practice.* Applied nursing research, 2002. **15**(3): p. 149-162.

43. Alarcon, J.B., et al., *Preclinical evaluation of microneedle technology for intradermal delivery of influenza vaccines.* Clinical and Vaccine Immunology, 2007. **14**(4): p. 375-381.

44. Harper, S.A., et al., *Prevention and control of influenza.* Mmwr, 2004. **53**(RR06): p. 1-40.

45. Hinman, A.R., et al., *Vaccine shortages: History, impact, and prospects for the future*.* Annu. Rev. Public Health, 2006. **27**: p. 235-259.

46. Kenney, R.T., et al., *Dose sparing with intradermal injection of influenza vaccine.* New England Journal of Medicine, 2004. **351**(22): p. 2295-2301.

47. Bricks, L.F., *Percutaneous or intradermal BCG vaccine?* Jornal de pediatria, 2004. **80**(2): p. 93-98.

48. Copeman, P.W. and J.E. Banatvala, *The skin and vaccination against smallpox.* Br J Dermatol, 1971. **84**(2): p. 169-73.

49. Naleway, A.L., et al., *Eczematous skin disease and recall of past diagnoses: implications for smallpox vaccination.* Ann Intern Med, 2003. **139**(1): p. 1-7.

50. Marquet, F., et al., *Characterization of Dendritic Cells Subpopulations in Skin and Afferent Lymph in the swine model.* PLoS One, 2011. **6**(1): p. e16320.

51. Godin, B. and E. Touitou, *Transdermal skin delivery: Predictions for humans from in vivo, ex vivo and animal models.* Advanced Drug Delivery Reviews, 2007. **59**(11): p. 1152-1161.

52. Wu, K.S., W.W. van Osdol, and R.H. Dauskardt, *Mechanical properties of human stratum corneum: Effects of temperature, hydration, and chemical treatment.* Biomaterials, 2006. **27**(5): p. 785-795.

53. DeBenedictis, C., et al., *Immune functions of the skin.* Clinics in Dermatology, 2001. **19**(5): p. 573-585.

54. Dean, C.H., et al., *Cutaneous delivery of a live, attenuated chimeric flavivirus vaccines against Japanese encephalitis (ChimeriVaxTM-JE) in non-human primates.* Human vaccines, 2005. **1**(3): p. 106-111.

55. Dean, H.J. and D. Chen, *Epidermal powder immunization against influenza.* Vaccine, 2004. **23**(5): p. 681-686.

56. Mitragotri, S., *Immunization without needles.* Nature Reviews Immunology, 2005. **5**(12): p. 905-916.

57. van der Maaden, K., W. Jiskoot, and J. Bouwstra, *Microneedle technologies for (trans)dermal drug and vaccine delivery.* Journal of Controlled Release, 2012. **161**(2): p. 645-655.

58. Van Damme, P., et al., *Safety and efficacy of a novel microneedle device for dose sparing intradermal influenza vaccination in healthy adults.* Vaccine, 2009. **27**(3): p. 454-459.

59. Quaak, S.G., et al., *DNA tattoo vaccination: effect on plasmid purity and transfection efficiency of different topoisoforms.* Journal of Controlled Release, 2009. **139**(2): p. 153-159.

60. van den Berg, J.H., et al., *Optimization of intradermal vaccination by DNA tattooing in human skin.* Hum Gene Ther, 2009. **20**(3): p. 181-9.

61. Coucke, D., et al., *Spray-dried powders of starch and crosslinked poly(acrylic acid) as carriers for nasal delivery of inactivated influenza vaccine.* Vaccine, 2009. **27**(8): p. 1279-1286.

62. Kendall, M.A.F., P.J. Wrighton Smith, and B.J. Bellhouse, *Transdermal ballistic delivery of micro-particles: investigation into skin penetration*. 2000, IEEE. p. 1621-1624 vol. 3.

63. Bellhouse, B.J. and M.A. Kendall, *Dermal powderject devices.* 2003.

64. Burkoth, T.L., et al., *Transdermal and transmucosal powdered drug delivery.* Crit Rev Ther Drug Carrier Syst, 1999. **16**(4): p. 331-84.

65. Kendall, M.A., *Needle-free vaccine injection.* Handbook Exp Pharmacol, 2010(197): p. 193-219.

66. Etzl, E.E., G. Winter, and J. Engert, *Toward intradermal vaccination: preparation of powder formulations by collapse freeze-drying.* Pharmaceutical Development and Technology, 2014. **19**(2): p. 213-222

.

2. Chapter - Stability of collapse lyophilized influenza vaccine formulations

This Chapter is already published in the International journal of pharmaceutics:

Anamur, C.*, G. Winter, and J. Engert**, Stability of collapse lyophilized influenza vaccine formulations. International journal of pharmaceutics, 2015. 483(1): p. 131-141.

* First author

** Corresponding author

The experiments in this publication were planned, structured and carried out by C. Anamur. Furthermore, the results were interpreted, summarized and the text was written by C. Anamur. Dr. Julia Engert gave her guidance in planning, discussion and interpretation of the experiments and results and corrected the manuscript for publication.

2.1 Abstract

A clear limitation of many liquid vaccines is the obligatory cold-chain distribution system. Therefore, distribution of a dried vaccine formulation may be beneficial in terms of vaccine stability, handling and transport. Collapse freeze-drying is a process which utilizes fairly aggressive but at the same time economic lyophilization cycles where the formulation is dried above its glass transition temperature.

In this study, we used collapse freeze-drying for a thermosensitive model influenza vaccine (Pandemrix®). The dried lyophilizates were further cryo-milled to engineer powder particles in the size range of approximately 20 µm to 80 µm which is applicable for epidermal powder immunization.

Vaccine potency and stability were neither affected by high temperature input during collapse lyophilization nor over a storage period of six months. Furthermore, cryo-milled vaccine lyophilizates showed good storage stability of up to three months at high storage temperature (40°C).

Stabilized collapse lyophilized vaccines do not need a cold-chain-distribution system. This technique can provide a powerful tool for the worldwide distribution of vaccine and for new application technologies such as engineered powder immunization.

Keywords:

Powder immunization; vaccination; influenza vaccine; collapse lyophilization; cryo-milling

2.2 Introduction

Vaccination is one of the most effective medical interventions to prevent viral infections [1]. The World Health Organization (WHO) recommends coverage of at least 70% - 80% of the population for effective immunization [2-4]. In addition, proper storage and handling of vaccines is very important since many vaccines feature low stability in liquid formulations, and often storage at 2-8°C is recommended [5]. Exposure to temperatures outside the recommended range can compromise vaccine stability and result in reduced vaccine potency, making cost-intensive cold-chain storage and distribution mandatory.

New strategies for vaccine stabilization as well as new and simple administration technologies are needed to improve accessibility to vaccination. A well-known process for pharmaceutical protein stabilization is lyophilization, which is a time and energy consuming process. Therefore, a more economical collapse lyophilization process was established. Collapse lyophilization is characterized by freeze-drying above the glass transition temperature (T_g`). Higher temperatures are exerted on the product while the time period which is necessary to dry the vaccine is shortened distinctively compared to conventional lyophilization [6]. Not only can the primary drying time be drastically shortened but also can a relaxation of the amorphous sugar matrix be achieved by exposure to the higher temperature in the end phase of the drying cycle. This leads to visually inhomogeneous but stable products [7, 8]. In addition to a faster and more economic process, collapse freeze-drying leads to more dense lyophilizates with a low specific surface area (SSA) [7, 9]. Smaller SSA of collapse lyophilizates presents lower interfaces for proteins to accumulate and subsequently interact with their surroundings. Due to the dry state of proteins in lyophilizates, degradation at higher temperature can often be avoided.

In terms of vaccine application, intradermal administration of vaccines using devices such as microneedles or epidermal powder immunization (EPI) could simplify the accessibility to vaccination [10-12]. The skin, not only organized as a mechanical barrier to pathogens, is also an active immune organ [13]. Highly specialized intradermal immune cells (Langerhans cells and dendritic cells) located in the epidermis can trigger immune response after an intradermal administration of vaccines

[13-15]. In addition, vaccine administration into the skin using EPIs is a minimally invasive type of application, which increases patient compliance and eliminates needle-stick injuries. The lack of tissue lesions, bleedings, and needle-stick injuries after EPI administration can help to minimize the risk of disease transmission [16, 17].
In our study, we used an influenza vaccine as a model because the antigen hemagglutinin (HA) is (very) thermo-sensitive and thus a suitable indicator for temperature related product changes. Furthermore, influenza vaccinations are in focus due to their socioeconomic importance [18-20]. Influenza infections circulate worldwide, can occur among people of all ages regardless of socioeconomic background, and are associated with high morbidity and mortality. In particular, people aged 65 or older and younger children are at risk [1,21-24]. Annual influenza epidemics in developing countries are a public health and economic concern when health care and surveillance systems are less developed, and thus an influenza infection can spread faster and more distinctive.
A commercially available H1N1 vaccine (Pandemrix®, GlaxoSmithKline, Rixensart, Belgium) was chosen. The process of preparation and stabilization by collapse lyophilization was controlled by monitoring stability and biological activity of hemagglutinin. Changes were detected using analytical methods such as a hemagglutination inhibition assay (HAI), westernblot analysis, and subvisible particle measurements. Quantification of hemagglutinin in the H1N1 vaccine was performed using reversed-phase liquid chromatography (RP-HPLC). In order to determine the quality of the lyophilizates, residual moisture and SSA of lyophilizates were measured. Collapse-freeze drying results in more compact collapse lyophilizates which will then form the basis for highly dense powder particles for epidermal powder administration [7]. The freeze-dried H1N1 model vaccine lyo cakes were subsequently ground by cryo-milling to achieve particles in the range of 20 µm – 80 µm.d. In this study, we demonstrate a successful stabilization and characterization of a thermo-sensitive model influenza vaccine for epidermal powder immunization.

2.3 Material and Methods

2.3.1 Materials

A H1N1 influenza vaccine (Pandemrix®, GlaxoSmithKline, Rixensart, Belgium) was used as a model vaccine and was kindly provided by the Bavarian State Ministry of Environment and Public Health. The commercial product contains 15 µg/ml hemagglutinin formulated in phosphate buffer with polysorbate 80, octoxynol 10 and thiomersal. Prior to administration, the vaccine is normally mixed with the adjuvant AS03 containing squalene, DL-α- tocopherol, and polysorbate 80. The adjuvant part was not used in our experiments. Sodium hydrogen phosphate monohydrate was purchased from Gruessing (Gruessing, Filsum, Germany), and sodium dihdydrogen phosphate dehydrate, sodium phosphate monobasic and dibasic, sodium hydroxide, and sodium chloride were obtained from Applichem (Applichem, Darmstadt, Germany). Trehalose was used as lyoprotectant and purchased from BDH Prolabo (VWR, Ismaning, Germany). Mannitol was used as bulking agent and obtained from Boehringer Ingelheim (Ingelheim, Germany). All other chemical were of at least analytical grade.

2.3.2 Methods

2.3.2.1 Tangential flow filtration (TFF) for vaccine concentration enrichment

The influenza vaccine was concentrated using a tangential flow filtration method as described by Kommareddy et al. [25]. A filtration cassette Minimate™ (PALL, Dreieich, Germany) with a cut-off pore size of 5 kDa was used. Prior to usage, the TFF cassette was sanitized with 0.5 M NaOH at 45°C for 45 min as recommended by the manufacturer (PALL, Dreieich, Germany). Subsequently, the TFF cassette was rinsed with highly purified water (Sartorius Arium Pro, Sartorius, Goettingen, Germany) until a neutral pH was measured using a seveneasy® pH-meter (Mettler

Toledo, Giessen, Germany). After saturation of the TFF-cassette membrane with 200 ml of circulating vaccine solution over a time period of 60 min, concentration of the vaccine was carried out at a temperature of 2-8°C. Concentration of H1N1 influenza vaccine (Pandemrix®) was performed at a flow rate of 100 ml/min as recommended by the manufacturer (PALL, Dreieich, Germany). A peristaltic pump (Masterflex, Ponndorf, Germany) was used to pressurize the membrane chamber while the vaccine solution was in contact with the membrane. The initial vaccine volume was reduced to 4%, which results in a hemagglutinin concentration which is 10 - 13 times higher than the initial concentration (final concentration 150 µg/ml). The final hemagglutinin concentration was determined by fluorescence detection following reversed phase high performance liquid chromatography (RP-HPLC) as described later. Subsequently, the concentrated vaccine was dialyzed against 10 mM phosphate buffer (0.22 µm filtered) (PALL life Sciences, Ann Arbor, USA) to reduce salts in order to avoid a phase separation during freeze-drying.

2.3.2.2 Adjustment of vaccine concentration

The amount of hemagglutinin in the concentrated vaccine solution was determined by RP-HPLC and calculated as follows: the area under the curve (AUC) of HA of the commercial product was compared to the AUC of modified vaccine solution. The hemagglutinin peak was recorded using a fluorescence detector (λ_{ex} 280 nm and λ_{em} 335 nm) and the AUC of the commercial product (15 µg/ml hemagglutinin) was determined. The AUC of the commercial product was then compared to the concentrated vaccine solution by TFF. Prior to lyophilization, the concentration of hemagglutinin was adjusted to 150 µg/ml with 10 mM phosphate buffer.

2.3.2.3 Preparation of a heat-stressed vaccine sample as control

Pandemrix® was heated to 70°C for 100 minutes in a Binder FED 53 heating chamber (Binder GmbH, Tuttlingen, Germany) to obtain a control vaccine for the analytics containing heat-stressed hemagglutinin.

2.3.2.4 Addition of lyoprotectants and bulking agents

The concentrated vaccine solution was mixed with trehalose and mannitol (1:1) (w/w) to obtain a final concentration of 15% solid content and a hemagglutinin concentration of 3.75 µg/mg in the lyophilizate. The mixture was gently stirred at approximately 50 rpm using a magnetic stirrer (IGAMAG RCT, IKA®-Werke GmbH & Co. KG, Staufen, Germany) to dissolve the excipients. The final concentration of 150 µg/ml in the final lyophilization mixture (H1N1 influenza vaccine-carbohydrate solution) was determined using fluorescence detection following RP-HPLC.

2.3.2.5 Lyophilization process

The final vaccine-carbohydrate solution (2.625 ml) was pipetted into DIN 10R vials (MGlas AG, Muennerstadt, Germany) with a resulting filling level of approximately 1 cm, semi-stoppered using Westar®RS.stoppers (Westpharma, Exton, USA) and transferred to the freeze-dryer. Lyophilization was performed using a Martin Christ Epsilon 2-6D freeze-dryer (Martin Christ, Osterode, Germany) equipped with a pirani pressure sensor. The middle shelf was loaded with 126 vials. Vials containing the final vaccine-carbohydrate solution were bordered by two rows of edge vials containing a 15% trehalose-mannitol (1:1) (w/w) solution in 10 mM phosphate buffer to obtain a homogenous temperature impact to the vaccine-carbohydrate formulation in the center. At the start of the lyophilization cycle, samples were equilibrated at 4°C for one hour and subsequently frozen to -50°C using a ramp within 1.5 hours. The freezing temperature was isothermally held for one hour. Afterwards, the temperature was increased to -40°C using a ramp of 0.33°C/min. When the process reached -40°C the chamber pressure was reduced to 1.98 mbar. After a short equilibration time the shelf temperature was increased to 45°C within 2 hours. Primary drying was carried out for 24 hours at 45°C. After the primary drying, the chamber pressure was further decreased to 0.3 mbar. These conditions (0.3 mbar / 45°C) were maintained for further 20 hours. At the end of the secondary drying, the temperature was reduced to the storage temperature of 4°C. Finally, the samples were stoppered at approximately 800 mbar with dry nitrogen gas atmosphere and crimped after unloading as described by Kis et al. [72].

The final protein (HA) concentration content of the HA in collapse lyophilizates were determined using RP-HPLC with fluorescence detection.

2.3.2.6 Cryo-milling of lyophilizates and sieving

Cryo-milling was performed using a Retsch CryoMill (Retsch Technology GmbH, Haan, Germany). Samples were cooled to -196°C using liquid nitrogen in stainless steel milling jars (Retsch Technology GmbH, Haan, Germany). An amount of approximately 1.5 g of the lyophilizates was filled into a stainless steel jar and two steel balls were added. A pre-cooling for 10 min with a milling frequency of 5 Hz was carried out before grinding was performed at 25 Hz for 15 sec. To avoid water condensation after the milling process, the chilled jar was placed into a custom made glovebox (workshop at the Ludwig-Maximilians-University Munich, Germany) which was flushed with nitrogen gas of low humidity (< 3%). Jars were left to equilibrate to room-temperature for two hours. Afterwards sieving through sieves (Retsch Technology GmbH, Haan, Germany) with mesh sizes of 20 µm, 40 µm, 80 µm and 125 µm was performed. Classifying by sieving was carried out for 10 minutes and the powder was weighed afterwards. These steps were repeated until the mass of the powder on each sieve did not differ more than 1% from the previous weighing. Aliquots of the ground and classified samples were filled in DIN 10R vials under dry nitrogen atmosphere and stoppered with Westar®RS.stoppers (Westpharma, Exton, USA).

2.3.2.7 Residual moisture content determination by Karl-Fischer titration

Residual moisture contents of all lyophilizates and the cryo-milled lyophilizates were analyzed to determine successfully stabilized collapse freeze-dried products. Residual moisture determination was performed using a Karl-Fischer direct injection method (737 KF Coulometer, Metrohm, Filderstadt, Germany). Sample aliquots between 10 mg to 50 mg were filled in DIN 2R vials (Mglas AG, Muennerstadt, Germany) in a Glovebox under dry nitrogen gas atmosphere (< 10%) measured with a thermo-hygrometer (TFA Dostmann, Wertheim, Germany). Each vial was filled with

approximately 2.5 ml methanol (Hydranal®-Methanol dry, Sigma-Aldrich, Taufkirchen, Germany) with very low water content and were placed into an ultrasonic bath for 15 minutes (Sonorex TK52, Bandelin electronics, Berlin, Germany). Finally, 1 ml of the solution was injected into the coulometric titrator. Results were calculated and are given as relative water content in percentage (m/m). Three independent measurements of samples of each storage temperature and time point were collected.

2.3.2.8 Specific surface area (SSA) determination

The Brunauer-Emmet-Teller (BET) krypton gas adsorption method was used to determine the SSA of lyophilizates and cryo-milled lyophilizates. The krypton adsorption on the surface of the specimen carried out in a liquid nitrogen bath (77.3 K) using an Autosorb 1 (Quantachrome, Odelzhausen, Germany). Weighed samples were outgassed for 2 hours at room temperature using the Autosorb 1 outgassing connection (Quantachrome, Odelzhausen, Germany). Sample measurement was performed applying an eleven point measurement curve. Data were collected using the Autosorb 1 software (Quantachrome, Odelzhausen, Germany), and the SSA was calculated using a multipoint BET method fit. Three independent measurements were performed. To identify the impact of HA to SSA, 10 mM phosphate buffer was also mixed with trehalose and mannitol (1:1) (w/w) to a 15% solid content (w/w).

2.3.2.9 Scanning electron microscopy (SEM)

Samples were attached onto an adhesive carbon tape (Bal-tec GmbH, Germany) and subsequently sputtered with carbon under high vacuum (MED 020, Bal-tec GmbH, Germany). Samples were viewed using a scanning-electron microscope (Supra 55VP, Zeiss SMT, Germany) under high vacuum. Scanning electron micrographs were recorded at 100 fold and 300 fold magnifications.

2.3.2.10 Storage conditions for lyophilizates and cryo-milled lyophilizates

Samples (lyophilizates and cryo-milled lyophilizates) were stored at temperatures of 2-8°C, 25°C, and 40°C in order to determine the stability of hemagglutinin over a period of up to six months at room humidity (65-80%). Data were collected after 2, 4, 12 weeks, and 6 months. Collapse freeze-dried samples (0.395 mg) were reconstituted with 2.23 ml highly purified water for further examination to obtain a final concentration of 15 µg/ml of the samples for each storage time point.

2.3.2.11 Reversed-phase liquid chromatography (RP-HPLC)

For the determination of the hemagglutinin content in the samples an RP-HPLC method was established using a Dionex HPLC system equipped with a Dionex P680 HPLC Pump, ASI-100 automated sample injector, Dionex Column oven, Dionex RF-2000 Fluorescence Detector and a Dionex UVD170u UV/VIS-detector (Dionex, Idstein, Germany). A Phenomenex Jupiter 5 µ, C18, 300 A column (250 x 4.6 mm) (Phenomenex, Aschaffenburg, Germany) was used for separation. Chromatographic separation was carried out at 60°C with a gradient elution over 30 min at a flow rate of 1.0 ml/min. Eluent A consisted of highly purified water with 0.1% trifluoric acid and eluent B comprised 75% 2-propanol, 25% acetonitrile and 0.1% trifluoric acid. At the start the eluent mixture consisted of 20% eluent B, which was increased to 36% within 10 min. During the next 4 min eluent B was increased to 95% and this concentration was held for further 4 min. Eluent B was abruptly reduced again to 20% after the plateau phase. The column was flushed for 12 min with eluent B at 20% to achieve re-equilibration. 25 µl of each sample was injected and hemagglutinin content was determined using the intrinsic fluorescence of hemagglutinin at λ_{ex} 280 nm and λ_{em} 335 nm. For each storage temperature and time point, three independent measurements of the specimens were analyzed. The lyophilized and cryo-milled samples were collected at each time point (2 weeks, 4 weeks 12 weeks and 6 months) and were compared against the heat stressed control vaccine (70°C/100 min), and the

liquid vaccine-carbohydrate solution stored at 2-8°C. Data acquisition and analysis was performed using Chromeleon 6.80 software (Dionex, Idstein, Germany).

2.3.2.12 Light obscuration measurements

Light obscuration was measured using a PAMAS SVSS-35 particle counter (PAMAS - Partikelmess- und Analysensysteme GmbH, Rutesheim, Germany) equipped with an HCB-LD-25/25 sensor. Particle diameters in the range of 1 to 200 µm were determined in reconstituted lyophilizates, H1N1 commercial product, heat stressed vaccine, and buffer medium. Prior to each measurement, the system was rinsed with 3.0 ml highly purified water. The measurement was started when the particle counts > 1 µm in highly purified water was below 10 particles/ml and no particles > 10 µm were detected. Subvisible particles were counted in a sample volume of 0.3 ml. The measurement was repeated three times for each storage temperature (2-8°C, 25°C, and 40°C) at every time point (2/4/12 weeks and 6 month). Data was collected using the PAMAS PMA software (PAMAS - Partikelmess- und Analysensysteme GmbH, Rutesheim, Germany). Results were given in cumulative particle per ml.

2.3.2.13 Turbidity measurements

Turbidity of reconstituted samples was determined using a Hach Lange Nephla nephelometer (Hach Lange GmbH, Düsseldorf, Germany). Samples (2.0 ml) were analyzed in pre-rinsed turbidity glass cuvettes with a flat bottom (Hach Lange GmbH, Düsseldorf, Germany). Turbidity was measured at a wavelength of $\lambda = 860$ nm and detected at an angle of 90°. Turbidity is reported in formazine nephelometric units (FNU). Each sample was measured twice. After the first measurement the cuvette was turned 90° and was measured again. For each time point and storage temperature, three specimens were analysed. Pandemrix® commercial product and Pandemrix® heat stressed vaccine as well as the buffer mediums were investigated and compared to the reconstituted lyophilizates for control purposes.

2.3.2.14 Sodium dodecyl sulphate-polyacrylamide gel electrophoresis (SDS-Page)

SDS-Page analysis was performed to determine proteins, protein fractions, degradation of antigen and the protein content of the vaccine. The different forms of a hemagglutinin (e.g. subunit, monomer, dimer, trimer of HA) were separated by their electrophoretic mobility. Reconstituted samples (15 µg/ml) were mixed with Laemmli buffer at a ratio of 1:1 (250 mM Tris(hydroxymethyl)-aminomethane, 1% of a 0.1% Bromphenol blue solution (Merck Darmstadt, Germany), 4% SDS (Sigma-Aldrich Taufkirchen, Germany), 23% of glycerol (AppliChem, Darmstadt, Germany). The mixtures were boiled at 95°C for 20 min in a block-thermostat Grant QBT (Grant Instruments, Cambridgeshire, Great Britain). 10 µl of each cooled sample was pipetted into a well of a Novex NuPAGE 10% Bis-Tris gel (life technologies, Carlsbad, USA). Mark12 protein standard ladder (life technologies, Carlsbad, USA) was used for comparison. Separation was performed with an electrophoresis module (Bio-Rad, Munich, Germany). The module was filled with a diluted Novex NuPAGE MES SDS-Runnung buffer 20x (life technologies, Carlsbad, USA) as recommended. Electrophoresis was carried out at 100 V for 15 min and 160 V for a further 45 min. The SDS-Page gel was then transferred for 60 minutes into a bath of Imperial Protein stain (Thermo Fischer scientific, Rockford, USA) to develop a Coomassie brilliant blue staining. Finally the SDS-Page gel was scanned (Epson Perfection V370, Epson, Japan), and the protein fractions were compared to the protein standard ladder.

2.3.2.15 Westernblot analysis

The structural integrity of hemagglutinin was tested by Westernblot analytics. A SDS-Page gel (10% Bis-Tris gel) was prepared according to the SDS-Page assay described above up to the staining step. Instead of a Mark12 Protein standard ladder, a MagicMark western protein standard (life technologies, Carlsbad, USA) was used. After protein separation, proteins were transferred to a nitrocellulose membrane (Hybond-ECL™, Amersham Bioscience, Freiburg, Germany) via tank electro-blotting for 90 min at 100 V. A blotting sandwich was prepared containing 10% Bis-Tris gel and nitrocellulose membrane, which were embedded in a layer of Rotilabo blotting

paper (Roth, Karlsruhe, Germany) and pads. The blotting sandwich was transferred into a box filled with cold Tank buffer cooled using a thermal pack (cooled to -80°C) within the blotting tank and storage in a chilled room at 2°-8°C to avoid excessive heat during electro-blotting. A 5x Tank buffer containing 240 mM Tris (hydroxymethyl)-aminomethane (Sigma-Aldrich, Taufkirchen, Germany), 195 mM Glycine (Applichem, Darmstadt, Germany) and highly purified water to 1000 ml was used. 20% of 5x Tank buffer was mixed with 20% methanol and highly purified water to the final volume. After blotting, the nitrocellulose membrane was shortly washed with 10% of a 10x Tris-buffered saline and Tween 20 solution (TBS-T). The 10x TBS-T contains 500 mM Tris(hydroxymethyl)-aminomethane (Merck, Darmstadt, Germany), 3.8 M NaCl (BDH Prolabo, VWR, Ismaning, Germany), 1% Tween 20 (Fluka, Sigma-Aldrich, Taufkirchen, Germany), diluted with highly purified water to the required quantity. Afterwards, the nitrocellulose membrane was incubated in a 5% milk powder blocking solution for 2 hours on a horizontal shaker (100 rpm per minute) (VWR Ismaning, Germany) and subsequently washed with TBS-T. Thereafter, incubation in 20 ml of 1% milk powder TBS-T solution with a murine monoclonal anti-hemagglutinin antibody (Sino biological Inc., Beijing, China) at a concentration of 1.5 µg/ml was carried out for 12 hours at 2-8°C. After a further washing step the nitrocellulose membrane was incubated with a secondary antibody, polyclonal anti-mouse-antibody with a fluorophor (λ_{ex} 778 nm and λ_{em} 795 nm) (LI-COR, Lincoln, USA) in a 20 ml of 1% milk powder-TBS-T solution for 2 hours in a horizontal shaker (100 rpm per minute) (VWR Ismaning, Germany). After the final washing step with TBS-T, the membrane was analyzed using a LI-COR Odyssey infrared imaging system (LI-COR, Lincoln, USA).

2.3.2.16 Hemagglutination inhibition assay (HAI)

Biological activity of hemagglutinin was tested by an adapted hemagglutination inhibition assay [26, 27]. A 25% chick whole-blood solution (Labor Dr. Merk & Kollegen GmbH, Ochsenhausen, Germany) was diluted with Dextrose-Gelatine-Veronal buffer (DGV-buffer) (Labor Dr. Merk & Kollegen GmbH, Ochsenhausen, Germany) to a final concentration of 0.5% (v/v). Each well of a 96 microtiter V-shaped well-plate (Nunc V96, Thermo Fischer scientific, Rockford, USA) was filled

with 50 µl of Agglutest buffer (Labor Dr. Merk & Kollegen GmbH, Ochsenhausen, Germany) excluding the first column. The first column of the microtiter plate was filled with 100 µl of each sample. Subsequently, two-fold dilution steps were performed each with a transfer of 50 µl. Finally, 50 µl of 0.5% chick whole-blood solution were added to each well. After agitating the microtiter plate at 350 rpm for 30 sec, the well-plate was incubated at 37°C for 45 min. The endpoint was determined by the characteristic red dot formation of sedimented erythrocytes in the center of the well. The amount of hemagglutinin at the end point can be calculated of the serial 2-fold dilution. Three independent samples of each storage temperature and time point were measured.

2.4 Results

2.4.1 Hemagglutinin quantification using RP-HPLC

Quantification of HA in all liquid vaccine samples as well as the reconstituted lyophilizates and cryo-milled lyophilizates was carried out using RP-HPLC. The retention time of hemagglutinin in all samples including the retention time of the commercially available product was approximately 17.40 min ± 0.15 min (Figure 2.4.1). The results indicated that neither the storage period up to six months nor the process of cryo-milling altered the hemagglutinin concentration detected by the fluorescence detector. The deviation of the fluorescence units [mV*min] of cryo-milled lyophilizates was slightly higher compared to non-cryo-milled lyophilizates. The stressed vaccine samples (70°C/100 min) unexpectedly exhibited a similar protein peak and fluorescence value as unstressed samples (Figure 2.4.1), no major changes to the hemagglutinin structure were observed.

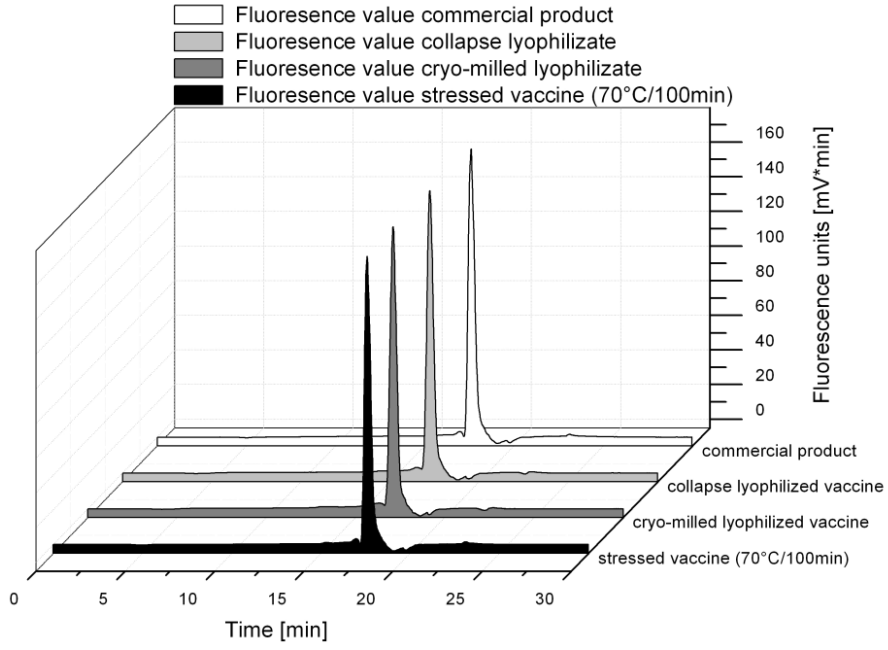

Figure 2.4.1: Fluorescence units of the commercially available product (15 µg/ml), stressed vaccine (15 µg/ml), and collapse lyophilized vaccine (15 µg/ml) after 6 months of storage Three independent measurements were performed (n=3)

2.4.2 Light obscuration measurements

All freeze-dried samples (lyophilizates and cryo-milled lyophilizates) were reconstituted with highly purified water to a final concentration of 15 µg/ml. The samples were analyzed by light obscuration to determine any formation of aggregates induced by the preparation process (concentration by TFF, collapse lyophilization, cryo-milling) or storage conditions. The reconstituted samples (lyophilizate and cryo-milled lyophilizate) were compared to the final vaccine-carbohydrate solution (15 µg/ml) stored at 2-8°C, the stressed vaccine (70°C/100 min, 15 µg/ml) stored at 2-8°C and 0.22 µm filtered trehalose-mannitol solution. The results of the subvisible particle measurements > 1 µm > 10 µm are shown in Figure 2.4.2.

Particle counts of particles > 1 µm were observed for the commercial product 2754 counts/ml ± 40 counts/ml, the heat stressed vaccine (70°C/100 min) 5005 counts/ml ± 73 counts/ml, collapse lyophilizates 4729 counts/ml± 879 counts/ml, and the cryo-milled lyophilized 5566 counts/ml ± 463 counts/ml. In all samples particle counts > 10 µm were below 600 counts/containment (10R vial), which is in line with the requirements by the European Pharmacopoeia (Ph. Eur.) for particle counts within a container (vial). Concentration by TFF and collapse lyophilization increased particles counts (>1 µm) to a level comparable to the stressed vaccine (Figure 2.4.2), stressed vaccine compared to t_0 of reconstituted lyophilizates). The additional cryo-milling step increased the particle count approximately two to threefold in comparison to the final vaccine-carbohydrate solutions at the start of the study (time point t_0). Measurements of reconstituted lyophilizates showed a homogenous particle distribution with low particle counts > 10 µm. On the contrary, subvisible particle distribution of cryo-milled lyophilizates depended on storage temperature and time period. Light obscuration measurements of cryo-milled samples stored at 2-8°C indicated higher counts of particles > 1 µm but lower counts for particles > 10 µm compared to the other storage temperatures. Lyophilizates stored at 25°C and 40°C had comparable counts of particles > 1 µm. Particle counts for cryo-milled lyophilizates stored at 25°C > 10 µm decreased over storage time whereas the reverse was seen for samples stored at 40°C.

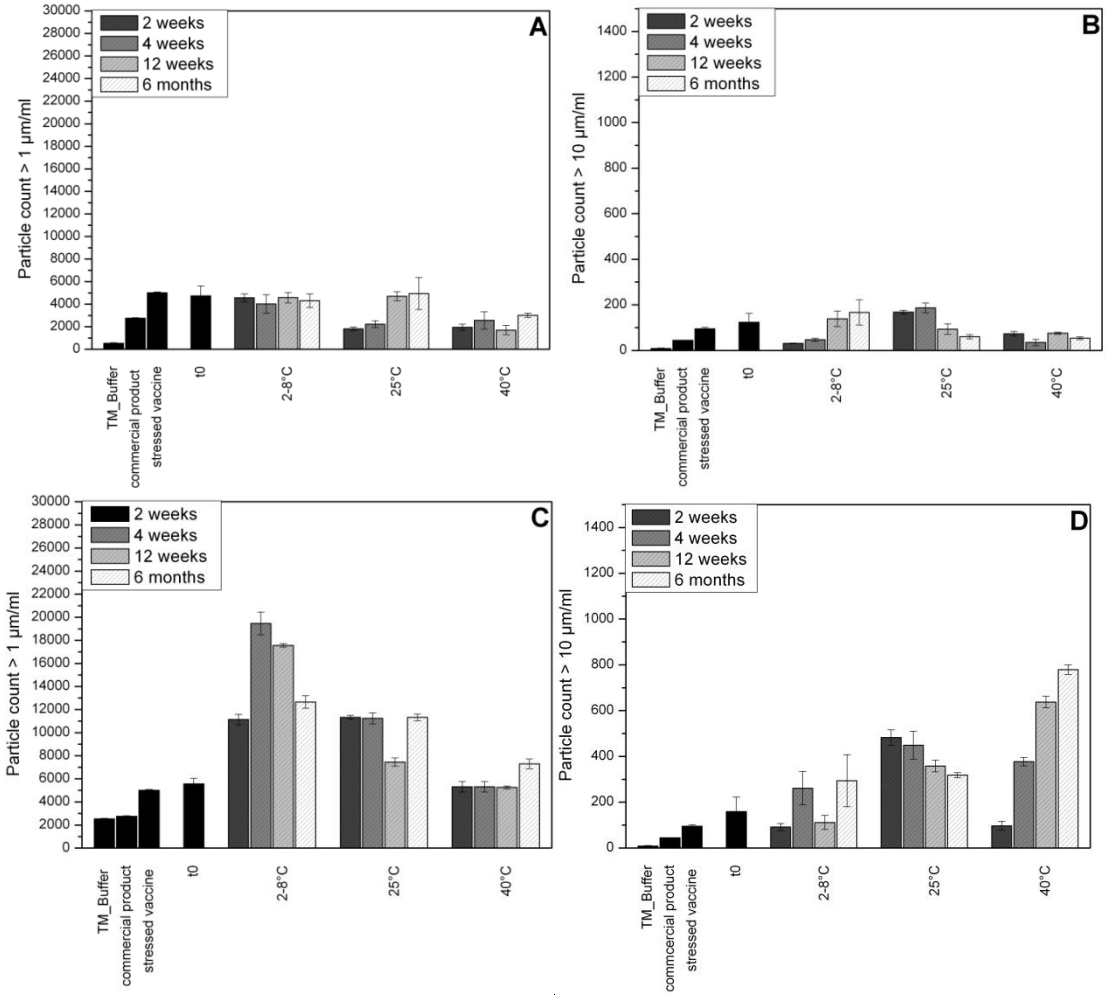

Figure 2.4.2: A) Subvisible particles > 1 µm of vaccine lyophilizates B) subvisible particles > 10 µm of lyophilizates C) subvisible particles > 1 µm of cryo-milled lyophilizates D) subvisible particles > 10 µm of cryo-milled lyophilizates stored at different storage temperatures and over a time period of six months. Three independent measurements were performed (n=3) for comparison of the buffer solution, commercial product, stressed vaccine (70°C/100min), lyophilizate, and cryo-milled lyophilizate.

2.4.3 Turbidity measurements

Generally, reconstituted lyophilizates showed a constant turbidity value over six months apart from reconstituted cryo-milled lyophilizates stored at 40°C The heat stressed vaccine as well as the cryo-milled lyophilizates showed an increased turbidity indicating an increased formation of agglomerations and therefore higher amounts of larger particles (Table 2.4.1). A rise in turbidity over time was detected in cryo-milled samples stored at 25°C and 40°C. The turbidity in cryo-milled lyophilizates stored at 40°C increased distinctly after three and six months of storage.

Table 2.4.1: Turbidity of vaccine lyophilizates and cryo-milled lyophilizates stored at different storage temperatures and over a time period of six months. Three independent measurements were performed (n=3) for comparison of the buffer solution, commercial product, stressed vaccine (70°C/100min), lyophilizate, and cryo-milled lyophilizate.

Sample	**Storage temperature [°C]**	**Turbidity [FNU]**	**Deviation [FNU]**	**Time point**
Trehalose-mannitol buffer	2-8	0.50	±0.01	All time points
Commercial product	2-8	3.11	±0.02	All time points
Vaccine stressed (70°C/100min)	2-8	5.27	±0.08	
Lyophilizate		11.56	±0.14	t0
Lyophilizate	2-8	11.43	±0.33	2 weeks
Lyophilizate	2-8	12.07	±0.04	4 weeks
Lyophilizate	2-8	14.01	±0.16	12 weeks
Lyophilizate	2-8	11.84	±0.15	6 months
Lyophilizate	25	11.27	±0.15	2 weeks
Lyophilizate	25	11.66	±0.18	4 weeks
Lyophilizate	25	11.85	±0.45	12 weeks
Lyophilizate	25	11.66	±0.10	6 months
Lyophilizate	40	11.64	±0.56	2 weeks
Lyophilizate	40	12.32	±0.06	4 weeks
Lyophilizate	40	11.63	±1.04	12 weeks
Lyophilizate	40	12.92	±0.06	6 months
Cryo-milled	2-8	11.89	±0.45	2 weeks
Cryo-milled	2-8	11.67	±0.02	4 weeks
Cryo-milled	2-8	12.07	±0.42	12 weeks
Cryo-milled	2-8	12.21	±0.55	6 months
Cryo-milled	25	11.01	±0.74	2 weeks
Cryo-milled	25	11.99	±0.17	4 weeks
Cryo-milled	25	13.18	±0.06	12 weeks
Cryo-milled	25	12.78	±0.67	6 months
Cryo-milled	40	11.54	±0.47	2 weeks
Cryo-milled	40	12.53	±0.14	4 weeks
Cryo-milled	40	16.24	±0.23	12 weeks
Cryo-milled	40	17.32	±0.35	6 months

2.4.4 Sodium dodecyl sulfate-Polyacrylamide gel electrophoresis (SDS-Page)

SDS-Page was performed to confirm hemagglutinin integrity. Hemagglutinin could potentially aggregate or fragment during processing and storage. The antigen consists of two subunits, HA1 (M_w of approximately 55 kDa) and HA2 (M_w of approximately 25 kDa). The monomer HA (M_w of 75 - 80 kDa) can form dimers (M_w of 150 - 160 kDa) and trimers (M_w of approximately 210 kDa). Bands in the SDS-Page gel were observed at the predicted M_w of HA1, monomer, dimer and trimer in all samples at

different storage temperatures (Figure 2.4.3) Cryo-milled lyophilizates demonstrated similar migration patterns compared to non-ground lyophilizates. Bands were also detected at the predicted molecular weight (M_w) (Figure 2.4.3B). However, 6 month storage at 40°C of cryo-milled lyophilizates induced immobile formation of aggregates in the well (Figure 2.4.3B). Generally, higher storage temperature of the cryo-milled samples resulted in higher visible amounts of agglomerations (Figure 2.4.3A vs. B).

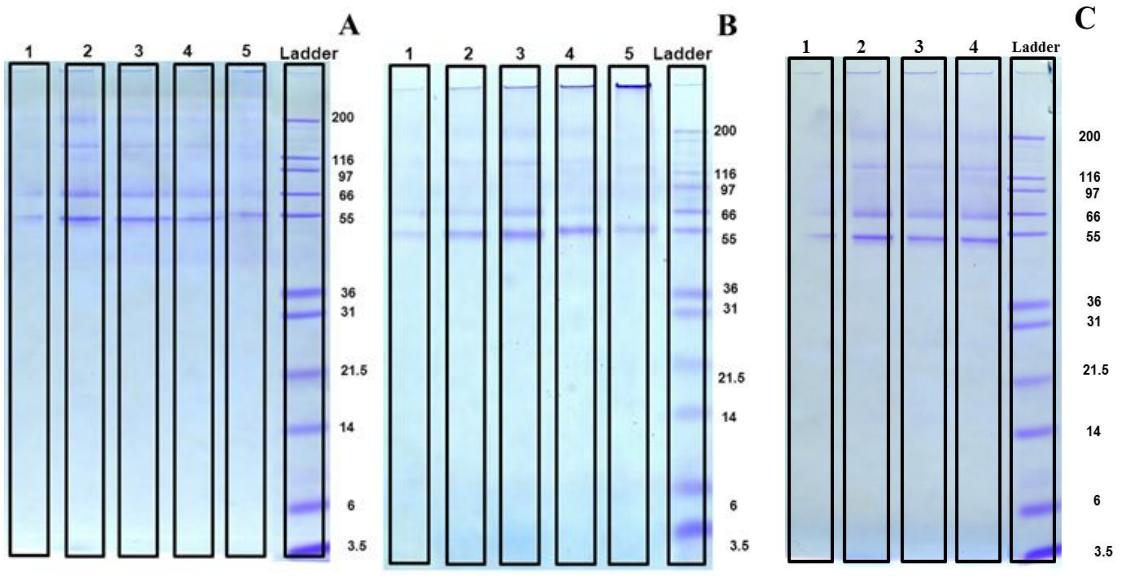

Figure 2.4.3: SDS-Page results after 6 months of storage A) lyophilizate and B) cryo-milled samples at different storage temperatures. Column A1 and B1) commercial product; column A2 and B2) liquid pre-lyophilizate-carbohydrate formulation; A3) lyophilizate stored at 2-8°C; A4) lyophilizate stored at 25°C; A5) lyophilizate stored at 40°C; B3) cryo-milled lyophilizate stored at 2-8°C; B4) cryo-milled lyophilizate stored at 25°C; B5) cryo-milled lyophilizate stored at 40°C; C2) lyophilizate; C3) cryo-milled lyophilizate; and C4) liquid pre-lyophilizate formulation.

2.4.5 Westernblot analysis

Westernblot was performed to test structural integrity and antigenicity of hemagglutinin in the H1N1 vaccine. The various states of hemagglutinin (HA1, monomer, dimer, and trimer) were not observed in every sample in the assays. The three states of hemagglutinin (monomer, dimer, and trimer) were only detected at time point t_0 in all samples (Figure 2.4.4C). Westernblot results of lyophilizates were consistent at all storage temperatures and over the time period of six months. Usually, monomer and dimer were observed at the predicted M_w (Figure 2.4.4) on the scans. Results of cryo-milled samples showed an alteration over the time period of six

months, especially for samples stored at 40°C. Nonetheless, the cryo-milled samples stored at 25°C demonstrated still a structural integrity of HA (six months of storage) (Figure 2.4.4B).

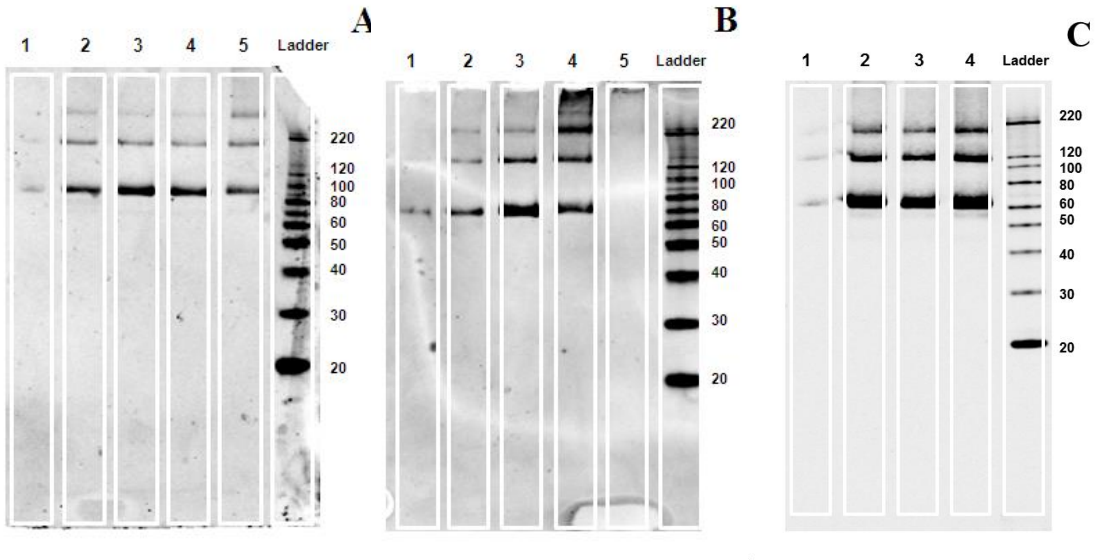

Figure 2.4.4: A) Westernblot results after 6 months of storage A) lyophilizate, B) cryo-milled samples and C) samples at t0 at different storage temperatures. Column A1, B1 and C1) commercial product; column A2 and B2) liquid pre-lyophilizate-carbohydrate formulation; A3) lyophilizate stored at 2-8°C; A4) lyophilizate stored at 25°C; A5) lyophilizate stored at 40°C;; B3) cryo-milled lyophilizate stored at 2-8°C; B4) cryo-milled lyophilizate stored at 25°C; B5) cryo-milled lyophilizate stored at 40°C;.C2) lyophilizate; C3) cryo-milled lyophilizate; and C4) liquid pre-lyophilizate formulation.

2.4.6 Hemagglutination inhibition assay (HAI)

Similar erythrocyte sedimentation was observed for all reconstituted lyophilizates and cryo-milled lyophilizates at a defined dilution (64 fold) independent of storage temperatures or time period (Figure 2.4.5). Hemagglutinin in heat stressed vaccine (70°C / 100 min) as a negative control was not able to cross-link the erythrocytes. Erythrocyte sedimentations were observed in each well in the 2–fold dilution row from the start. HAI of lyophilizates demonstrated a consistent dilution of hemagglutinin (at 64 fold dilution), where the sedimentation of erythrocytes occurred as red dots at the bottom of the wells (Figure 2.4.5). Hemagglutination of erythrocytes took also place at a dilution of 64 fold in samples of cryo-milled lyophilizates. However, a slightly increased deviation was observed in cryo-milled lyophilizates (Figure 2.4.5A). Hemagglutinin showed consistently good biological activity over the time period of

six months and at different storage temperatures. Therefore, the stage of dilution where the hemagglutination could not be established, was similar as in the first sample at t_0 (64 fold dilution, equal to 0.23 µg/ml of hemagglutinin). The end point determined as red dots with sedimented erythrocytes were clearly distinguishable to the diffuse patch of erythrocyte in non-hemagglutinated wells.

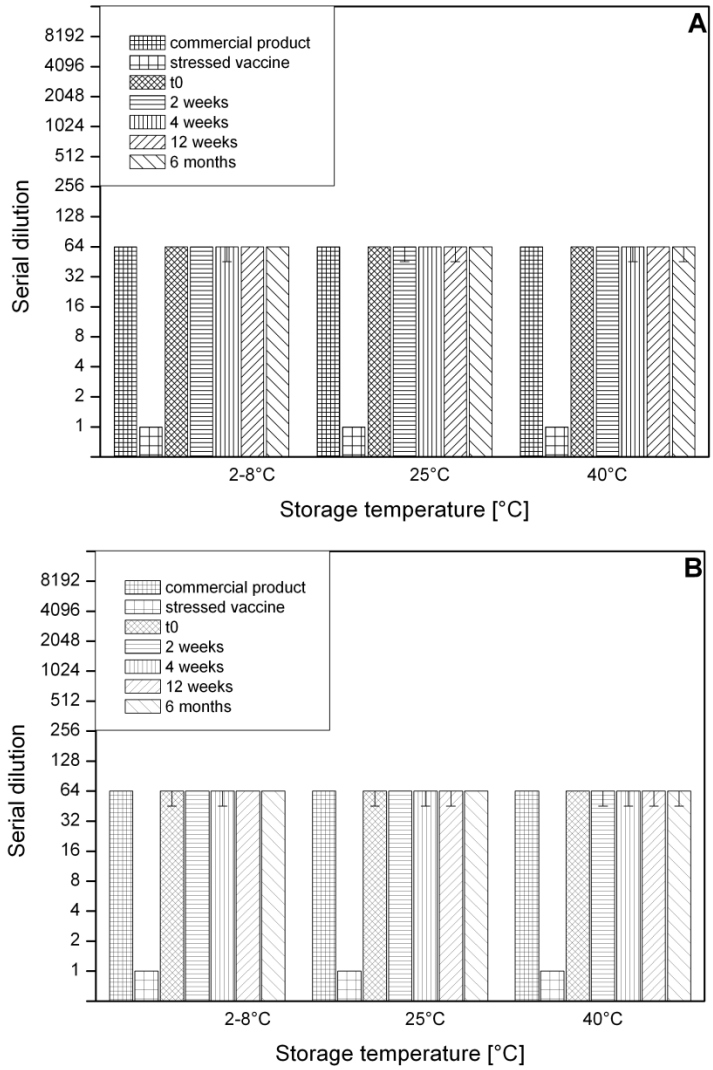

Figure 2.4.5: Results of hemagglutination inhibition assay of A) lyophilizates and B) cryo-milled lyophilizates at different storage temperatures and different time points. Three independent measurements were performed (n=3).

2.4.7 Determination of the residual moisture content

Generally, lyophilizates exhibited low residual moisture contents over time, reaching only 1.5% after 6 month at 40°C and approximately 1% for all other storage temperatures. Cryo-milled samples had 2-2.5% residual moisture after the milling. The residual moisture was below 3%, only at 40°C the residual moisture increased to 3.5% after storage (Figure 2.4.6).

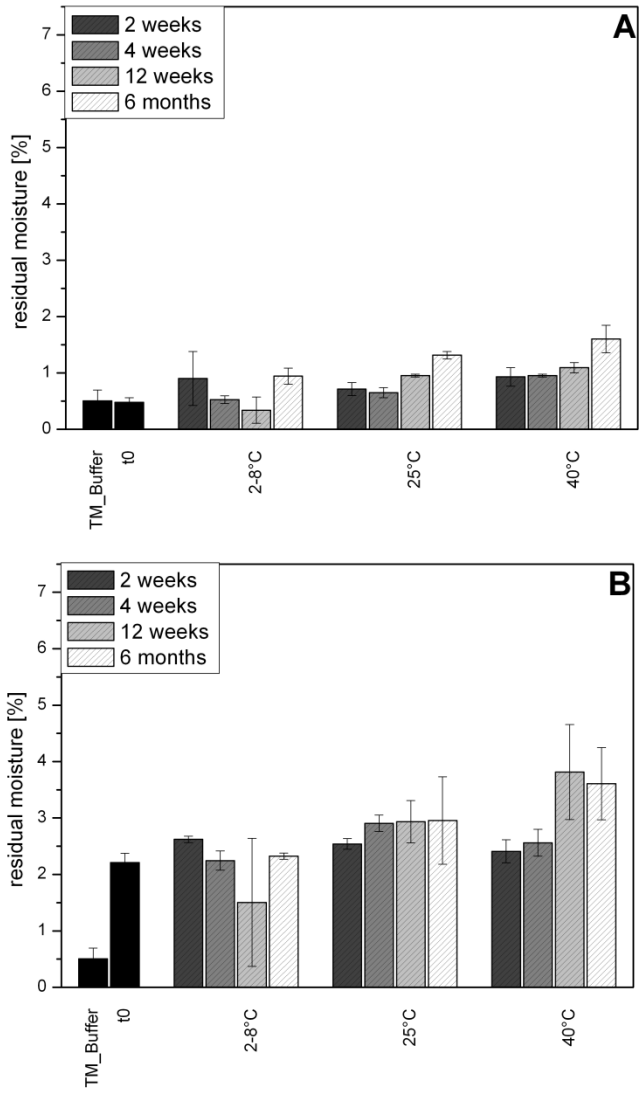

Figure 2.4.6: Residual moisture content of A) vaccine lyophilizates and B) cryo-milled vaccine lyophilizates stored at different storage temperatures and over a time period of six months. Three independent measurements were performed (n=3)

2.4.8 Scanning electron microscopy (SEM)

Electron microscopy was performed to confirm the structure of the collapse lyophilizate. Characteristic large pores for collapse lyophilizates were clearly detectable (Figure 2.4.7A and B) in the electron micrographs of lyophilizates. The surface was rough with sharp edges (Figure 2.4.7A and B). After cryo-milling, particles in the SEM micrographs of lyophilizates displayed the expected powder size between 20 µm and 80 µm but with a different surface morphology (Figure 2.4.7C and D). Distinguishing a single particle from formation of particle agglomerates was, however, not possible using SEM analysis.

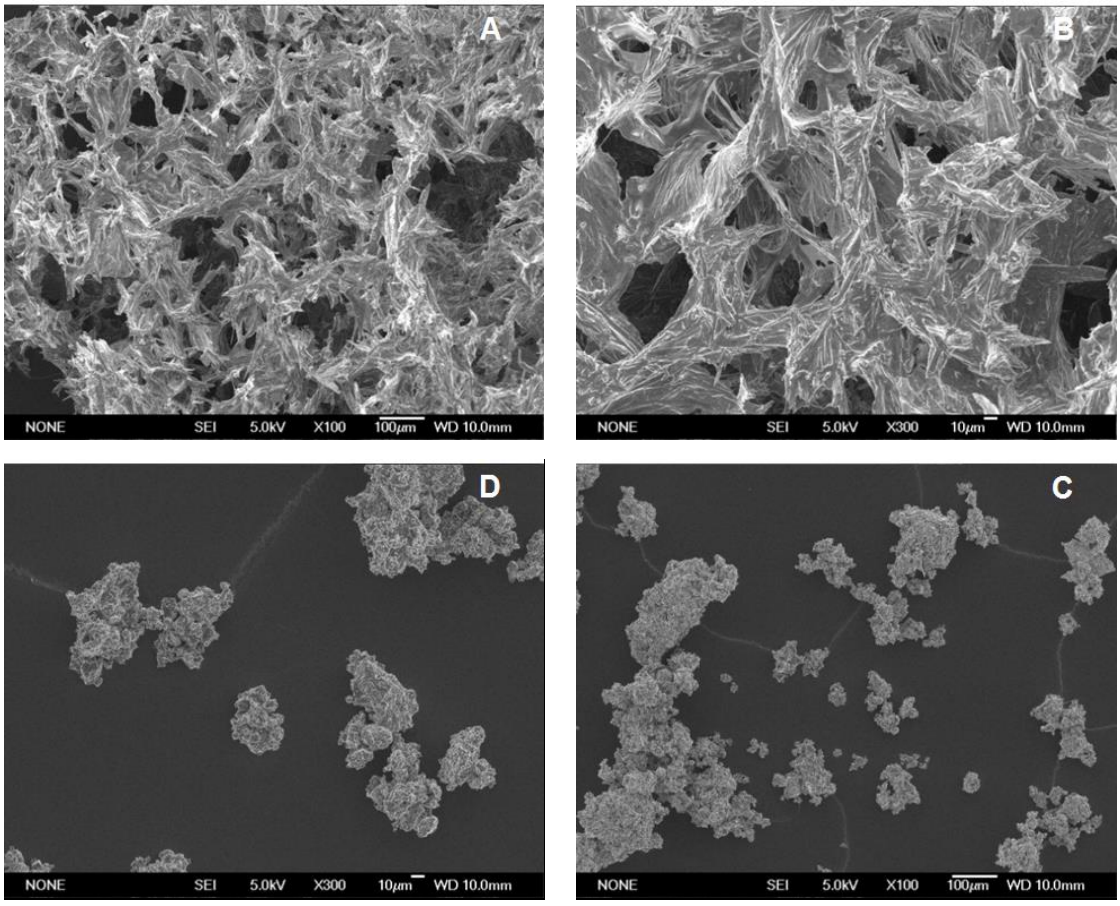

Figure 2.4.7: Scanning electron micrographs A and B) lyophilizates (A: magnification: 100 fold; B: magnification: 300 fold); C and D) cryo-milled lyophilizates (C: magnification: 100 fold; D: magnification: 300 fold).

2.4.9 Determination of the specific surface area (SSA)

Placebo collapse lyophilizates (carbohydrate solution) with trehalose-mannitol formulations (1:1) (w/w) and a 15% solid content (w/w) in a 10 mM phosphate buffer had a SSA of 0.5901 m²/g ± 0.0211 m²/g. Vaccine samples containing hemagglutinin demonstrated a lower SSA value compared to placebo samples (Table 2.4.2). The cryo-milling process increased the SSA almost to the value of non-ground placebo formulation.

Table 2.4.2: Specific surface area (SSA) results measured using a BET-method. Three independent measurements were performed (n=3).

Sample	**SSA [m^2/g]**	**Standard deviation [m^2/g]**
Trehalose:mannitol (1:1) 15% solid content (w/w)	0.5990	0.0211
Vaccine (trehalose:mannitol) 15% solid content [3.75 µg/mg]	0.2794	0.0482
Cryo-milled vaccine (trehalose:mannitol) 15% solid content [3.75 µg/mg]	0.5055	0.0627

2.5 Discussion

In this work, we aimed to stabilize influenza vaccine as a model for temperature sensitive vaccines using collapse lyophilization. We were able to demonstrate that influenza vaccine in lyophilizates, prepared by collapse lyophilization, showed a sufficient stability at different storage temperatures over a time period of six months.

The commercial vaccine and lyophilizates were characterized using RP-HPLC. Unexpectedly, RP-HPLC results did not reveal any alterations of the hemagglutinin structure (and/or function) induced by e.g. heat stress. All samples investigated showed comparable retention times and intrinsic fluorescence values. In contrast to this finding, the heat stressed samples lost their ability to cross-link erythrocytes which was supported by the HAI results.

Further results from the HAI assay demonstrated that preparation and storage of collapse lyophilized at different temperatures vaccine had no detectable impact on biological activity. Consistently, inhibition of hemagglutination was observed in samples over the time period of six months at any storage temperatures (2°C-8°C, 25°C and 40°C) up to dilutions of 1: 64. In addition, larger particles measured by light obscuration corresponding with less free and active hemagglutinin did not affect HAI results. Therefore, no reduction in biological activity of lyophilizates caused by formation of agglomerates was observed. Generally, counts of less than 6000 particle counts/ml > 1 µm can be considered as a low value for lyophilizates [86]. Moreover, counts of subvisible particles matched perfectly the requirements of Ph. Eur. In addition, constant turbidity results of reconstituted lyophilizates supported the findings of subvisible particle measurement (Table 2.4.1).

Electrophoretic assays were performed to gain more insight into the structure of the agglomerates. SDS-Page is a suitable method to determine alterations of hemagglutinin induced by e.g. preparation stress, storage time and/or temperature. Unchanged migration distance and estimated M_w of hemagglutinin subunits and/or oligomers (HA1, monomer, dimer and trimer) support our assumption that collapse lyophilisation did not introduce detrimental modifications to hemagglutinin structure. Slightly different intensities of the bands might be attributed to surface irregularities of SDS-Page gel and/or the imaging technique using a scanner. Fluctuations in band

intensities were also observed in Westernblot analysis. A shift from smaller (HA1 and monomer) to larger hemagglutinin oligomers (dimer and trimer) could be deducted from the increasing intensities of the dimer and trimer bands (Figure 2.4.3 and Figure 2.4.4) over the observed time period of six months. This also is in line with the results of light obscuration measurement.

Physico-chemical stability of the freeze-dried samples was investigated by assessing moisture content, SSA and microscopic characteristics of the final lyophilizates. Moisture in lyophilizates can support chemical and microbiological degradation and therefore reduce vaccine stability. The determined values of residual moisture of up to 1.5% for lyophilizates and 3% for cryo-milled lyophilizates are too low to affect lyophilizates integrity [29]. Collapse freeze-drying was performed to additionally reduce the SSA and to obtain more dense lyophilizates. SSA of the lyophilizates was measured directly after the collapse freeze-drying. The storage temperatures (2-8°C, 25°C, and 40°C) of lyophilizates were below T_g of the sugar matrix (trehalose:107°C ; mannitol 92°C) [30, 31]. While the storage temperature is below T_g, SSA of lyophilizate would not show a temperature induced alteration of the sugar matrix [32, 33]. However, the combination of storage temperature and residual moisture did not compromise the lyophilizate stability over a time period of six months.

Additionally, we prepared powder particles by cryo-milling for EPI. The range of 20-80 µm of powder particles was described and determined as sufficient to penetrate the skin without causing harm and pain [17, 34, 35]. Like the lyophilizates, cryo-milled samples were analyzed to determine the stability of the vaccine (hemagglutinin) and the stability of the powder particles. Stability can be compromised due to the additional cryo-milling step which leads to an increase of SSA. Nonetheless, comparable AUCs of the cryo-milled samples to lyophilizates were measured using RP-HPLC. However, the higher deviation of cryo-milled samples in fluorescence values indicated a thermodynamic process (data not shown). As described above, RP-HPLC was not suitable to determine any stress impact. Therefore, biological activity was assessed using HAI, which revealed a slower sedimentation of erythrocytes in samples of cryo-milled lyophilizates and a less clear distinction between diffuse erythrocyte patch and red hemagglutinated erythrocyte dot after the incubation time. The altered hemagglutination might have been induced by additional stress factors during the cryo-milling process as e.g. mechanical and freeze-thaw stress.

Agglomeration processes were observed in light obscuration measurements. Stress during cryo-milling led to larger particle formation and formations of agglomerates. Hemagglutinin-oligomers of the monomers/subunits (SDS-Page and Westernblot) were detected in the electrophoretic assays which could be a result of a combination of cryo-milling process and storage at high temperatures. The alteration of hemagglutinin could reduce the affinity of the specific anti-hemagglutinin antibody to the antigen or even prevent binding completely. Both causes can result in a diminishing or a lack of bands in Westernblot results.

Generally, we showed a successful stabilization of influenza vaccine using a fast and economic collapse lyophilization. Our technique appears to be capable of generating adequately stable hemagglutinin lyophilizates which can be stored at different temperatures (2 -8°C, 25°C and 40°C) and over a time period of up to six months. Collapse freeze-dried vaccine powder particles showed a high stability in the refrigerator (2 -8°C) or at ambient temperatures (25°C). Storage at 40°C resulted in a poorer stability of the antigen due to an increased alteration of hemagglutinin.

2.6 Conclusion

We have demonstrated that stabilization of influenza vaccine is possible using collapse lyophilization. In the future, this technique could enable a more economical distribution of stabilized vaccine to regions in which a cold chain system for liquid vaccines is hard to maintain. The stabilization of highly temperature sensitive hemagglutinin by an aggressive collapse lyophilization seems promising. Furthermore, the lyophilized vaccine demonstrated a high resistance against elevated storage temperatures compared to the commercial liquid vaccine formulation. The different storage temperatures (2-8°C, 25°C and 40°C) did not affect the stability of the lyophilized vaccine.

Although the stability of the powder particles was decreased compared to non-processed lyophilizates when stored at 40 °C, vaccine powder particles for EPI seemed to be stable at 2-8°C or ambient room temperature (25°C) storage.

High stability in combination with new developments in administration (EPI) could make vaccination more accessible and would close the gap between required and available vaccination.

2.7 Acknowledgments

This study was supported by a grant from the Federal Ministry of Education and Research, Germany, grant no. 13N11318. The authors would like to thank Christian Minke (Department of Chemistry, Ludwig-Maximilians-University Munich), for his assistance with electron microscopy and Prof. Dr. Stefan Zahler (Department of Pharmacy, Pharmaceutical Biology, Ludwig-Maximilians-University Munich) for his assistance with Westernblot analysis.

2.8 References

1. Scuffham, P.A. and P.A. West, *Economic evaluation of strategies for the control and management of influenza in Europe.* Vaccine, 2002. **20**(19–20): p. 2562-2578.

2. Hethcote, H.W., *An immunization model for a heterogeneous population.* Theoretical Population Biology, 1978. **14**(3): p. 338-349.

3. Coleman, P.G. and C. Dye, *Immunization coverage required to prevent outbreaks of dog rabies.* Vaccine, 1996. **14**(3): p. 185-186.

4. Guyer, B., et al., *Immunization coverage and its relationship to preventive health care visits among inner-city children in Baltimore.* Pediatrics, 1994. **94**(1): p. 53-58.

5. Layne, S.R., *Human influenza surveillance: the demand to expand.* Emerging Infectious Diseases, 2006. **12**(4): p. 562-568.

6. Schersch, K., et al., *Systematic investigation of the effect of lyophilizate collapse on pharmaceutically relevant proteins, part 2: stability during storage at elevated temperatures.* Journal of Pharmaceutical Sciences, 2012. **101**(7): p. 2288-2306.

7. Kis, E., G. Winter, and J. Myschik, *Can Collapse Freeze Drying Provide High Density Protein Sugar Particles for Ballistic Powder Injection?* Scientia Pharmaceutica, 2010. **78**: p. 653.

8. Schersch, K., et al., *Systematic investigation of the effect of lyophilizate collapse on pharmaceutically relevant proteins I: Stability after freeze-drying.* Journal of Pharmaceutical Sciences, 2010. **99**(5): p. 2256-2278.

9. Etzl, E.E., G. Winter, and J. Engert, *Toward intradermal vaccination: preparation of powder formulations by collapse freeze-drying.* Pharmaceutical Development and Technology, 2014. **19**(2): p. 213-222.

10. Loudon, P.T., et al., *GM-CSF increases mucosal and systemic immunogenicity of an H1N1 influenza DNA vaccine administered into the epidermis of non-human primates.* PloS One, 2010. **5**(6): p. e11021.

11. DeMuth, P.C., et al., *Vaccine delivery with microneedle skin patches in nonhuman primates.* Nature Biotechnology, 2013. **31**(12): p. 1082-1085.

12. DeMuth, P.C., et al., *Releasable Layer-by-Layer Assembly of Stabilized Lipid Nanocapsules on Microneedles for Enhanced Transcutaneous Vaccine Delivery.* ACS Nano, 2012. **6**(9): p. 8041-8051.

13. DeBenedictis, C., et al., *Immune functions of the skin.* Clinics in Dermatology, 2001. **19**(5): p. 573-585.

14. Bonifaz, L.C., et al., *In vivo targeting of antigens to maturing dendritic cells via the DEC-205 receptor improves T cell vaccination.* Journal of Experimental Medecine, 2004. **199**(6): p. 815-24.

15. Dean, H.J. and D. Chen, *Epidermal powder immunization against influenza.* Vaccine, 2004. **23**(5): p. 681-686.

16. Moingeon, P., C. de Taisne, and J. Almond, *Delivery technologies for human vaccines.* British Medical Bulletin, 2002. **62**(1): p. 29-49.

17. Mitragotri, S., *Immunization without needles.* Nature Reviews Immunology, 2005. **5**(12): p. 905-916.

18. Zambon, M.C., *Epidemiology and pathogenesis of influenza.* Journal of Antimicrobial Chemotherapy, 1999. **44**(suppl 2): p. 3-9.

19. Andreasen, V., *Dynamics of annual influenza A epidemics with immuno-selection.* Journal of Mathematical Biology, 2003. **46**(6): p. 504-536.

20. De Jong, J.C., et al., *Influenza virus: a master of metamorphosis.* Journal of Infection, 2000. **40**(3): p. 218-228.

21. Carrat, F. and A. Flahault, *Influenza vaccine: The challenge of antigenic drift.* Vaccine, 2007. **25**(39–40): p. 6852-6862.

22. Ryan, J., et al., *Establishing the health and economic impact of influenza vaccination within the European Union 25 countries.* Vaccine, 2006. **24**(47–48): p. 6812-6822.

23. Belshe, R.B., *Current status of live attenuated influenza virus vaccine in the US.* Virus Research, 2004. **103**(1–2): p. 177-185.

24. Taubenberger, J.K. and S.P. Layne, *Diagnosis of influenza virus: Coming to grips with the molecular era.* Molecular Diagnosis, 2001. **6**(4): p. 291-305.

25. Kommareddy, S., et al., *Preparation of highly concentrated influenza vaccine for use in novel delivery approaches.* Journal of Pharmaceutical Sciences, 2013. **102**(3): p. 866-875.

26. Cross, G., *Hemagglutination inhibition assays.* Seminars in Avian and Exotic Pet Medicine, 2002. **11**(1): p. 15-18.

27. Zambon, M.C. and J.S. Ellis, *Molecular methods for diagnosis of influenza.* International Congress Series, 2001. **1219**(0): p. 267-273.

28. Hawe, A., et al., *Pharmaceutical feasibility of sub-visible particle analysis in parenterals with reduced volume light obscuration methods.* European Journal of Pharmaceutics and Biopharmaceutics, 2013. **85**(3, Part B): p. 1084-1087.

29. Mohammed, A.R., et al., *Lyophilisation and sterilisation of liposomal vaccines to produce stable and sterile products.* Methods, 2006. **40**(1): p. 30-38.

30. Crowe, L.M., D.S. Reid, and J.H. Crowe, *Is trehalose special for preserving dry biomaterials?* Biophysical Journal, 1996. **71**(4): p. 2087-2093.

31. Kim, A.I., M.J. Akers, and S.L. Nail, *The physical state of mannitol after freeze-drying: Effects of mannitol concentration, freezing rate, and a noncrystallizing cosolute.* Journal of Pharmaceutical Sciences, 1998. **87**(8): p. 931-935.

32. Wang, W., *Lyophilization and development of solid protein pharmaceuticals.* International Journal of Pharmaceutics, 2000. **203**(1–2): p. 1-60.

33. Heljo, V., et al., *The Effect of Water Plasticization on the Molecular Mobility and Crystallization Tendency of Amorphous Disaccharides.* Pharmaceutical Research, 2012. **29**(10): p. 2684-2697.

34. Smalls, L.K., R. Randall Wickett, and M.O. Visscher, *Effect of dermal thickness, tissue composition, and body site on skin biomechanical properties.* Skin Research and Technology, 2006. **12**(1): p. 43-49.

35. Partidos, C.D., *Delivering vaccines into the skin without needles and syringes.* Expert Review of Vaccines, 2003. **2**(6): p. 753-61.

3. Chapter - Stability of lyophilized influenza vaccine under long-term storage conditions and in presence of oily components

3.1 Introduction

Storage stability emerges as a major issue during the development of vaccine formulations. In order to achieve long term stability during storage, liquid vaccines are normally stored at 2-8°C due to an accelerated degradation or protein inactivation at temperatures outside this range. These temperature-dependent limitations make cost-intensive cold-chain storage and distribution mostly mandatory, which is why new strategies for vaccine stabilization are becoming increasingly important to stabilize the product such as transferring the liquid vaccine into a dry state [1-4]. This principle can avoid or at least reduce water and temperature triggered protein degradation [5].

This work focused on the stabilization of a model vaccine using freeze-drying. In general, proteins can be stabilized and freeze-dried using lyoprotectants and cryoprotectants during the cycle [6]. In order to optimize the process, a more aggressive collapse lyophilization cycle was implemented to stabilize a thermo-sensitive model vaccine and to reduce the specific surface area (SSA) simultaneously [7-10]. A lower SSA was targeted to obtain more dense lyophilizates which could be ground into dense and hard lyophilizate particles. These stable vaccine particles could provide a vehicle for new and easy to handle vaccine administrations technologies. The skin could be targeted as an easily accessible tissue to administer the vaccine particles using the concept of epidermal powder immunization (EPI). New studies have shown a high potential of improved immune response after skin vaccination [11-18]. Using EPI, stable particles could be administered through the mechanical barrier (stratum corneum) into the epidermis to address the vaccine to the located antigen presenting cells (APCs) and induce a sufficient immune response. The stabilized vaccine using collapse freeze-drying and new minimal-invasive and easy handled administration strategies (e.g.: EPI) could prevent a fast spreading of the influenza disease [19]. Furthermore, the minimally invasive skin vaccination induce less pain and bleedings compared to the conventional intramuscular (i.m.) injection and could improve patient compliance and could eliminates the risk of disease transmission [20, 21].

Influenza vaccine was chosen as the model vaccine because of its high thermo-sensitivity to monitor the impact of heat induced degradation [22-25]. Monitoring the sensitive influenza model vaccine, incorporated into a carbohydrate matrix, could

reveal induced degradations during the preparation, stabilization and storage at different storage temperatures (2-8°C, 25°C and 40°C) over a time period of 12 months. As previously described (**Chapter 2**), a set of analytics was established to characterize the stability and activity of the vaccine, such as the hemagglutination inhibition assay (HAI), SDS-Page and westernblot analysis, subvisible particle measurements, reversed-phase liquid chromatography (RP-HPLC), and the residual moisture assay.

The effects of adjuvants in vaccines should also be considered. Generally, adjuvants are mixed with the vaccines prior to application to induce an improved and/or moderated immune response, to reduce the needed antigen amount, and/or a superfluous booster application [26, 27]. The stabilized model vaccine (Pandemrix®, GlaxoSmithKline, Rixensart, Belgium) is administered with the adjuvant AS03. In order to provide the adjuvant advantages to the new administration technology (EPI), the vaccine was characterized in presence of the adjuvant and its oily components (DL-α-tocopherol, polysorbat 80, squalene, and paraffin).

In this study, we demonstrate a successful stabilization and characterization of a thermo-sensitive model influenza vaccine for epidermal powder immunization over a time period of 12 months and a characterization of the vaccine in presence of oily components.

3.2 Material and Methods

3.2.1 Materials

In addition to the materials described in **Chapter 2**, H1N1 influenza vaccine (Pandemrix®, GlaxoSmithKline, Rixensart, Belgium), sodium hydrogen phosphate monohydrate (Gruessing, Filsum, Germany), sodium dihdydrogen phosphate dehydrate, sodium phosphate monobasic and dibasic, sodium hydroxide, and sodium chloride (Applichem, Darmstadt, Germany), trehalose (VWR, Ismaning, Germany), mannitol (Boehringer Ingelheim, Ingelheim, Germany), the following materials were used: the adjuvant AS03 of the H1N1 influenza vaccine (Pandemrix®, GlaxoSmithKline, Rixensart, Belgium) containing squalene, DL-α- tocopherol, and polysorbate 80 is normally mixed with the vaccine prior to administration. In order to determine the vaccine stability in presence of oily components, the vaccine was mixed with the adjuvant (AS03) or with the oily ingredients of AS03 DL-α-tocopherol, polysorbat 80, and squalene, which were purchased from Sigma-Aldrich (Taufkirchen, Germany) and paraffin (100 cSt) was obtained from Merck KGaA (Darmstadt, Germany).

3.2.2 Methods

The preparation of lyophilizates and lyophilizate particles using the tangential flow filtration (TFF), the determination of concentration and adjustment of the vaccine concentration using RP-HPLC, the collapse freeze-dry cycle, and cryo-milling were previously described in detail in **Chapter 2.**

Furthermore, the characterization of the vaccine and the lyophilizate stability (reconstituted with 2.23 ml highly purified water to obtain 7.5 µg HA/0.5 ml) under storage conditions of 2-8°C, 25°C, and 40°C at ambient humidity (65-80%) over a time period of 12 month was performed using the same assays as described in **Chapter 2**.

The following analytics were used in particular: residual moisture content determination by Karl-Fischer titration, reversed-phase liquid chromatography (RP-

HPLC), light obscuration measurements, turbidity measurements, sodium dodecyl sulphate-polyacrylamide gel electrophoresis (SDS-Page), westernblot analysis, and the hemagglutination inhibition assay (HAI).

3.2.2.1 Determination of vaccine stability in presence of oily components (AS03, oily components of AS03, and paraffin) using HAI

In order to determine the stability of the vaccine in presence of oily components, the commercial product (H1N1 vaccine) and/or the reconstituted lyophilizate was mixed with the adjuvant (AS03), oily components of AS03, or paraffin. The oily part of the adjuvant (AS03) consisted of 27.41 mg/dose (0.5 ml) and was comprised of 10.69 mg squalene, 11.86 mg DL-α- tocopherol, and 4.86 mg polysorbate 80. In order to determine the impact of the oily substances to the vaccine stability during the fixation with the oily components on the intradermal powder applicator, each solution, commercial product (CP) (7.5 µg/0.5 ml) or reconstituted lyophilizate (7.5 µg/0.5 ml), was mixed with 27.41 mg of the adjuvant (paraffin) or proportionally to the oily components (squalene, DL-α-tocopherol or polysorbate 80).

In contrast to the final application using the vaccine applicator, where lyophilized vaccine particles were fixed with oily components, vaccine stability characterization in the presence of oily components was performed with vaccine solutions to maximize the contact and interaction between vaccine and adjuvant. The experiments to determine the stability were based on separation (RP-HPLC) or agglutination (hemagglutination inhibition assay) in a liquid environment.

The impact of AS03 (or the oily components) on the assay was determined by the addition of AS03 to 10 mM PBS buffer instead of the vaccine solution while the robustness of the assay in presence of the oily components was characterized by mixing paraffin into the vaccine solution.

Due to the high portion of oily components (up to 27.41 mg/0.5 ml) compared to the low vaccine dose (7.5 µg/0.5 ml) and the impact on the assay, the separation of the oily components was performed using a centrifuge at 10000 rpm (Sigma 4K15, Sigma Zentrifugen, Osterode am Harz, Germany) for 15 minutes. The liquid parts were extracted using a pipette after the phase separation had taken place. These steps were

repeated 10 times in order to separate as many oily components as possible from the mixture to minimize the impact of the oily components to the assay.

3.2.2.2 Determination of vaccine stability in presence of oily components (AS03, oily components of AS03, and paraffin) using RP-HPLC

In order to characterize the vaccine stability, the oily components and the vaccine in presence of the oily components were determined using RP-HPLC as previously described in **Chapter 2**. Samples (commercial product, reconstituted lyophilizate, and PBS buffer) were mixed with the oily components as described above (**Chapter 3.2.2.1**) and 25 µl of each sample was injected, separated using a reversed phase Phenomenex Jupiter 5 µ, C18, 300 A column (250 x 4.6 mm) (Phenomenex, Aschaffenburg, Germany), and detected using the intrinsic fluorescence of hemagglutinin at λ_{ex} 280 nm and λ_{em} 335 nm.

The samples mixed with the oily components were collected and were compared with the heat stressed control vaccine (70°C/100 min) and the commercial product solution stored at 2-8°C. Data acquisition and analysis were performed using the Chromeleon 6.80 software (Dionex, Idstein, Germany).

3.3 Results

3.3.1 Hemagglutinin (HA) quantification using RP-HPLC

The determination of the HA content within the samples using the intrinsic fluorescence was performed using RP-HPLC. The retention time of HA at approximately 17.40 min ± 0.15 min was still unchanged for the storage samples at time point T5 (12 months) compared to the prior time points (t0, 2, 4, 12 weeks, and 6 months) and the commercial product described in **Chapter 2 (**Figure 3.3.1A and B). Nonetheless, a second peak for the cryo-milled lyophilizates stored at 40°C was observed at 19.42 min ± 0.09 min with an area under the curve (AUC) of 18.25 mV*min ± 9.1 min (Figure 3.3.1C). The results of the lyophilizates indicated uninfluenced storage stability while the cryo-milled samples demonstrated an alteration at high storage temperature (40°C) over 12 months. Similar protein peaks and fluorescence values were also observed for the stressed vaccine which demonstrated degraded vaccine as previously described in **Chapter 2**.

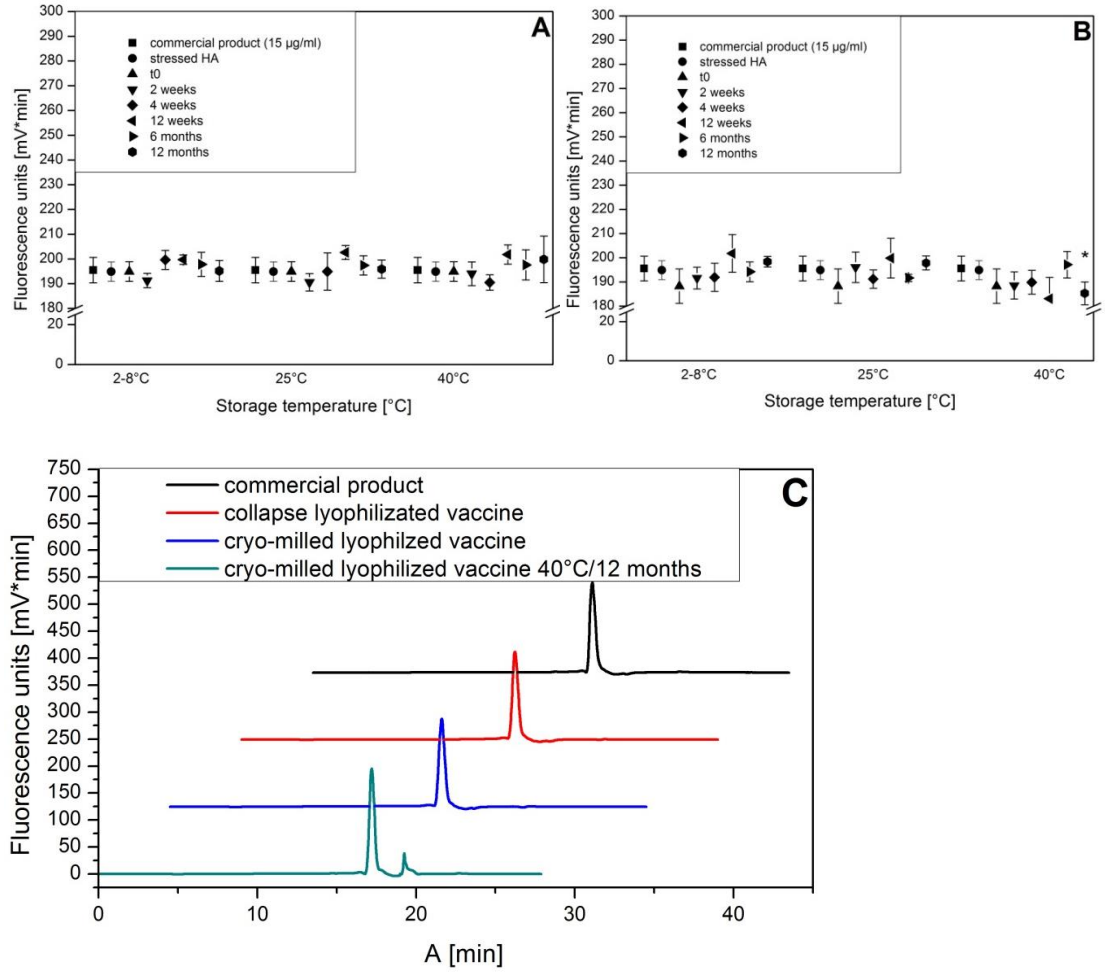

Figure 3.3.1: A) Fluorescence units of the commercially available product (15 µg/ml), stressed vaccine (15 µg/ml), and collapse lyophilized vaccine (15 µg/ml) after 12 months of storage at 2-8°C, 25°C, and 40°C. B) Fluorescence units of the commercially available product (15 µg/ml), stressed vaccine (15 µg/ml), and cryo-milled lyophilizates (15 µg/ml) after 12 months of storage at 2-8°C, 25°C, and 40°C). C) Chromatograms of cryo-milled lyophilized vaccine ($t_{12months}$/40°C) and comparison to commercial product, lyophilized vaccine (t_0) and cryo-milled lyophilizate (t_0) (second peak: RT: 19.42 min; AUC 18.25 mV*min ± 9.1 min). Three independent measurements were performed (n=3)

3.3.2 Light obscuration measurements

The freeze-dried samples were reconstituted and adjusted with highly purified water (2.625 ml) to a final concentration of 15 µg/ml. Vaccine alterations could induce formations of larger, particle forming aggregates, which could be determined using light obscuration measurements. In order to compare the degree of alteration, induced by the storage conditions over the observed storage time period, samples were compared to the results of the vaccine-carbohydrate solution (prior to lyophilization)

(15 µg/ml) stored at 2-8°C, the stressed vaccine (70°C/100 min, 15 µg/ml) stored at 2-8°C and the 0.22 µm filtered trehalose-mannitol solution. The results of the subvisible particle measurements > 1 µm, > 10 µm, and > 25 µm are shown in Figure 3.3.2

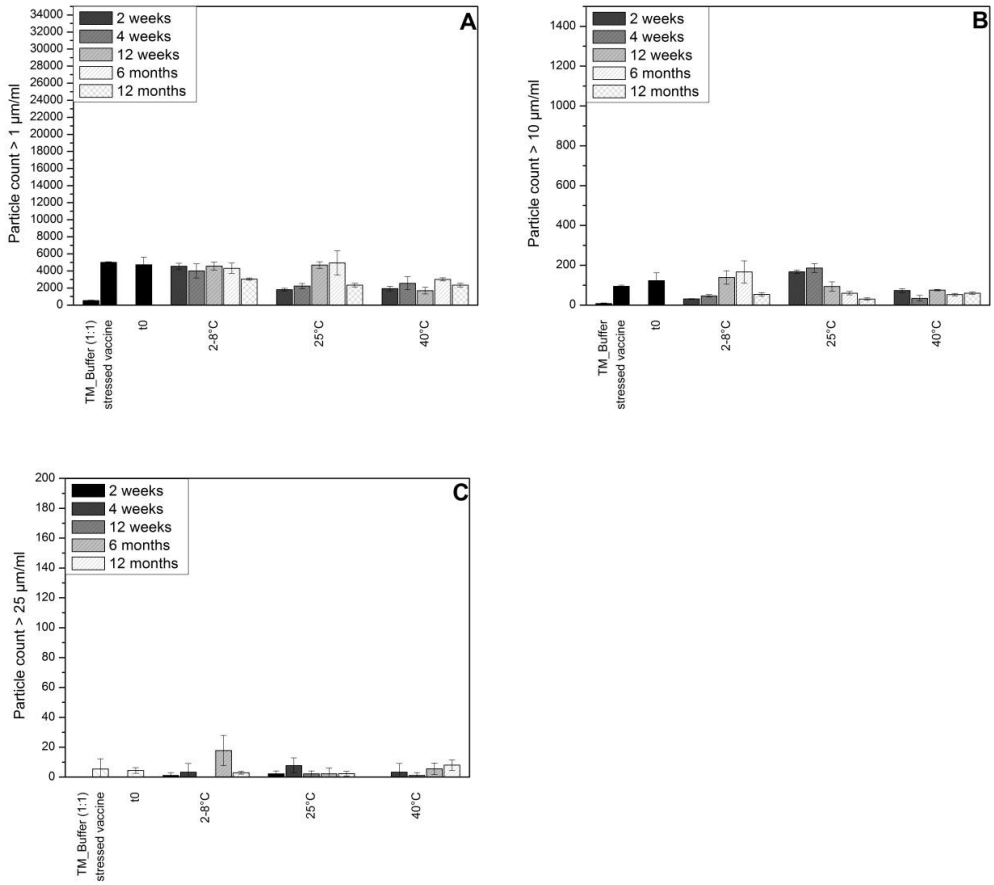

Figure 3.3.2 A) Subvisible particles > 1 µm of vaccine lyophilizates B) subvisible particles > 10 µm of lyophilizates C) subvisible particles > 25 µm of vaccine lyophilizates stored at different storage temperatures and over a time period of 12 months. Three independent measurements were performed (n=3) for comparison of the buffer solution, the stressed vaccine (70°C/100min) and the lyophilizate

The particle count > 1 µm of the lyophilizates increased slightly up to 3058 counts/ml ± 132 counts/ml while the cryo-milled samples resulted in a 5-8 fold higher count of approximately 24636 counts/ml ± 350 counts/ml compared to the commercial product with only 2754 counts/ml ± 40 counts/ml. Nevertheless, in all samples particle counts > 10 µm were below 600 counts/container (DIN 10R vial), which is in line with the requirements by the European Pharmacopoeia (Ph. Eur. 2.9.19). The threshold of 600 counts/containment (DIN 10R vial) was only exceeded by the cryo-milled samples stored at 40°C/6 months at 779 counts/ml ± 21 counts/ml which stabilized below 600 counts/ml at time point T5.

Moreover, the results of the cryo-milled samples demonstrated an opposed trend for particle counts > 1µm compared to particles > 10µm, particularly samples stored under 40°C conditions. Noteworthy was an increase of particle counts > 10 µm up to a storage period of 6 months (779 counts/ml ± 21 counts/ml) followed by a drop after 12 months (400 counts/ml ± 10 counts/ml). At the same time a leap of particle counts > 1 µm was observed from 7301 counts/ml ± 424 counts/ml to 24636 counts/ml ± 350 counts/ml for the (same) samples stored at 40°C (Figure 3.3.3:A and B).

Thus, comparable to the particle counts > 1 µm, a low count of particles > 25 µm was observed for the lyophilizates, while cryo-milled samples resulted in 5-7 fold higher particle counts (Figure 3.3.2C and Figure 3.3.3C).

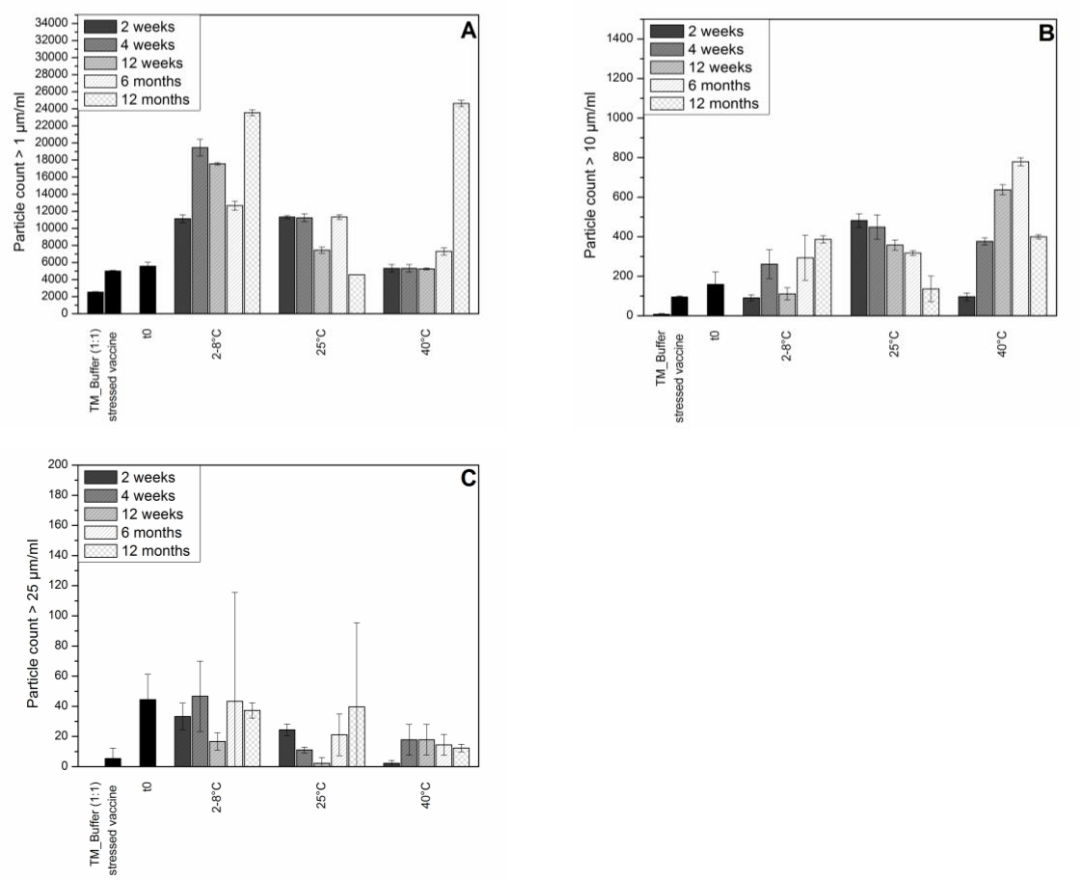

Figure 3.3.3: A) Subvisible particles > 1 µm of cryo-milled lyophilizates B) subvisible particles > 10 µm of cryo-milled lyophilizates C) subvisible particles > 25 µm of cryo-milled lyophilizates stored at different storage temperatures and over a time period of 12 months. Three independent measurements were performed (n=3) for comparison of the buffer solution, the commercial product, the stressed vaccine (70°C/100min) and the lyophilizate

3.3.3 Turbidity measurements

As demonstrated in **Chapter 2** for the turbidity results after 6 month of storage, the lyophilizates showed still a constant turbidity (Figure 3.3.4 and Table 3.3.1) while an increased turbidity over the time was observed for the cryo-milled samples. The lyophilization process induced an increase of turbidity compared to the commercial product or only heat stressed vaccine solution. While the turbidity of cryo-milled samples started at the same turbidity level as the lyophilized samples, the increase over the time might be a result of formations of small particle agglomerates. These trends continued for the samples stored for 12 months. The leap of particle counts for the cryo-milled lyophilizates stored at 40°C/12 months was reflected in the turbidity results for these samples. It should be kept in mind that the turbidity results of cryo-milled samples stored at 2-8°C and 25°C were only 1-2 FNU (Formazine Nephelometric Units) higher than the unmilled lyophilizates.

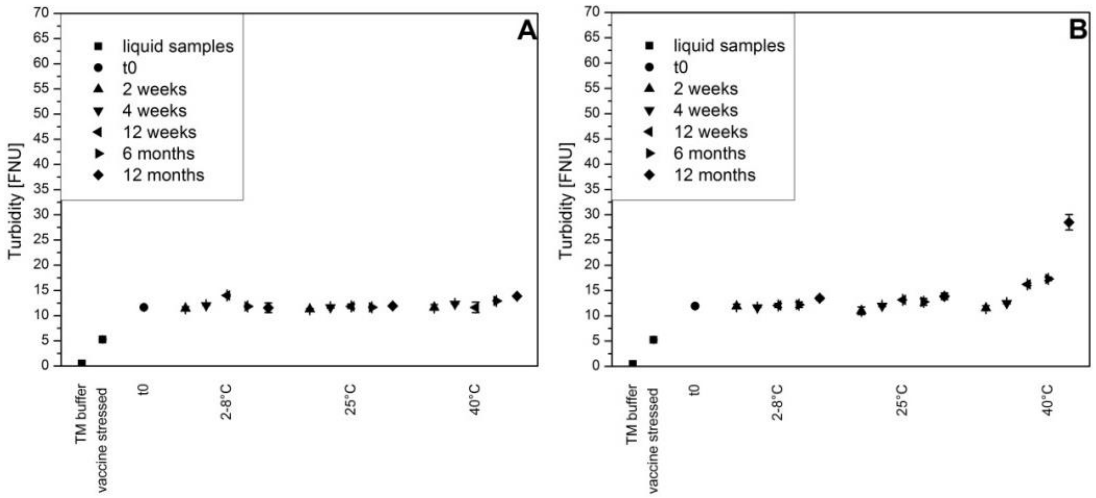

Figure 3.3.4: Turbidity of A) vaccine lyophilizates and B) cryo-milled lyophilizates stored at different storage temperatures and over a time period of 12 months. Three independent measurements were performed (n=3). To compare the stored samples, turbidity measurements of the buffer solution, the commercial product, and the stressed vaccine (70°C/100min) were additionally performed.

Table 3.3.1: Detailed turbidity results of the buffer solution, the commercial product, the stressed vaccine (70°C/100min), the vaccine lyophilizates, and the cryo-milled lyophilizates stored at different storage temperatures and over a time period of 12 months. Three independent measurements were performed (n=3).

Sample	Storage temperature [°C]	Turbidity [FNU]	Deviation [FNU]	Time point
Trehalose-mannitol buffer	2-8	0.50	±0.01	All time points
Commercial product	2-8	3.11	±0.02	All time points
Vaccine stressed (70°C/100min)	2-8	5.27	±0.08	
Lyophilizate		11.56	±0.14	t0
Lyophilizate	2-8	11.43	±0.33	2 weeks
Lyophilizate	2-8	12.07	±0.04	4 weeks
Lyophilizate	2-8	14.01	±0.16	12 weeks
Lyophilizate	2-8	11.84	±0.15	6 months
Lyophilizate	2-8	11.55	±0,96	12 months
Lyophilizate	25	11.27	±0.15	2 weeks
Lyophilizate	25	11.66	±0.18	4 weeks
Lyophilizate	25	11.85	±0.45	12 weeks
Lyophilizate	25	11.66	±0.10	6 months
Lyophilizate	25	11.93	±0.22	12 months
Lyophilizate	40	11.64	±0.56	2 weeks
Lyophilizate	40	12.32	±0.06	4 weeks
Lyophilizate	40	11.63	±1.04	12 weeks
Lyophilizate	40	12.92	±0.06	6 months
Lyophilizate	40	13.86	±0.15	12 months
Cryo-milled	2-8	11.89	±0.45	2 weeks
Cryo-milled	2-8	11.67	±0.02	4 weeks
Cryo-milled	2-8	12.07	±0.42	12 weeks
Cryo-milled	2-8	12.21	±0.55	6 months
Cryo-milled	2-8	13.48	±0.35	12 months

Table 3.3.3.1 continued

Sample	Storage temperature [°C]	Turbidity [FNU]	Deviation [FNU]	Time point
Cryo-milled	25	11.01	±0.74	2 weeks
Cryo-milled	25	11.99	±0.17	4 weeks
Cryo-milled	25	13.18	±0.06	12 weeks
Cryo-milled	25	12.78	±0.67	6 months
Cryo-milled	25	13.87	±0.66	12 months
Cryo-milled	40	11.54	±0.47	2 weeks
Cryo-milled	40	12.53	±0.14	4 weeks
Cryo-milled	40	16.24	±0.23	12 weeks
Cryo-milled	40	17.32	±0.35	6 months
Cryo-milled	40	28.50	±1.51	12 months

3.3.4 Sodium dodecyl sulfate-Polyacrylamide gel electrophoresis (SDS-Page)

While hemagglutinin (HA) is composed of two subunits (HA1 M_w of approximately 55 kDa and HA2 M_w of approximately 25 kDa), the monomer HA (M_w of 75 - 80 kDa) can aggregate to a dimer (M_w of 150 - 160 kDa) or a trimer (M_w of approximately 210 kDa). In order to characterize the integrity of hemagglutinin during the storage period of up to 12 months, an electrophoretic separation (SDS-Page) was also performed. Changes of intensity and the shares of the different states of HA (monomer, dimer, and trimer) can be observed within 12 months of storage compared to the starting point at t0 (Figure 3.3.5C). While the results of the lyophilizates showed slight changes independent of the storage temperature, a trend of agglomerate formations was observed for the cryo-milled samples. The cryo-milled lyophilizates stored at 40°C/12 months formed large visible agglomerates in the well which limited the migration through the gel (Figure 3.3.5B). Moreover, only pale bands in the dyed gel could be detected in these samples (40°C/12 months) for the different states of HA. Thus, minor alteration of band intensities and distribution were observed in the SDS-

Page gels for the cryo-milled lyophilizates stored at lower temperatures (2-8°C and 25°C) compared to t0 or the lyophilizates (2-8°C, 25°C, and 40°C).

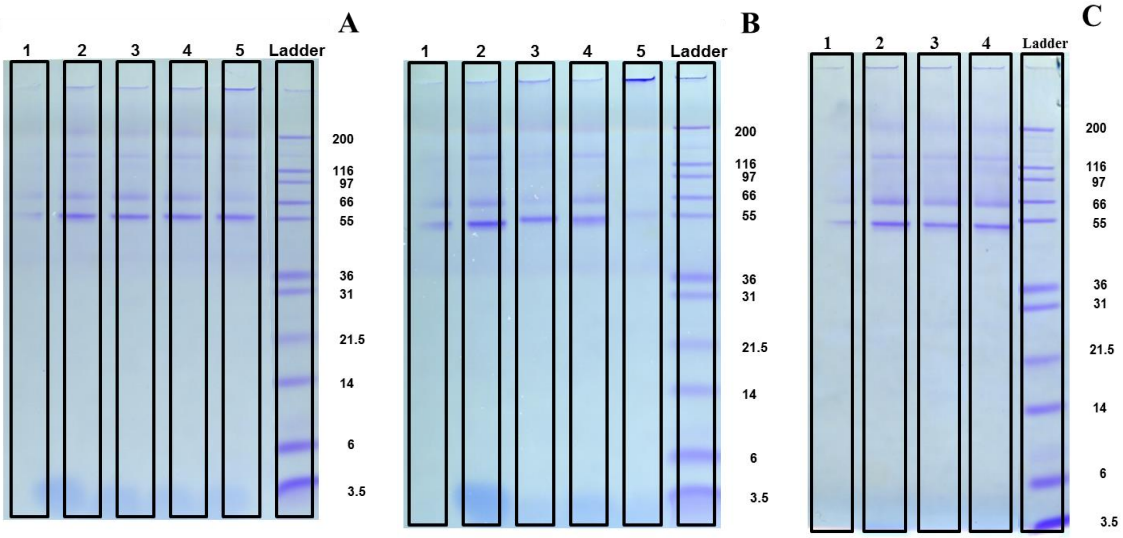

Figure 3.3.5: SDS-Page results after 12 months of storage A) lyophilizate and B) cryo-milled samples at different storage temperatures. Column A1, B1 and C1) commercial product; column A2 and B2) liquid pre-lyophilizate-carbohydrate formulation; A3) lyophilizate stored at 2-8°C; A4) lyophilizate stored at 25°C; A5) lyophilizate stored at 40°C; B3) cryo-milled lyophilizate stored at 2-8°C; B4) cryo-milled lyophilizate stored at 25°C; B5) cryo-milled lyophilizate stored at 40°C; C2) lyophilizate; C3) cryo-milled lyophilizate; and C4) liquid pre-lyophilizate formulation.

3.3.5 Westernblot analysis

While performing westernblot analysis, changes of structural integrity and antigenicity of hemagglutinin in the H1N1 vaccine could be determined more precisely due to a magnification of band intensities induced by the formation of antigen-antibody-complexes. In contrast to the westernblot results of the lyophilizates after six months of storage (demonstrated in **Chapter 2**) the lyophilizates stored at 40°C and the cryo-milled samples stored at 2-8°C and 25°C resulted in blurred band boundaries. Moreover, a tendency to larger agglomerates from monomer to dimer or trimer were detected in both groups (lyophilizates and cryo-milled samples) compared to the band intensities at the starting point t0 (Figure 3.3.6C). In addition, a complete lack of bands was observed for cryo-milled lyophilizates stored at 40°C/12 months (Figure 3.3.6B).

Nonetheless, the detected bands of HA independent of the state (monomer, dimer, and trimer) were at the predicted M_w on the scans (Figure 3.3.6).

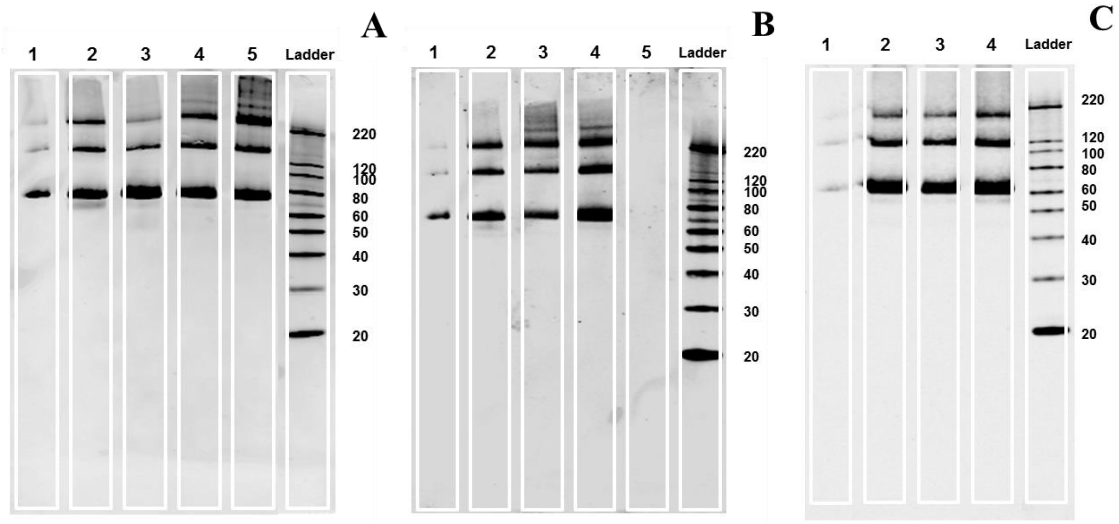

Figure 3.3.6: A) Westernblot results after 12 months of storage A) lyophilizate, B) cryo-milled samples at different storage temperatures and C) samples at t0. Column A1, B1 and C1) commercial product; column A2 and B2) liquid pre-lyophilizate- carbohydrate formulation; A3) lyophilizate stored at 2-8°C; A4) lyophilizate stored at 25°C; A5) lyophilizate stored at 40°C;; B3) cryo-milled lyophilizate stored at 2-8°C; B4) cryo-milled lyophilizate stored at 25°C; B5) cryo-milled lyophilizate stored at 40°C;.C2) lyophilizate; C3) cryo-milled lyophilizate; and C4) liquid pre-lyophilizate formulation.

3.3.6 Hemagglutination inhibition assay (HAI)

Consistent results were observed for the reconstituted lyophilizates and cryo-milled lyophilizates independent of storage temperatures or time period (Figure 3.3.7). The sedimentation of the erythrocytes took place at the 64 fold serial dilution. Yet, the sedimentation at a 64 fold dilution corresponded to 0.23 µg/ml of hemagglutinin. While the heat stressed hemagglutinin (70°C/100 min) was no longer able to cross-link the erythrocytes due to heat-induced degradation, the sedimentation occurred in the first well of the 2 fold serial dilution row. However, an increased incidence of deviation could be observed for the cryo-milled samples, particularly at higher storage temperature during the time period of 12 months (Figure 3.3.7B versus A). The end points could visually be determined as red dots consisting of the sedimented erythrocytes and could be distinguished to the diffuse patch of erythrocyte in non-hemagglutinated wells.

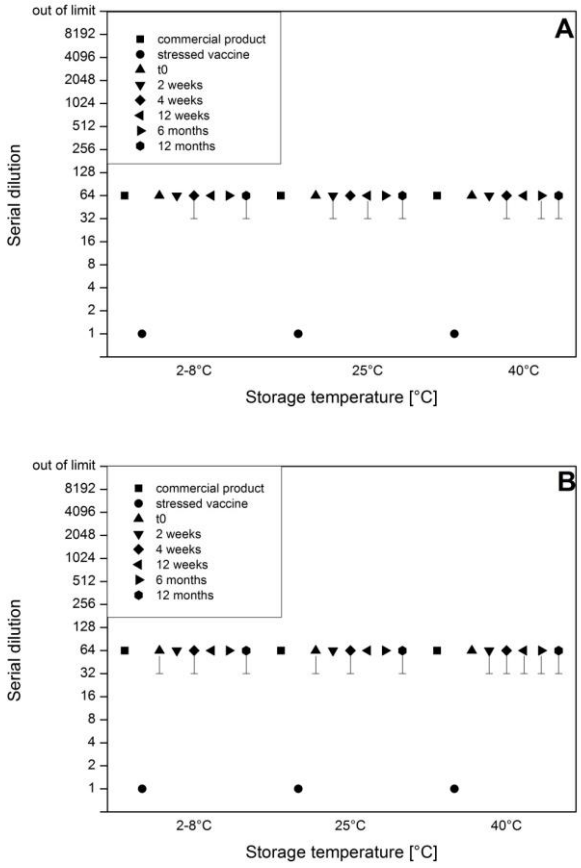

Figure 3.3.7: Results of the hemagglutination inhibition assay of A) lyophilizates and B) cryo-milled lyophilizates at different storage temperatures and different time points. Three independent measurements were performed (n=3).

3.3.7 Determination of the residual moisture content

As previously described in **Chapter 2**, results of the residual moisture content of lyophilizates stabilized at a value < 1.5% while the cryo-milled samples exhibited with a 2-3 fold higher value after a time period of 12 months. Nevertheless, the residual moisture content of the cryo-milled lyophilizates plateaued < 3.5% after at the last time point (t5, 12 months) of storage (Figure 3.3.8).

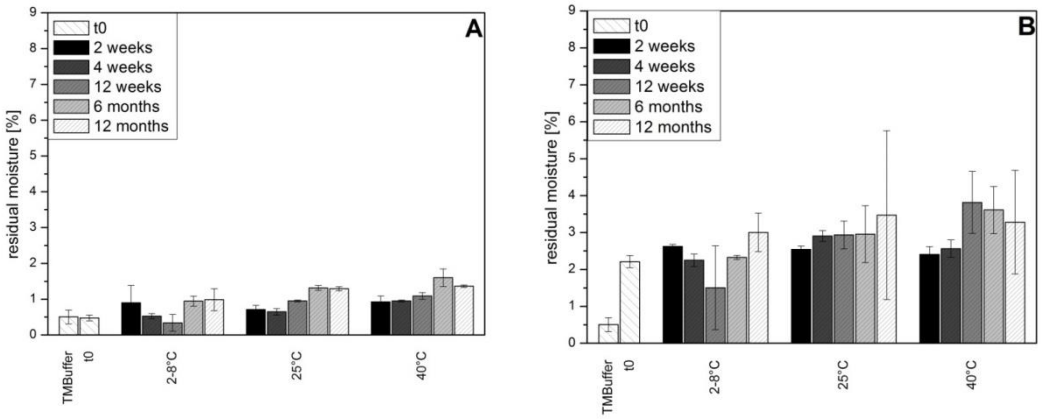

Figure 3.3.8: Residual moisture content of A) vaccine lyophilizates and B) cryo-milled vaccine lyophilizates stored at different storage temperatures and over a time period of 12 months. Three independent measurements were performed (n=3)

3.3.8 Determination of vaccine stability in presence of oily components (AS03, oily components of AS03, and paraffin) using HAI

Vaccine stability determinations in presence of oily components using the hemagglutination inhibition assay were unexpectedly of poor quality and had conflicting results. Samples mixed with oily components deviated between three dilution steps while samples with non-extracted AS03 (or oily components) without using centrifugation and separation of the oily components reached the limitation of the assay at > 4096 fold dilution (Figure 3.3.9). Moreover, after an extraction of AS03 (oily components) using centrifugation and separation of the oily components from the aqueous solution plateaued at 128 fold dilution independent of a presence of hemagglutinin (PBS buffer+AS03+extraction versus CP+AS03+extraction). The sedimentation of the erythrocytes should occur directly at the first well in a mixture without hemagglutinin, while the hemagglutination should be delayed to a higher dilution step in presence of hemagglutinin (64 fold serial dilutions). Unexpectedly, some oily components added to the commercial product (squalene and paraffin), induced a prior erythrocyte sedimentation than the anticipated hemagglutination at

64 fold serial dilution where the hemagglutination of the commercial product occurred. Furthermore, separately tested oily components revealed Polysorbate 80 as the main element which caused the delayed or rather inhibited erythrocyte sedimentation.

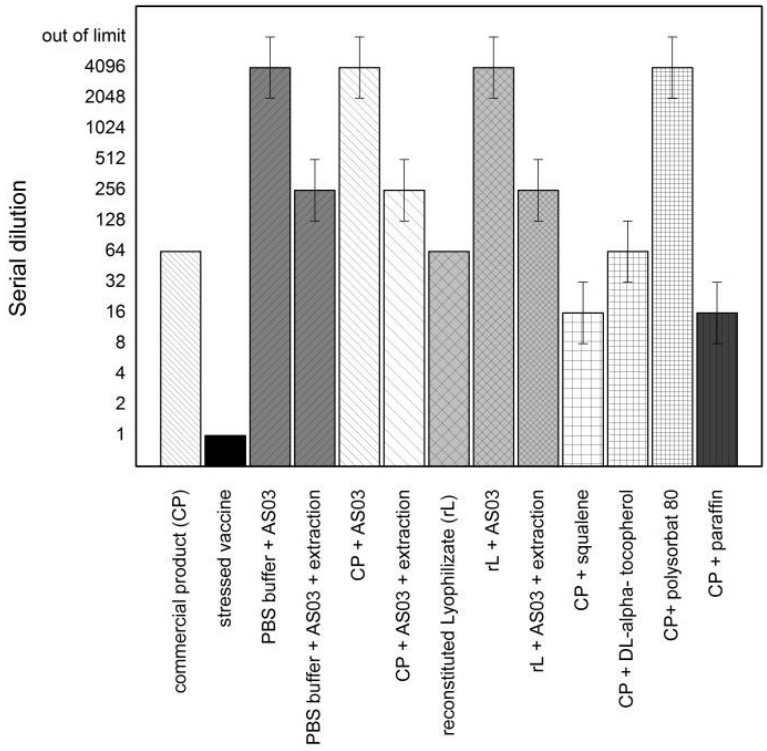

Figure 3.3.9: Results of the hemagglutination inhibition assay of samples (commercial product, reconstituted lyophilizates, and 10 mM PBS buffer) mixed with oily components (AS03, squalene, DL-α-tocopherol, Polysorbate 80, and paraffin). Three independent measurements were performed (n=3).

3.3.9 Determination of vaccine stability in presence of oily components (AS03, oily components of AS03, and paraffin) using RP-HPLC

Samples with hemagglutinin but without oily components were characterized using RP-HPLC using fluorescence detection as a benchmark. For these samples, comparable peak values and retention time (17.40 min ± 0.15 min) were observed

(Figure 3.3.10). The chromatogram of AS03 exhibited a very broad peak, which was a composition of the squalene and DL-α-tocopherol peak. Polysorbate 80 and/or paraffin resulted in baselines without any detectable peaks due to a lack of excitable compounds (λ_{ex} 280 nm and λ_{em} 335 n) (Figure 3.3.11). Moreover, results showed a partially overlay of the broad AS03 peak over the distinct hemagglutinin peak in mixed samples (commercial product (CP) or reconstituted lyophilizates (rL) + AS03) (Figure 3.3.12). Furthermore, the process of extraction (centrifugation and separation of the oily component from the aqueous part) resulted in a partial loss of hemagglutinin which was indicated by a lower peak value while peaks of the residual oily components were still detectable. The observable peaks of the oily components indicated a limitation of the extraction using centrifugation (Figure 3.3.12 and Figure 3.3.13). DL-α-tocopherol (high but thin peak shape) was still detectable in the samples while squalene (flat but broad peak shape) was almost completely extracted from the mixture after 10 centrifugation cycles (Figure 3.3.13). Polysorbate 80, which demonstrated a high impact on vaccine activity (HAI) (Figure 3.3.7) could not be detected using RP-HPLC and fluorescence detection.

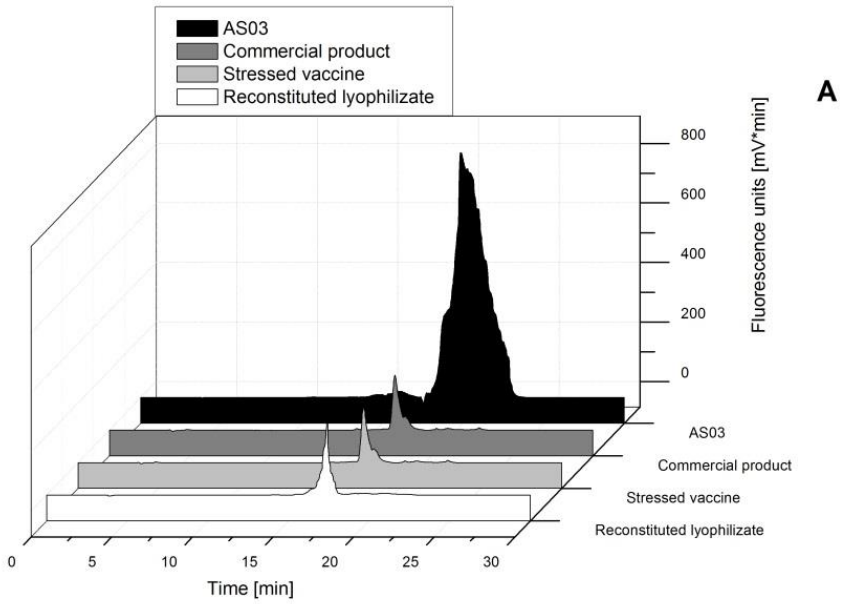

Figure 3.3.10: Fluorescence units of the commercially available product (15 µg/ml), stressed vaccine (15 µg/ml), collapse lyophilized vaccine (15 µg/ml), AS03, Three independent measurements were performed (n=3)

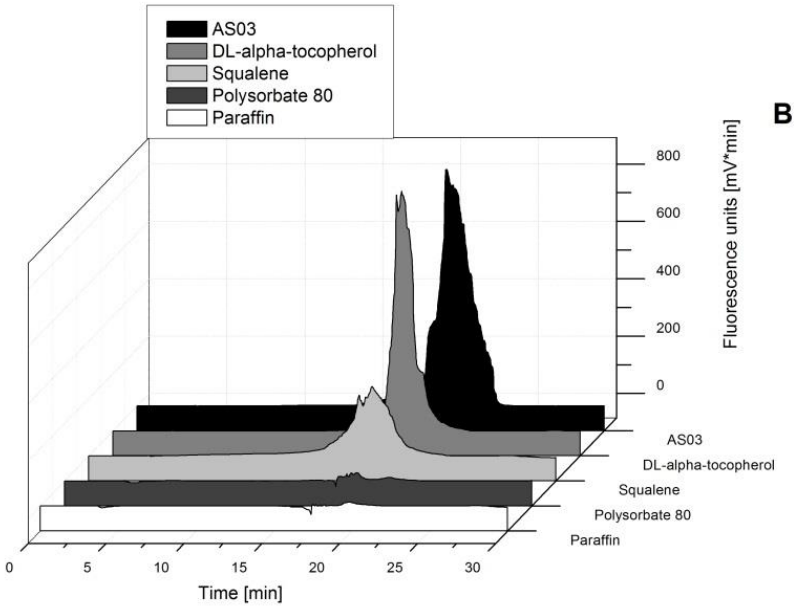

Figure 3.3.11: Fluorescence units of the commercially available product (15 µg/ml), AS03, oily components of AS03 (squalene, DL-α-tocopherol, Polysorbate 80), paraffin. Three independent measurements were performed (n=3)

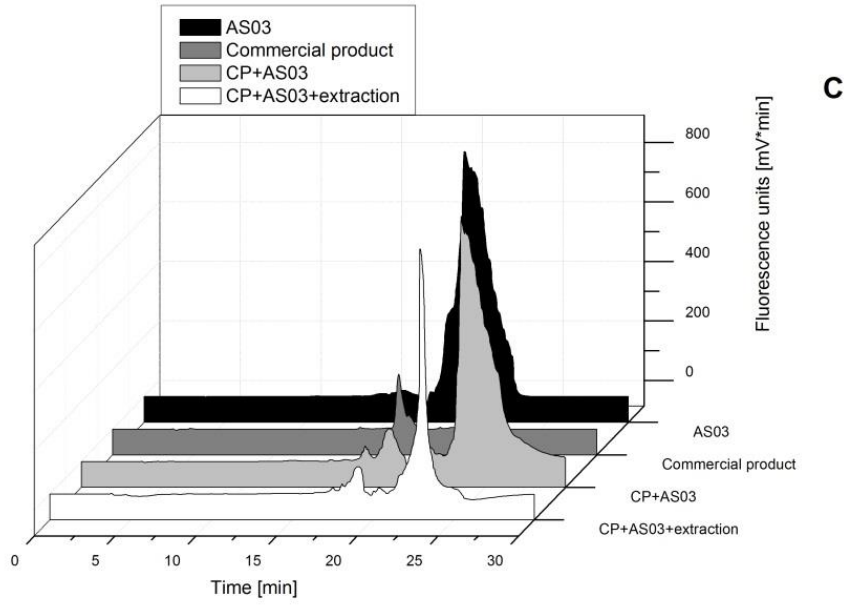

Figure 3.3.12: Fluorescence units of the commercially available product (15 µg/ml), AS03, mixtures of the commercial product with AS03 (CP+AS03) and additional separation of the oily components (CP+AS03+extraction). Three independent measurements were performed (n=3)

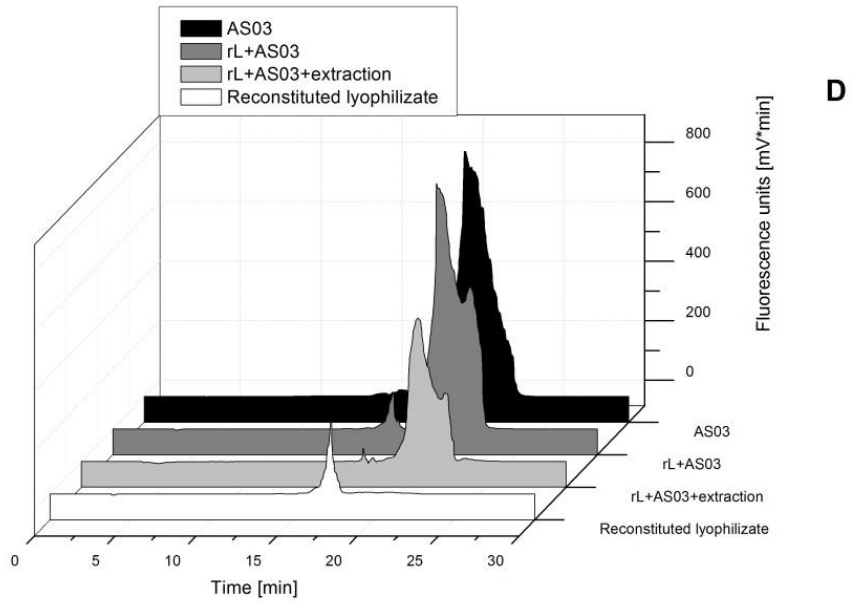

Figure 3.3.13: Fluorescence units of the AS03, mixture of the reconstituted lyophilizate with AS03 (rL+AS03) and an additional separation of the oily components (rL+AS03+extraction). Three independent measurements were performed (n=3)

3.4 Discussion

In this chapter, the storage stability of collapse freeze-dried (and cryo-milled) influenza vaccine was characterized. The samples were stored under different storage conditions (2-8°C, 25°C, and 40°C) over a time period of 12 months. Hemagglutinin as the main antigenic protein in the vaccine was used as a temperature sensitive indicator molecule to identify the stress impact during processing and/or storage. While the results in **Chapter 2** demonstrated a successful stabilization of the vaccine using an cost efficient collapse freeze-dry cycle over 6 months of storage, this chapter focused on the long-time storage stability (12 months) of the vaccine lyophilizates and the characterization of hemagglutinin in presence of oily components such as AS03 (adjuvant), squalene, DL-α-tocopherol, polysorbate 80, and paraffin. The storage stability was analysed using the assays already established in **Chapter 2**.

Stabilized vaccine lyophilizates resulted in consisted fluorescence values (RP-HPLC) under all storage conditions (2-8°C, 25°C, and 40°C) over the observed time period. In contrast, the cryo-milled samples demonstrated a compromised result at high storage temperature. The storage stability of cryo-milled vaccine lyophilizates at ambient temperatures (25°C) opened the possibility to handle the stabilized vaccine without a cold-chain-system. While the long-term heat stress (40°C/12 months) resulted in major vaccine alteration indicated by a second peak (Figure 3.3.1) in the cryo-milled samples the shortly heated vaccine (70°C/100 minutes) demonstrated still an unchanged peak value and retention time. Notable was the chromatographically observable change of the cryo-milled lyophilizates (40°C/12 months) but the biological activity of hemagglutinin was not affected by the degradation as detected in the consistent HAI results. The diverging results of both assays could occur due to a less sensitive hemagglutinin activity determination using the HAI assay compared to the high sensitive intrinsic fluorescence characterization of minor structural changes during RP analysis. The progressed degradation was also detected in the electrophoretic assays (SDS-Page and western blot analysis) (Figure 3.3.5 and Figure 3.3.6). The alteration of cryo-milled samples led to formation of aggregates, which resulted in a reduced ability of protein migration through the gel. Moreover, a changed protein structure could be assumed due to a modified binding affinity of the specific anti-HA-

antibody, which resulted in diminished or rather lack of detectable antigen-antibody-complexes (Figure 3.3.6).

The formation of small agglomerates, resulting from progressed protein degradation at higher storage temperature, was also observed in light obscuration measurements and turbidity analysis. While the turbidity at time-point t_0 was comparable between lyophilizates and cryo-milled samples, the steady turbidity increase of cryo-milled samples might be indicating a self-reinforcing process of degradation. The drastic alterations of the particle sizes between the last two time points (6 months and 12 months) could be a result of the progressing degradation. The higher residual moisture of the cryo-milled samples might catalyze the alteration. In contrast to the compromised stability of the cryo-milled samples at high storage temperatures, consistent results of stable products were observed for the cryo-milled samples stored at 2-8°C and ambient temperature (25°C). Unprocessed lyophilizates demonstrated a high resistance against induced heat stress over 12 months.

The second focus of this work was to characterize the vaccine stability in presence of oily components. Light obscuration measurements, turbidity analysis and electrophoretic characterization could not be used to determine the stability of hemagglutinin due to a huge impact of the oily components to the principles of the assays. Using the hemagglutination inhibition assay and RP-HPLC seemed expedient to determine the vaccine modifications. Nonetheless, oily components, added to the commercial product, reconstituted lyophilizates, or buffer resulted in unreproducible results performing the HAI assay. In order to accomplish the activity assay, an extraction of the oily components using centrifugation was tried out but the effect was limited (Figure 3.3.9). The chromatograms using RP-HPLC revealed remaining DL-α-tocopherol in the solutions after the extraction (Figure 3.3.13) which significantly effected the assay. Moreover, the HAI assay revealed that Polysorbate 80, as an ingredient of AS03 or as an individual component, disturbed mainly the activity assay and led to false results. It is likely that Polysorbate 80 as a surfactant had an impact on the erythrocyte membranes. The changed or even destroyed membranes prevent the hemagglutination and could result in inconclusive results. Even though the characterization of the vaccine in presence of oily components could be performed using RP-HPLC the validity was limited. Using only this chromotographical assay, structural changes could be characterized but neither the activity of hemagglutinin nor

protein degradations without any separations as shown for the commercial product versus the heat stressed vaccine could be detected (Figure 3.3.13 and Figure 3.3.13). In order to characterize the stability of hemagglutinin in presence of the oily components, new analytical assays should be conducted. Moreover, the activity of the antigen could be determined in animal experiments during a vaccination study. However, a minor activity loss cannot be determined using this concept of animal experiments because vaccinations are not subjected to dosage-response relationships [104, 105].

This work showed a stabilization of collapse-freeze-dried lyophilizates at different storage temperatures (2-8°C, 25°C, and 40°C) over a time period of 12 months while storage cryo-milled samples were limited to 2-8°C and 25°C. The characterization of the vaccine in presence of oily components was not achieved due to the high impact of the ingredients to the assays.

3.5 Conclusion

The stabilization of the thermo-sensitive hemagglutinin can be established using a collapse-freeze dry-cycle. The lyophilizates showed a consistent stability at different storage temperatures over the observed time period of 12 months while the storage conditions should be more restricted for cryo-milled samples. However, storage stability of all samples at ambient temperatures is a huge improvement compared to the strict refrigerator storage of the liquid influenza vaccines.

Yet, the characterizations of the vaccine in presence of oily components (adjuvants) need further investigation because of the limitations of the established analytical methods.

In this work, the long-term storage stability of lyophilized influenza vaccine was demonstrated. While the stability of unprocessed lyophilizates was confirmed under all storage conditions the cryo-milled samples could be stored at ambient temperatures over a time period of 12 months. This storage stability of the vaccine particles opens the possibility to distribute vaccines for intradermal vaccination without any cold-chain-system.

3.6 References

1. Layne, S.R., *Human influenza surveillance: the demand to expand.* Emerging Infectious Diseases, 2006. **12**(4): p. 562-568.

2. Diminsky, D., et al., *Physical, chemical and immunological stability of CHO-derived hepatitis B surface antigen (HBsAg) particles.* Vaccine, 1999. **18**(1–2): p. 3-17.

3. Yuan, L., et al., *Vaccine storage and handling. Knowledge and practice in primary care physicians' offices.* Canadian family physician, 1995. **41**: p. 1169.

4. Brandau, D.T., et al., *Thermal stability of vaccines.* Journal of Pharmaceutical Sciences, 2003. **92**(2): p. 218-231.

5. Nail, S.L. and L.A. Gatlin, *Freeze drying: principles and practice.* Pharmaceutical dosage forms: Parenteral medications, 1993. **2**: p. 163-233.

6. Wang, W., *Lyophilization and development of solid protein pharmaceuticals.* International Journal of Pharmaceutics, 2000. **203**(1–2): p. 1-60.

7. Kis, E., G. Winter, and J. Myschik, *Can Collapse Freeze Drying Provide High Density Protein Sugar Particles for Ballistic Powder Injection?* Scientia Pharmaceutica, 2010. **78**: p. 653.

8. Etzl, E.E., G. Winter, and J. Engert, *Toward intradermal vaccination: preparation of powder formulations by collapse freeze-drying.* Pharmaceutical Development and Technology, 2014. **19**(2): p. 213-222.

9. Schersch, K., et al., *Systematic investigation of the effect of lyophilizate collapse on pharmaceutically relevant proteins I: Stability after freeze-drying.* Journal of Pharmaceutical Sciences, 2010. **99**(5): p. 2256-2278.

10. Schersch, K., et al., *Systematic investigation of the effect of lyophilizate collapse on pharmaceutically relevant proteins, part 2: stability during storage at elevated temperatures.* Journal of Pharmaceutical Sciences, 2012. **101**(7): p. 2288-2306.

11. Bonifaz, L.C., et al., *In vivo targeting of antigens to maturing dendritic cells via the DEC-205 receptor improves T cell vaccination.* Journal of Experimental Medecine, 2004. **199**(6): p. 815-24.

12. DeBenedictis, C., et al., *Immune functions of the skin.* Clinics in Dermatology, 2001. **19**(5): p. 573-585.

13. Dean, H.J. and D. Chen, *Epidermal powder immunization against influenza.* Vaccine, 2004. **23**(5): p. 681-686.

14. Loudon, P.T., et al., *GM-CSF increases mucosal and systemic immunogenicity of an H1N1 influenza DNA vaccine administered into the epidermis of non-human primates.* PloS One, 2010. **5**(6): p. e11021.

15. DeMuth, P.C., et al., *Vaccine delivery with microneedle skin patches in nonhuman primates.* Nature Biotechnology, 2013. **31**(12): p. 1082-1085.

16. DeMuth, P.C., et al., *Releasable Layer-by-Layer Assembly of Stabilized Lipid Nanocapsules on Microneedles for Enhanced Transcutaneous Vaccine Delivery.* ACS Nano, 2012. **6**(9): p. 8041-8051.

17. Marquet, F., et al., *Characterization of Dendritic Cells Subpopulations in Skin and Afferent Lymph in the.* 2011.

18. Burgess, D.J., *Immunotherapy: A skin test to predict melanoma vaccine efficacy.* Nature Reviews Cancer, 2012. **12**(11): p. 737-737.

19. Fiore, A.E., et al., *Prevention and control of influenza with vaccines: recommendations of the Advisory Committee on Immunization Practices (ACIP), 2010.* MMWR. Recommendations and Reports: Morbidity and mortality weekly report. Recommendations and reports/Centers for Disease Control, 2010. **59**(RR-8): p. 1.

20. Moingeon, P., C. de Taisne, and J. Almond, *Delivery technologies for human vaccines.* British Medical Bulletin, 2002. **62**(1): p. 29-49.

21. Mitragotri, S., *Immunization without needles.* Nature Reviews Immunology, 2005. **5**(12): p. 905-916.

22. Ortiz, J.R., et al., *Strategy to enhance influenza surveillance worldwide.* Emerging Infectious Diseases Journal, 2009. **15**(8): p. 1271-8.

23. Scuffham, P.A. and P.A. West, *Economic evaluation of strategies for the control and management of influenza in Europe.* Vaccine, 2002. **20**(19–20): p. 2562-2578.

24. Andreasen, V., *Dynamics of annual influenza A epidemics with immuno-selection.* Journal of Mathematical Biology, 2003. **46**(6): p. 504-536.

25. De Jong, J.C., et al., *Influenza virus: a master of metamorphosis.* Journal of Infection, 2000. **40**(3): p. 218-228.

26. Aguilar, J.C. and E.G. Rodriguez, *Vaccine adjuvants revisited.* Vaccine, 2007. **25**(19): p. 3752-62.

27. Lefevre, E.A., et al., *Immune Responses in Pigs Vaccinated with Adjuvanted and Non-Adjuvanted A(H1N1)pdm/09 Influenza Vaccines Used in Human Immunization Programmes.* PLoS One, 2012. **7**(3): p. e32400.

28. Dutcher, J., et al., *Alloimmunization following platelet transfusion: the absence of a dose- response relationship*. Vol. 57. 1981. 395-398.

29. Bock, H.L., et al., *A new vaccine against tick-borne encephalitis: initial trial in man including a dose-response study.* Vaccine, 1990. **8**(1): p. 22-24.

4. Chapter – Intradermal administration of particles

4.1 Introduction

In the search of new ways of needle-free vaccination the skin can be one of the vaccination targets. Intradermally applied vaccines have to be administered through the stratum corneum, which is formed by cornified keratinocytes and serves as the main physical barrier. The vaccination needs to be displayed directly to the immunocompetent cells which migrate and present the antigen fragments to other immune cells in the draining lymph nodes [1-6].

Skin thickness has a major impact on the efficacy of intradermal immunization, as it can vary significantly between different body parts [2, 7]. Investigated skin areas of subjects of different body mass index (BMI), age, gender, and ethnic origin demonstrated an average thickness between 1.5 mm to 2.7 mm: e.g. 1.5 mm at the thigh; 1.8 mm at the deltoid and suprascapular; 2.7 mm at the upper abdomen [2, 8, 9]. Consistent skin thickness promises an easier handling for intradermal vaccination compared to a needle lengths adjustment for i.m. vaccine injections due to varying thickness of subcutaneous fat and muscle thickness [2, 10].

So far results of clinical trials were inconsistent when examining the benefit of intradermal vaccination. However, the predominant view in literature reported mostly an equivalent or superior immune response for intradermal vaccination [4-6, 11]. Generally vaccines for intradermal application can be categorized in: (I) induction of superior immune response compared to i.m. or s.c. administration, (II) inconsistent results of observed immune response in different clinical trials, and (III) vaccines remaining to be investigated for intradermal administration [2]. A superior immune response can be a result of wider vaccine distribution and addressing immunocompetent cells within the tissue after intradermal vaccination while the vaccine deposition of i.m. administration is locally limited and immune cells have to migrate to the vaccination area [2, 3, 12]. Moreover, the epidermis promises a painless vaccine application due to a lack of sensory nerve endings in the upper skin layers [12, 13].

Epidermal powder immunization could deliver powdered vaccines to the skin as an immunologically active site and would combine the advantages of needle-free and skin vaccination. Moreover, pain and adverse side effects could be minimized or even

eliminated due to the small volume and low penetration depth of vaccine particles. In addition to that, the high thermo-stability of dried vaccines could make cold chain maintenance superfluous [3, 9, 12, 14-16]. In preliminary test, the administration of model and vaccine particles into a skin model was tested by our group using an experimental ballistic device (BK01) [17].

This chapter will present a new ballistic device for epidermal powder immunization which is based on the patents of P. Lell and will show the successful deposition of model particles into the epidermis to target the Langerhans cells [18]. Labelled polystyrene particles were mainly used to characterize the properties of particle acceleration using the ballistic device and the penetration into the skin. Additionally, labelled carbohydrate particles were applied which could easily be detected in the skin to bridge the results from the polystyrene model particles to vaccine carbohydrate particles. The mechanical properties of human skin during the impact of particles were simulated using pig skin while gelatine skin models were used to trace the distribution of the particles [17].

4.2 Material and Methods

4.2.1 Materials

Fluorescence labelled and collapse lyophilized particles were used to determine the depth of particle penetration. Fluorescein isothiocyanate (FITC) was purchased from Sigma-Aldrich (Sigma-Aldrich, Taufkirchen, Germany). Sodium hydrogen phosphate monohydrate was purchased from Gruessing (Gruessing, Filsum, Germany). Sodium dihdydrogen phosphate dihydrate, sodium phosphate monobasic and dibasic, sodium hydroxide and sodium chloride were obtained from Applichem (Applichem, Darmstadt, Germany). Trehalose used as a lyoprotectant was purchased from BDH Prolabo (VWR, Ismaning, Germany) and mannitol as a bulking agent was obtained from Boehringer Ingelheim (Ingelheim, Germany).

Fluorescence (FITC) labelled polystyrene (PS) particles (19.78 µm, 41.14 µm, 60.28 µm) were purchased from microparticles GmbH (Berlin, Germany) as model particles. Paraffin (100 cSt) was obtained from Merck KGaA (Darmstadt, Germany) and the components of the adjuvant system AS03, DL-α-tocopherol, polysorbat 80, and squalene were purchased from Sigma-Aldrich (Taufkirchen, Germany). Customized 500 µm glass spheres were purchased from Carl Roth (Karlsruhe, Germany). Hematoxylin and eosin stain, 25% hydrochloric acid, 96% ethanol, and carbol-xylol were obtained from Merck (Darmstadt, Germany). Xylol was purchased from W.Gaeen GmbH&Co. (Munich, Germany). Eukitt solution was purchased from Vitro-Clud (Langenbrunck GmbH, Emmendingen, Germany). Hydrochloric acid (36%) and sodium hydroxide (32%) were purchased from Applichem (Darmstadt, Germany) to dissolve skin samples and cell strainers (70 µm) were obtained from BD Biosciences (Erembodegem, Belgium) to prepare the skin suspension. For gelatin skin models GELITA Pharmaceutical Gelatin made from pig skin with strength of 180 Bloom was purchased from DGF STOESS AG (Eberbach, Germany). 1,2,3-Propantriol (Glycerol) (purity, 99%) and polyethylene glycol 400 (PEG 400) were obtained from AppliChem (Darmstadt, Germany). Potassium carbonate was obtained from Sigma-Aldrich (Taufkirchen, Germany).

4.2.2 Methods

4.2.2.1 Preparation of collapse lyophilized particles

The fluorescence labelled and collapse lyophilized particles were prepared using 300 ml of a 10 mM phosphate buffer at pH 7.0 saturated with FITC. The solution was additionally filtered using a 0.22 µm cellulose acetate syringe filter (VWR Ismaning, Germany). The saturated FITC solution was mixed with trehalose and mannitol (1:1) (w/w) to obtain a final concentration of 15% solid content. The FITC-carbohydrate solution was gently stirred at approximately 50 rpm using a magnetic stirrer (IGAMAG RCT, IKA®-Werke GmbH & Co. KG, Staufen, Germany) to dissolve the additives. The mixed solution was filtered again with a 0.22 µm cellulose acetate syringe filter to remove any undissolved residues.

4.2.2.2 Lyophilization processes (as described previously in Chapter 2)

A Martin Christ Epsilon 2-6D freeze-dryer (Martin Christ, Osterode, Germany) equipped with a pirani pressure sensor was used to perform the collapse lyophilization. A volume of 2.625 ml of the FITC carbohydrate formulation was transferred into each of 100 vials DIN 10R (Mglas AG, Muennerstadt, Germany) and were placed in the center of a lyophilization shelf. Vials containing FITC-carbohydrate solution were surrounded by edge-vials filled with a 15% (w/w) trehalose-mannitol (1:1) (w/w) solution. All vials were finally semi-stoppered using Westar®RS.stoppers (Westpharma, Exton, USA) and transferred to the freeze-dryer.

The collapse lyophilization cycle started with an equilibration period at 4°C for 1 hour and subsequent freezing to -50°C using a ramp within 1.5 hours. The temperature of -50°C was (isothermally) held for one hour. Afterwards, the temperature was increased to -40°C using a ramp of 0.33°C/min. At -40°C, the chamber pressure was reduced to 1.98 mbar.

After an equilibration time of 10 minutes the shelf temperature was increased to 45°C within 2 hours. Primary drying was carried out for 24 hours and unchanged shelf-temperature. The chamber pressure was further decreased to 0.03 mbar, after the

primary drying. The secondary drying was continued for further 20 hours at 45°C. The temperature was reduced to the storage temperature of 4°C, at the end of the collapse lyophilization cycle. Finally, the samples were stoppered at approximately 800 mbar in dry nitrogen gas atmosphere and crimped after unloading.

4.2.2.3 Cryo-milling and sieving

The FITC lyophilizates were cryo-milled using a Retsch CryoMill (Retsch Technology GmbH, Haan, Germany). Samples in a stainless steel milling jar (Retsch Technology GmbH, Haan, Germany) were cooled to -196°C using liquid nitrogen during the cryo-milling cycle. Approximately 1.5 g of the lyophilizates was filled into the milling jar and two steel balls were additionally included. A pre-cooling for 10 min. with a milling frequency of 5 Hz was carried out before grinding was performed at 25 Hz for 15 sec. After the cryo-milling cycle, water condensation was avoided by placing the milling jar into a Glove box (customized from a university associated workshop) under dry nitrogen gas atmosphere (< 10%) measured with a thermo-hygrometer (TFA Dostmann, Wertheim, Germany). The equilibration of the milling jar to room-temperature was realized within two hours. The powder was sieved with a Retsch sieve (Retsch Technology GmbH, Haan, Germany) with mesh sizes of 20 µm, 40 µm, 80 µm and 125 µm. Classifying by sieving was carried out for 10 minutes and weighed afterwards. Classifying steps were repeated until the mass of powder on each sieve did not differ more than 1% to the previous weighing. Aliquots of ground and classified samples were filled in DIN 10R vials under dry nitrogen atmosphere and stoppered with Westar®RS.stoppers.

4.2.2.4 Preparation of oily part of AS03

The oily part of AS03 contains 10.69 g of squalene, 11.86 g DL-α-tocopherol, and 4.86 g polysorbat 80. All components were mixed using a magnetic stirrer at approximately 50 rpm. The oily mixture was stored at 2-8°C until usage.

4.2.2.5 Experimental particle applicator device

The experimental particle applicator was based on pyrotechnical acceleration to administer particles into the skin (Figure 4.2.1). The device was divided in two functional parts. The pharmaceutical part was designed to provide a sterile environment for particles and was composed of support plate, membrane holder, customized bilayer of arched membranes, combustor chamber and an oleogel. The pyrotechnical part provided the acceleration energy and composed of a gas-generator (**Chapter 6**), and the igniter. After the electrically ignition of the gas-generator the pressure was directed by the combustor design and transmitted through the oleogel filling of the combustion chamber to the modified bilayer membranes. Membranes and oily fixed particles accelerated together, induced by the pulse energy. While the acceleration of the membranes slowed down, the fixed particle membranes detached from the surface. Further details of the device development are described in **Chapter 5**.

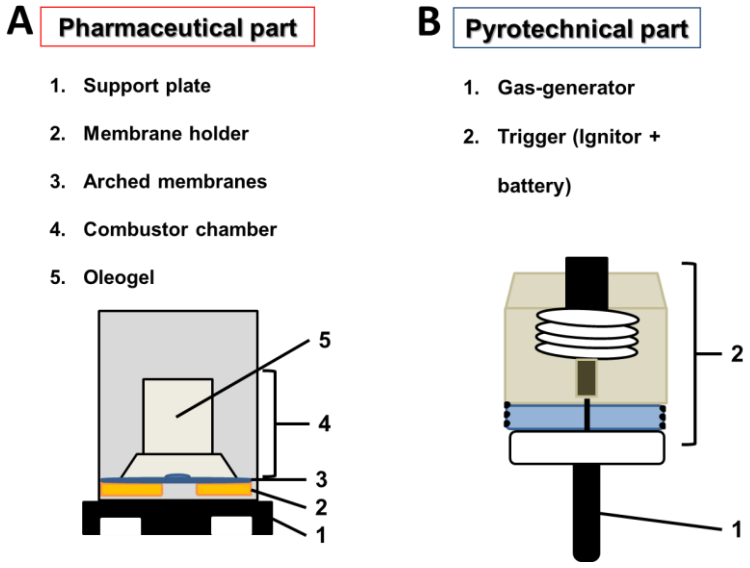

Figure 4.2.1: Experimental particle applicator, separated into the two functional parts A) the pharmaceutical part, B) the pyrotechnical part. C) The prototype of the powder applicator.

4.2.2.6 Particle loading

The experimental device provided a circular surface area of approximately 0.78 cm^2 for particles. Particle loading on the membrane of the experimental device was performed on a clean bench (Herasafe, Thermo Fischer scientific, Rockford, USA). To fix particles, the upper membrane was previously coated with an oily component, such as paraffin (Merck KGaA, Darmstadt, Germany) or the oily part of AS03 (DL-α-tocopherol, polysorbat 80, and squalene) using a sterile swab (Copan, Brescia, Italia). The sterile swab was led through the nozzle of the experimental device and the oily coating was homogenously spread on the membrane (Figure 4.2.2). Afterwards, a customized funnel was gently put through the nozzle. The particles (FITC labelled TM (trehalose-mannitol) particles or FITC labelled PS particles) were scattered through the funnel on the coated membrane until the membrane surface was overfilled (Figure 4.2.2). The device was inverted and the funnel was carefully taken out to avoid a swirling of the particles in the pharmaceutical part of the device. Subsequently the inverted particle applicator was tapped on the bench to detach loose particles and approximately an amount of 1.7-2.0 mg kept attached on the membrane (Figure 4.2.2). Finally, the pharmaceutical part was sealed with a customized foil (IIS, Andernach, Germany) to inhibit a permeation of dust and moisture.

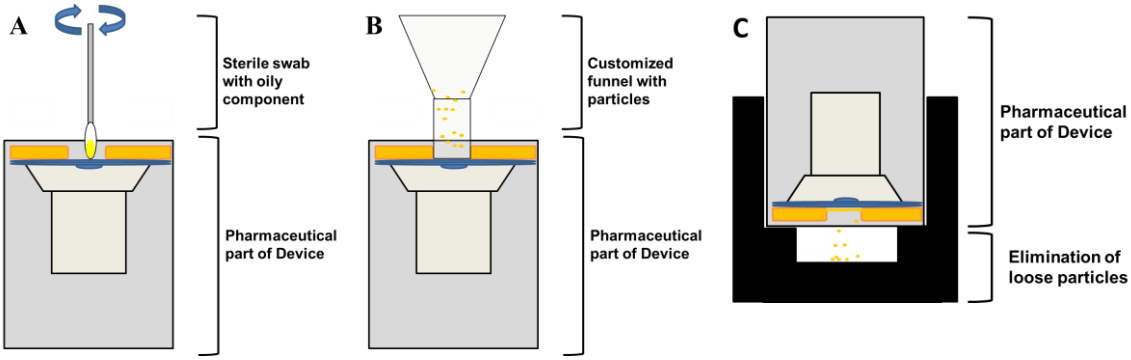

Figure 4.2.2: Schematic representation of particle loading on membrane of pharmaceutical part.

4.2.2.7 Animal keeping and skin preparation and particle administration ex vivo and in vivo

Skin parts of commercial cross-breed pigs (LWxPI) were used for *ex vivo* and *in vivo* experiments to determine the penetration depth of the administered particles. In a first step, an examination of the intradermal particle penetration in *ex vivo* skin was realized. The specimens were analyzed for administered particles to adjust the particle penetration depth by optimizing the particle velocity. Subsequently, the experiments were conducted *in vivo* using the modified particle velocity.

All procedures and the experimental protocol for animal experiments were officially approved by the Government Office of Upper Bavaria, Munich, Germany (authorization reference number 55.2.1.54-2532-87-12; 30.08.2012).

In order to adjust the velocity of the particles *ex vivo* experiments were performed using frozen skin parts (ventral side) from five to six week old piglets. The frozen samples were gently thawed and equilibrated to ambient temperature (25°C) within 2 hours. Previous to application, the bristles were gently trimmed. Particle loaded device was placed on the marked administration site. Directly after particle administration, the skin samples with administered particles were frozen again on dry ice. Afterwards, the samples were embedded in a tissue freezing media (Leica, Nussloch, Germany) and frozen at -80°C until the specimens were prepared for histological examinations. Depending on the histological results of the *ex vivo* preparations the device was modified to optimize the safety and penetration depths.

Six five-week old piglets from farm were transported to the Clinic for Swine (Oberschleissheim, Germany). Water and food was available ad libitum. After a 2 week adaptation phase, the piglets were weighed and clinically examined and monitored by veterinarians.

The *in vivo* particle administrations to anaesthetized animals with 5 Vol% Isoflurane ((Isoba® MAC 1,5 Vol% Essex Tierarznei) and O_2 were performed with the modified device. These animals were also euthanized (as described above) to excise the respective skin patches after 90 minutes of particle application.

In both experiments particles were administered to skin areas ambilateral to the mammilla complex. These were carefully cleaned with tissues and the bristles were trimmed cautiously to avoid any skin irritation. The concerned areas were marked

using a permanent marker. Each lappet was subdivided in five applications sites each a size of 6 cm x 6 cm. In contrast to the *ex vivo* experiments, the skin parts of the in vivo experiments were directly frozen on dry ice after the particle administration to the marked sites and were subsequently embedded in a tissue freezing medium for histological examination. Number of animals could be minimized by using larger skin lappets to optimize the device during the *ex vivo* experiments.

4.2.2.8 Microscopic examination of skin slices

Skin specimens embedded in the tissue freezing medium were sliced with 10 µm thickness using a cryotom Research Cryostat Leica CM35050S (Techno-Med GmbH, Bielefeld, Germany). Subsequently, the slices were placed on SuperFrost microscope slides (VWR, Ismaning, Germany). Afterwards, the specimens were microscopically examined using a BZ8100 Biozero Micrsocope (Keyence, Neu-Isenburg, Germany), equipped with objectives Nikon S Plan Fluor (20x/0.45) and Plan Apo (10x/0.45) (Nikon GmbH, Duesseldorf, Germany).

4.2.2.9 Microscopic examination of Hematoxylin and eosin stained (HE stain) skin slices

In addition to a microscopical examination of samples, specimens of the intradermal particle administration were dyed using a hematoxylin and eosin stain (HE stain). Previously prepared skin slices were embedded in HE stain for 5 min. and subsequently washed with tap water for further 5 min. Samples were shortly moved through a 0.5% hydrochloric acid-ethanol solution with an additional washing step afterwards. Thereafter, the samples were briefly put into a 1% eosin solution and then washed again with water. The prepared slices were dried in ascending/increasing ethanol concentrations (50%, 70%, 80%, 96%, and 100%) for 1 min for each concentration. Finally, specimens were shortly covered with carbol-xylol and xylol. The slices were fixed with the Eukitt solution on microscope slides. Specimens were microscopically examined using a BZ8100 Biozero Micrsocope (Keyence, Neu-Isenburg, Germany).

4.2.2.10 Particle size determination using Scanning electron microscopy (SEM)

Particle samples (polystyrene model particles and cryo-milled carbohydrate particles) were carefully transferred onto an adhesive carbon tape (Bal-tec GmbH, Germany) and subsequently sputtered with carbon under high vacuum (MED 020, Bal-tec GmbH, Germany). Specimens were viewed using a scanning-electron microscope (Supra 55VP, Zeiss SMT, Germany) under high vacuum. Scanning electron micrographs were recorded at magnifications of 100 fold and 300 fold.

4.2.2.11 Preparation of gelatin skin models for determination of penetrated particle counts

As described in Deng et al. highly purified water was mixed with glycerol in a 200 ml Erlenmeyer flask and heated to 55°C using the magnetic hot-plate stirrer (Stable Micro Systems Ltd., Surrey, UK). Gelatin was added in a ratio to glycerol of 2:9 (w/w) and dissolved by stirring at 700 rpm for 30 minutes. Afterwards, the mixture was filled into petri-dishes, which were pre-treated with 70% isopropanol to prevent bubble formation on the surface. Petri-dishes were placed in a fume exhaust hood to dry for 24 hours. Finally the skin models were stored for at least two weeks in a desiccator containing a saturated potassium carbonate aqueous solution with a relative humidity of 43% [17].

4.2.2.12 Dissolving pig skin and skin model to determine penetrated particle count

Polystyrene spheres were administered to the gelatin skin model and pig skin to determine the particle count ejected by the device. Excess particles, which did not penetrate into the material properly, were removed with an air pressure gun (2 bar / nozzle diameter 3 mm / distance 7 cm) in an angle of 90° for 5 sec. These particles were visualized using a Keyence light microscope VHX-500F equipped with an objective VH-Z20R (Keyence GmbH, Neu-Isenburg, Germany).

Gelatin skin models with administered polystyrene particles (41 µm) were given into a falcon tube (50 ml), filled with highly purified water and dissolved at 95°C using a magnetic hot-plate stirrer. Solutions were centrifuged at 10000 rpm (Sigma 4K15, Sigma Zentrifugen, Osterode am Harz, Germany) for 15 min. The clear supernatants were exchanged three times and finally the particles were collected in 1.5 ml of highly purified water in an Eppendorf-cup (Eppendorf, Hamburg, Germany). A complete transfer from the gelatin solution to the highly purified water was verified using a UV lamp to detect residual particles in the gelatin solution.

The native skin samples were treated with 25 ml of hydrochloric acid (36%) for 2 hours at ambient temperature in order to retrieve the polystyrene particles. The suspension was neutralized with sodium hydroxide (32%), filtered through a cell strainer (70 µm), mixed with Isopropanol (100%) (25 ml), and centrifuged at 10000 rpm for 30 min. The addition of isopropanol led to a separation of bigger cell fragments and lipids from the smaller cell fragments and polystyrene particles. Bigger fragments and lipids were skimmed using a pipette while cell fragments and particles were collected in 1.5 ml suspension.

4.2.2.13 Micro-flow-Imaging (MFI)

Polystyrene particles in samples were detected using a micro-flow imaging system (Brigthwell Technologies Inc., Ottawa, Canada). The system was pre-equalized with 250 µl of the sample solution / suspension with a flow rate of 0.1 ml/min. Afterwards 750 µl with a flow rate of 0.1 ml/min of gelatin-glycerol solutions and / or dissolved skin suspensions were analyzed to detect the spherical particles. Results were evaluated using DPA4100 software (Brigthwell Technologies Inc., Ottawa, Canada).

4.2.2.14 Determination of particle velocity

In order to determine the velocity of the accelerated particles, a system of flash cams was installed at the premises of the cooperation partner (Pyroglobe, Hettenshausen, Germany). The flash cams were positioned in an angle of 90° to each other to include the flight direction into the velocity calculations (Figure 4.2.3). Accelerated particles were repeatedly photographed by each flash cam and an overlay of images was finally

generated. Flash cam 1 took a picture every 10 µs, while flash cam 2 took a picture every 15 µs. The overlays of the flash cams were used to determine the velocity of the particles using the velocity-time theorem.

Previous to the velocity determination, a straight edge was photographed to determine the magnification of the flash cams. The visual correction of the magnification was implemented into the velocity calculations.

The experimental particle applicator was positioned in the focus of both flash cams. The ignition of the particle applicator and the flash cams were triggered by a photo flash (Metz, Zirndorf, Germany).

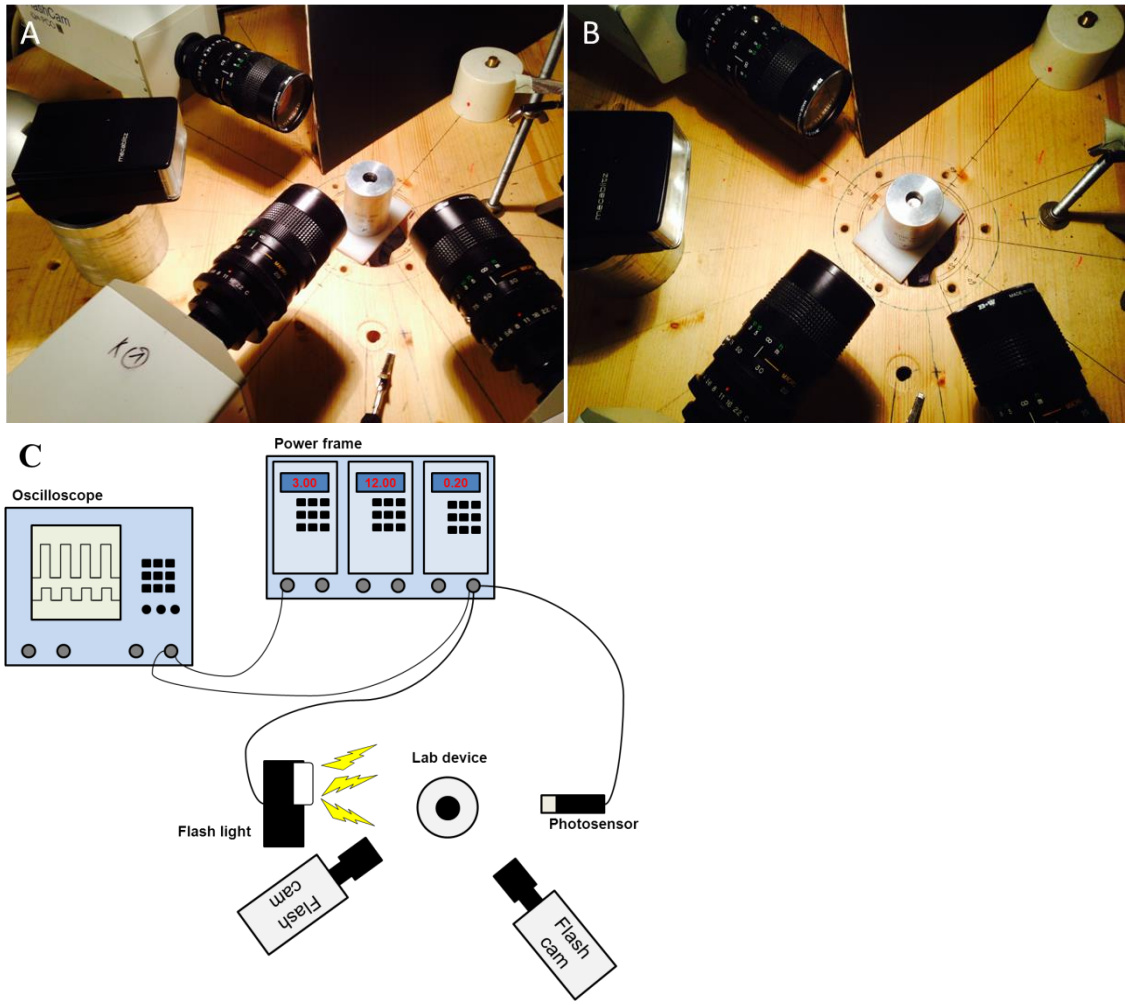

Figure 4.2.3: Experimental set-up of Flash cams to determine particle velocity. The powder applicator was positioned in the focus of the Flash cams. Emission of the particles and velocity measurement was triggered by the photo flash.

4.3 Results

4.3.1 Determination of particle velocity (in cooperation with Dr. P. Lell, C. Fellner, Pyroglobe, Hettenshausen, Germany)

Previous to the animal experiments, particle velocity was optimized using only one single 500 µm glass sphere as a standard model, while the smaller polystyrene particles were used as a model for velocity determination of the ejected powder cloud. Due to the limitations of process observation, we assumed that acceleration took place within the first 3-6 mm. The sudden pressure of the gas-generator hit the membrane and led to acceleration of the attached particles. After the acceleration path (3-6 mm), the particles could keep the momentum while the membranes slowed down. The glass sphere (ϱ= 2.3 g/cm^3) was accelerated to approximately 620 m/s (Figure 4.3.1A and B). We tested different sizes of polystyrene particles (ϱ= 1.1 g/cm^3) (19.78 µm, 41.14 µm, and 60.28 µm) to cover the range between 20 µm to 80 µm. All particle sizes showed comparable velocities with 516 m/s for 20 µm, 518 m/s for 40 µm and 521 m/s for 60 µm, respectively (Figure 4.3.1C to H and Table 1). A similar result of 526 m/s was obtained for the FITC-labelled lyophilizate particles (ϱ= 1.3 g/cm^3) (Figure 4.3.1and J).

Regarding the shapes of the powder clouds that are emitted from the device it can be stated that the powder clouds that form after emission of polystyrene and lyophilizate particles from the device show comparable shapes. Interestingly the monodispersed polystyrene particles demonstrated a mainly consistent pattern in cloud shape and a distinct cloud front, whereas a more unpredictable/irregular shape was observed for the polydispersed FITC labelled lyophilized particles.

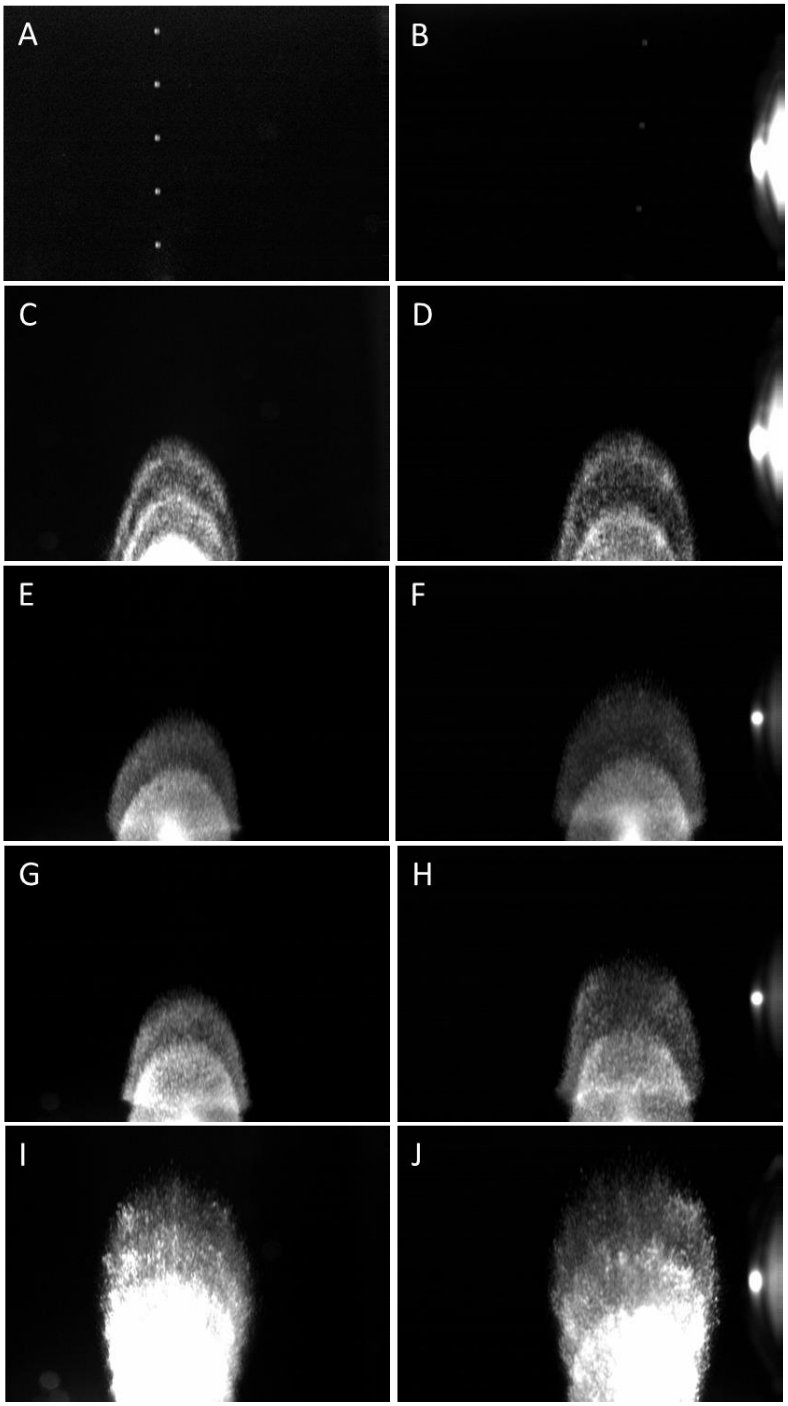

Figure 4.3.1: Overlay of particles accelerated by the experimental device. Flash cam 1 (delay time 10 µs) is positioned in a 90° angle to flash cam 2 (delay time 15 µs). A) overlay of 500 µm glass sphere taken by flash cam 1; B) overlay of 500 µm glass sphere taken by flash cam 2; C) overlay of 20 µm FITC labelled polystyrene particles taken by flash cam 1; D) overlay of 20 µm FITC labelled polystyrene particles taken by flash cam 2; E) overlay of 40 µm FITC labelled polystyrene particles taken by flash cam 1; F) overly of 40 µm FITC labelled polystyrene particles taken by flash cam 2; G) overlay of 60 µm FITC labelled polystyrene particles taken by flash cam 1; H) overlay of 60 µm FITC labelled polystyrene particles taken by flash cam 2; I) overlay of 20 µm-80 µm FITC labelled lyophilized particles taken by flash cam 1; J) overlay of 20 µm-80 µm FITC labelled lyophilized particles taken by flash cam 2.

Table 4.3.1 Calculated velocity of particles accelerated by the experimental device

Particle	**Size (µm)**	**Velocity[m/s] ±standard deviation n=2**	**Density [g/cm3]**
Glass sphere	500	624 ± 13.7	2.3
Polystyrene particles	20	516 ± 11.5	1.1
Polystyrene particles	40	518 ± 15.1	1.1
Polystyrene particles	60	521 ± 9.1	1.1
Lyophilizate particles	20 – 80	526 ± 12.2	1.3

4.3.2 Scanning electron microscopy (SEM)

Particle sizes were confirmed using the scanning electron microscopy. The three different polystyrene particle sizes demonstrated a high monodispersity (Figure 4.3.2A - F) and uniform spherical shapes (Figure 4.3.2B, D, and F). On the contrary, the electro micrographs displayed the broad distribution of the lyophilizate particles between the expected sizes of 20 µm to 80 µm (Figure 4.3.2G and H). Furthermore, heterogeneous shapes and rough surfaces of lyophilizate particles were evident but all examined particles were in the same magnitude as the comparator polystyrene particles.

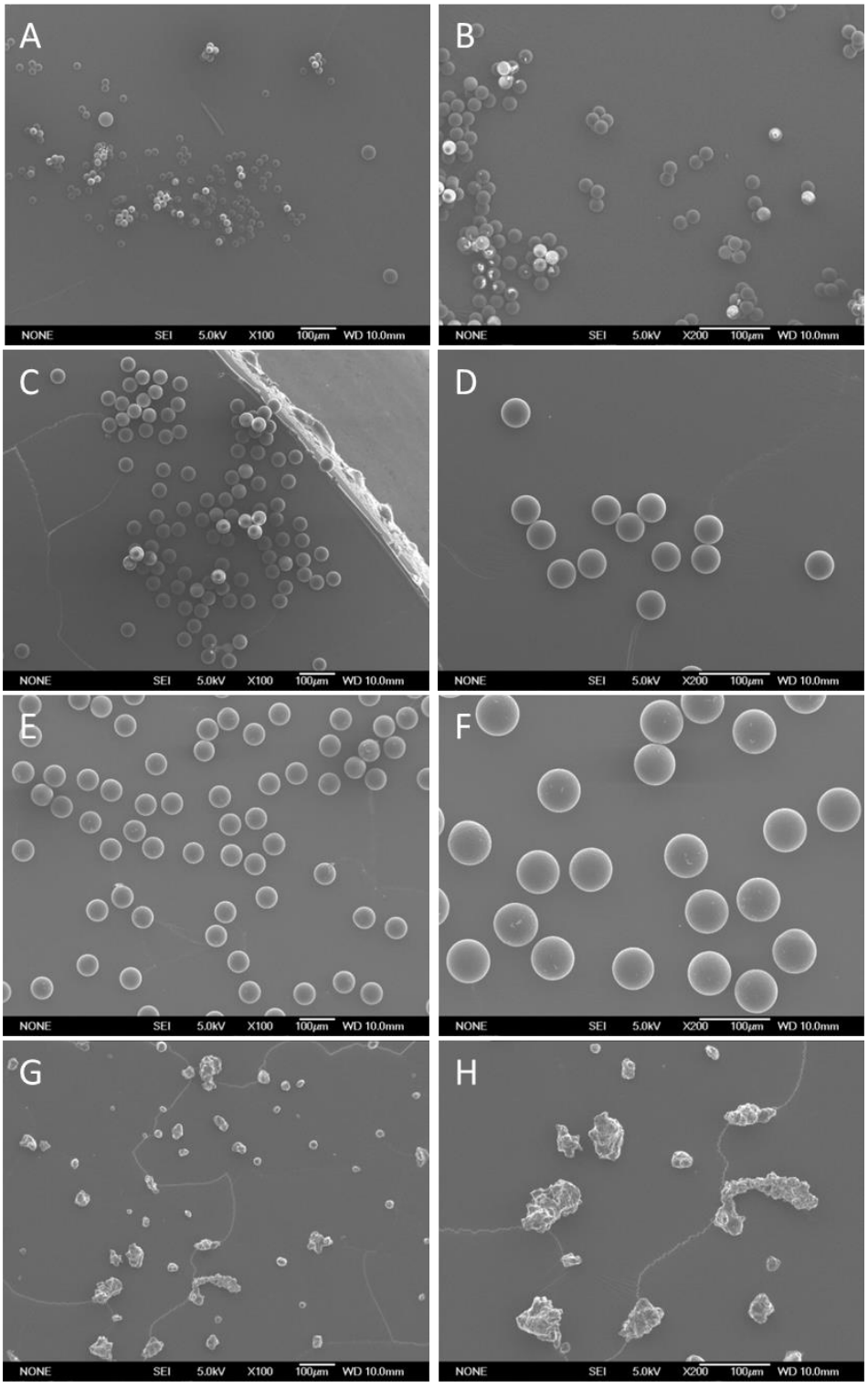

Figure 4.3.2: Scanning electron micrographs A and B) polystyrene particles 20 µm (A: magnification: 100 fold; B: magnification: 200 fold); C and D) polystyrene particles 40 µm (C: magnification: 100 fold; D: magnification: 200 fold); E and F) polystyrene particles 60 µm (E: magnification: 100 fold; F: magnification: 200 fold); G and H) FITC lyophilizates 20 µm-80 µm (G: magnification: 100 fold; H: magnification: 200 fold).

4.3.3 Microscopic examination of skin slices

Only 40 µm polystyrene particles as model particles and 20 µm-80 µm FITC labeled lyophilizate particles were used to determine the penetration depth into the skin (*ex vivo* and *in vivo*). Polystyrene particles were clearly detectable in *ex vivo* skin slices of 10 µm thickness (Figure 4.3.3). The different sizes of spheres were caused by the different positions of the 40 µm polystyrene particles within the cutting level of the skin sample. Nevertheless, polystyrene particles penetrated in a depth of approximately 50-100 µm (Figure 4.3.1A-C). The administration of the polystyrene particles to the layer between epidermis and dermis (stratum basale) could be determined due to differently stained cell-types in the *ex vivo* skin slices (Figure 4.3.3D). The administration of the polystyrene particles was not just a circumscribed phenomenon; a distribution over the complete administration site was successfully demonstrated (Figure 4.3.3C and Figure 4.3.4). Lesion-free particle administrations could be demonstrated due to a lack of tissue scaring in histological samples.

While the polystyrene particles can distinctively be discovered, a clear determination of lyophilizate particles was not possible due to their instant dissolution and distribution to surrounding tissue (Figure 4.3.3E and G). Therefore, the penetration depths of the FITC labeled lyophilizate particles could only be estimated in a range between 20 µm to 150 µm by the fluorescent area. A lesion-free distribution over the complete administration site of the FITC-labelled lyophilizate particles was also observed (Figure 4.3.3G). In order to confirm the *ex vivo* results of lesion-free particle penetration into the required depths in a living tissue, *in vivo* administration experiments were subsequently performed. In HE stained skin slices, the PS particles could be detected as spherical vesicles without any color which were washed out by the organic solvents.

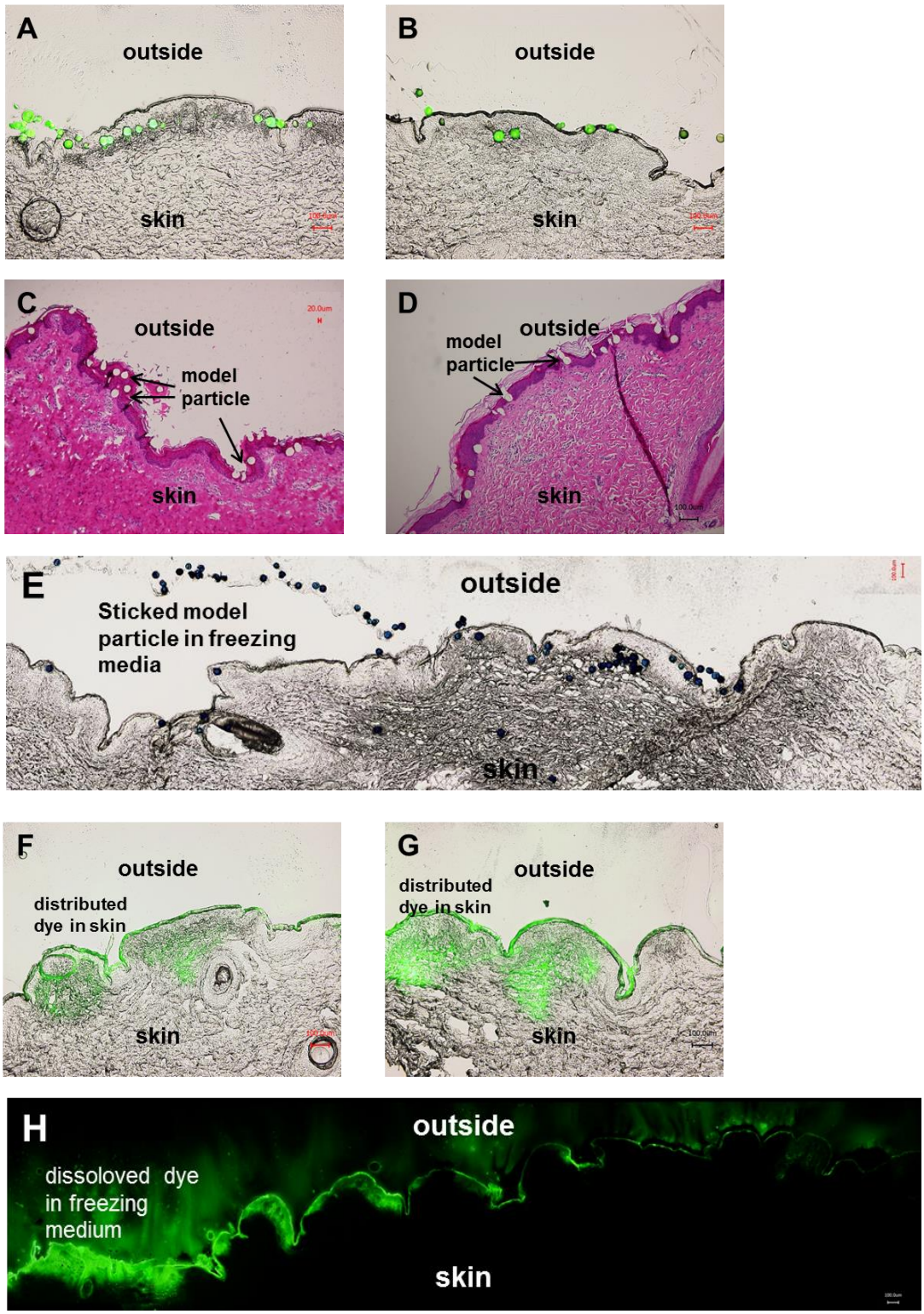

Figure 4.3.3: Overlay of particle penetration into the skin of German Landrace pigs during the *ex vivo* experiments. A and B) overlay of 40 µm FITC labeled polystyrene particles in skin; C and D) HE stained skin slices with penetrated particles; E) overview of the application site of 40 µm polystyrene particles; F and G) overlay of 20 µm-80 µm FITC lyophilizate particles in skin; H) overview of the application site of 20 µm-80 µm FITC lyophilizate particles.

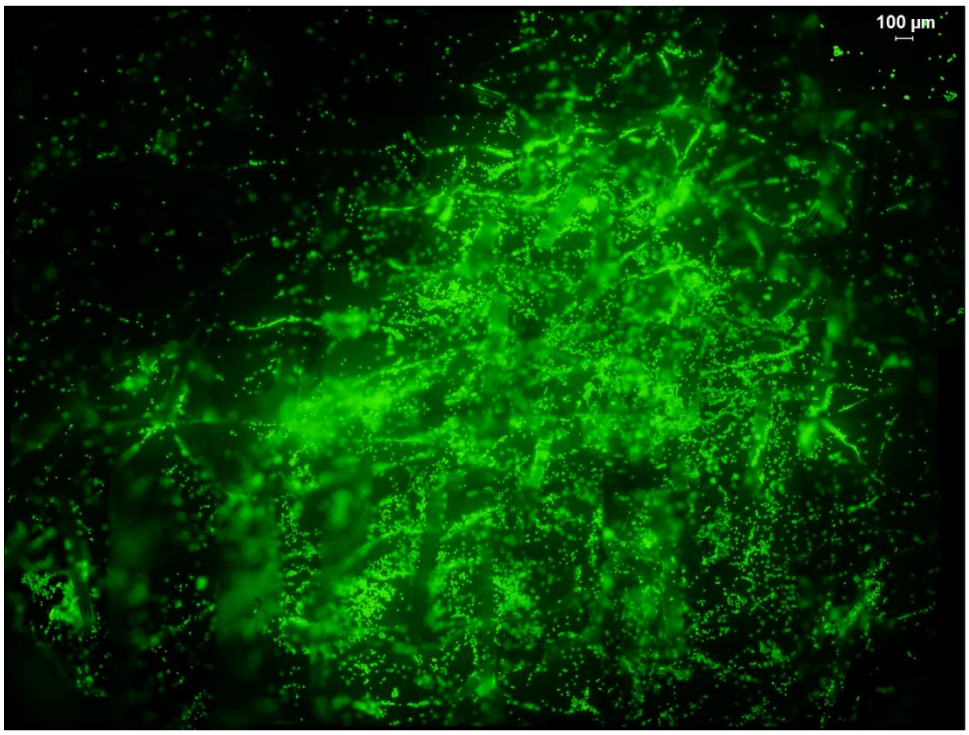

38

Figure 4.3.4: Distribution of 20 µm PS particles applied on *ex vivo* pig skin using the ballistic particle applicator.

Particle penetration was also observed in *in vivo* skin specimens (Figure 4.3.5). Clearly detectable polystyrene particles in the *in vivo* skin slices were located in a depth of approximately 50-120 µm. (Figure 4.3.5A – D). Particles penetrated the skin through the stratum corneum up to the stratum basale, which could be observed in the histological skin slices (Figure 4.3.5C and D). On the contrary, the FITC-labeled lyophilizate particles were not distinctively detectable (Figure 4.3.6E and F). The diffused fluorescent dye of dissolved FITC-lyophilizates was observed in penetration depths between 20 to 120 µm.

Generally, a detection of FITC-labeled lyophilizates in histologically stained *in vivo* skin slices to determine the penetrated tissue layer was not possible (Figure 4.3.6G and H) due to elimination of the dye during the staining procedure. Yet, an administration of the lyophilizates over the complete administration site could be demonstrated in unstained skin slices (Figure 4.3.6I). The application of the particles in in vivo skin revealed no tissue lesions and scaring, as demonstrated also in the histologically stained skin slices after particle administration (Figure 4.3.6C; D; G and H).

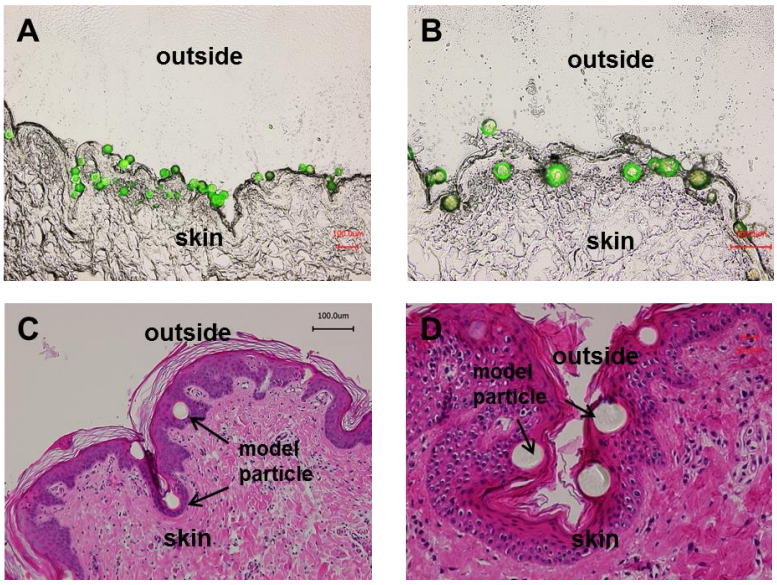

Figure 4.3.5: Overlay of particles penetration into the skin of German Landrace pigs during the *in vivo* experiments. A and B) overlay of 40 µm FITC labeled polystyrene particles in skin slices prepared using the cryotom; C and D) images of 40 µm FITC labeled polystyrene particles in histologically stained skin slices

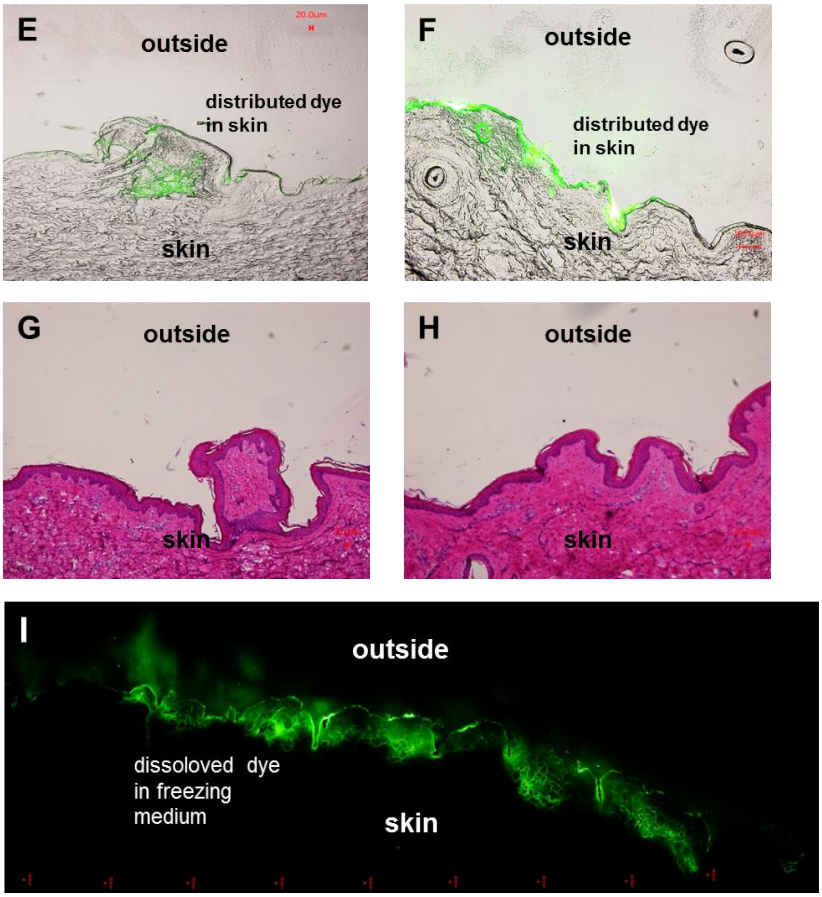

Figure 4.3.6: Overlay of particles penetration into the skin of German Landrace pigs during the *in vivo* experiments. E and F) overlay of 20 µm-80 µm FITC lyophilizate particles in skin slices prepared using the cryotom; G and H) images of 20 µm-80 µm FITC lyophilizate particles in histologically stained skin slices; I) overview of the application site of 20 µm-80 µm FITC lyophilizate particles.

4.3.4 Determination of penetrated particle count in pig skin and skin model using MFI

The total amount of particles loaded on the device was determined using FITC labelled polystyrene particle (41 µm), by firstly following the loading procedure as described in Figure 4.2.2. Afterwards, the particles were rinsed off the membrane with highly purified water and the particle count was determined using MFI. A single dose (100%) of polystyrene particles (41 µm) loaded on the device was washed into 1.5 ml highly purified water and was amounted to 2400 particles per ml +/- 180 (n=4) (i.e. a single dose contained about 3600 particles (41 µm)). An application to the gelatin skin model with low mechanical resistance (gelatin-glycerol (2/9)) was performed to collect all detached particles and to calculate the loaded dose which was set free by the device. The gelatin skin model was dissolved and the particles were transferred to highly purified water to avoid any differences in viscosity of the solution. Approximately 93% ± 7% (n=4) of the particles penetrated into the gelatin skin model (i.e. 3600 particles to 3096 particles were detached from the device per dose).

Microscopic images and particle counts (MFI) revealed a large number of polystyrene spheres, which did not penetrate into the pig skin. The major part only (loosely) adhered to the surface and could be removed (easily) by pressurized air (Figure 4.3.7 and Figure 4.3.8). After removal of polystyrene spheres, particles remained on or in the skin. Particle agglomerations on bristles and in skin folds were distinctly removed by the process while penetrated particles still stuck in the epidermis (Figure 4.3.7).

After dissolving the skin and transferring the particles in highly purified water the amount of particles which had penetrated the skin was determined as about 25% of the emitted dose (i.e. 900 particles to 774 particles could penetrate the skin per dose)

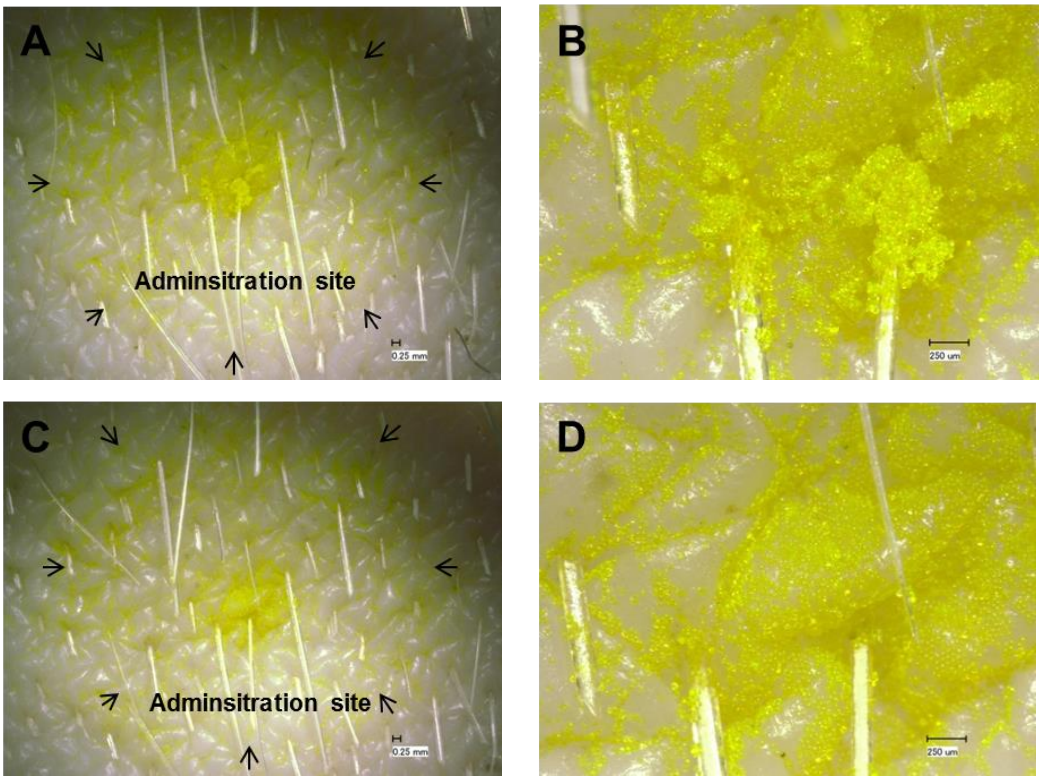

Figure 4.3.7: Skin samples with administered polystyrene particles A) overview prior to removal, B) close-up prior to removal, C) overview after removal, D) close-up after removal

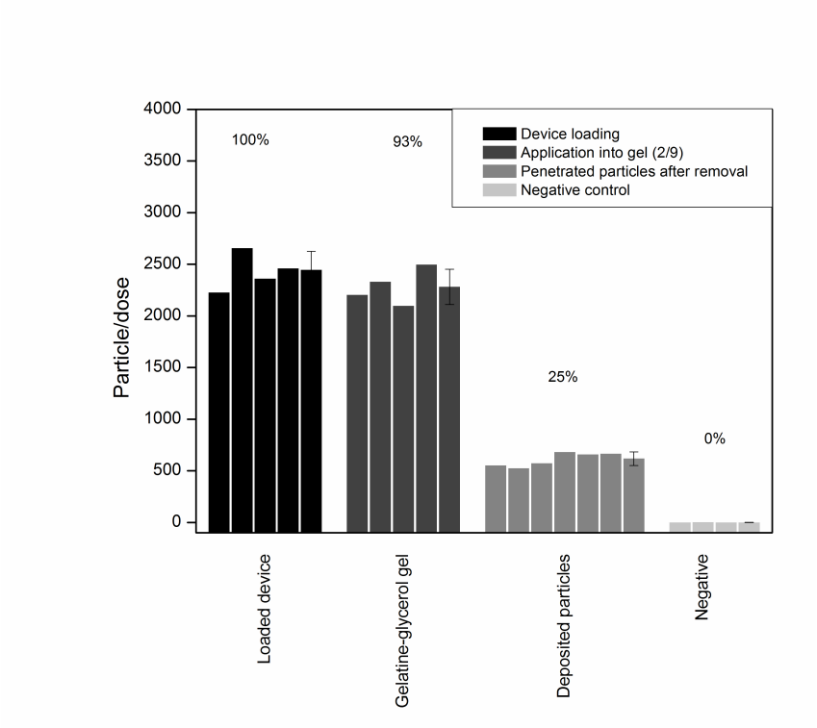

Figure 4.3.8: Polystyrene Particle (41 µm) count in skin samples and skin model using the MFI before and after removal of non-penetrated particles into the *ex vivo* skin. Particle loaded on device was washed in 1 ml highly purified water to use MFI. *Ex vivo* skin without particle application was also used as negative sample (n=4).

4.4 Discussion

4.4.1 Device and particle velocity

In this work, an experimental, pyrotechnical and intradermal powder applicator was tested which was capable to generate particle velocities of over 500 m/s for polystyrene (ϱ= 1.1 g/cm^3) and lyophilizate (ϱ= 1.3 g/cm^3) particle clouds to breach successfully the stratum corneum and to deposit the particles in the tissue below. Particles in a range between 20 µm to 80 µm showed to be large enough to gain enough momentum to penetrate into the skin but were still small enough to avoid bleedings and pain due to the low penetration depth (Figure 4.3.3). Blood vessels and receptors for pain are located in deeper parts of the skin (dermis) in 500 µm-1500 µm (Figure 4.3.3) [123]. For sake of comparison a single glass sphere (ϱ= 2.3 g/cm^3, size = 500 µm) was used as a standard model particle to precisely calculate velocities resulting from the actuation of the device (Figure 4.2.3A and B). The glass sphere was accelerated to more than 600 m/s due to its high density and size compared to polystyrene and lyophilizate particles (Figure 4.2.3A and B).

Accurate velocity determinations of particle clouds were limited compared to the single glass sphere due to the cloud front composed of a high number of small particles 20-80 µm).

The cloud front, which resulted after accelerating lyophilizate particles was rather diffuse and blurred and may mainly be attributed to the polydispersity and the irregular shape of the particles (Figure 4.3.1G and H) lyophilized. Size, surface structure and particle shape were already studied using electron microscopy (**Chapter 2**), but their impact on acceleration and penetration properties needs further elucidation. The sizes of the polystyrene model particles were chosen to cover the range of the lyophilizate particles from 20 µm to 80 µm. The only slight increase of velocity with increasing particle sizes was found to be negligible due to uncertainty of particle velocity measurements.

4.4.2 Application of particles to skin

The examination of particle penetration in *ex vivo* skin demonstrated a successful deposition of the particles around the stratum basale to deliver the particles directly to the antigen presenting cells (LC and DC). While the polystyrene particles were clearly detectable, FITC-labelled lyophilizates dissolved immediately after penetration as desired. As a result, the FITC dye diffused in the tissue. The intended dissolving of lyophilizate particles results in a broader deposition of e. g. an administered vaccine in the skin and might therefore increase vaccination efficacy after intradermal administration.

Despite the differences in shape, density and dispersity, polystyrene and lyophilizate particles demonstrated a comparable penetration pattern over the complete application site (**Appendix** and Figure 4.6.2). We demonstrated in preliminary tests that the shape of the particles had no impact to the penetration depths (Figure 4.6.3).

Skin properties as thickness, tissue composition or moisture vary e. g with age and can have a wide influence on penetration properties and penetration depth [20]. Penetration depth and distribution of particles (polystyrene and lyophilizate particles) in *ex vivo* skin, with one additional freeze-thaw cycle and lack of vascularization and nutrient supply, were comparable to *in vivo* specimens. In order to determine the tissue layer of the deposited particles, a HE staining was performed. While the polystyrene particles were still detectable, the lyophilizates were washed out during the process of the HE-staining of the skin slices (Figure 4.3.6 G and H). Therefore, skin slices were prepared without staining using the cryotom to investigate deposition of the FITC-labeled lyophilizates in the epidermis Figure 4.3.6E and F and Figure 4.6.2).

Summarizing the results of the penetration experiments it can be stated that the new device is capable of accelerating particles to a velocity that suffices to make them penetrate the epidermis of pig skin. Quantitative assessment of penetrated particles showed, that about 25% of the initial applicator loading were finally traceable in the skin tissue. Penetrated particles could create a remaining sinkhole in the stiff stratum corneum and pressurized air simply might remove them from there again. Therefore this technique of excessed particle removal might be reconsidered by using other suitable procedures as e. g. tape striping or rinsing with water. However, the removal

method is a “worst-case- scenario” so that slightly more, up to 1/3 of the particles could had penetrated the skin. Therefore, dose deposition of 1/4 to 1/3 shall be the basis of our calculations.

4.5 Conclusion

In summary, we have tested an experimental pyrotechnical device to deposit particles into the epidermis, where immunocompetent cells (LCs and DCs) are located. Reproducible velocities and cloud shapes of particles could be shown and results confirmed a successful administration of particles into desired penetration depths and over the complete administration site of about 3.1 cm^2.

Further examinations need to be undertaken to increase the count of penetrating particles e.g. higher particle velocity or increasing particle density.

A successful particle loading on the device using oily components (described in **Chapter 3**) and an almost complete detachment (93%) of the particle from the device demonstrated a calculable dose administration. In order to increase the dose deposition into the skin, particle velocity, particle size or density should be modified to increase the momentum of the particles to breach the mechanical barrier (stratum corneum). The particle shape played a tangential role to the penetration depths (Figure 4.6.3). The deposition of the particles in the desired depth (stratum basale) may result in an improved immune response combined with lack of bleedings and pain.

4.6 Appendix

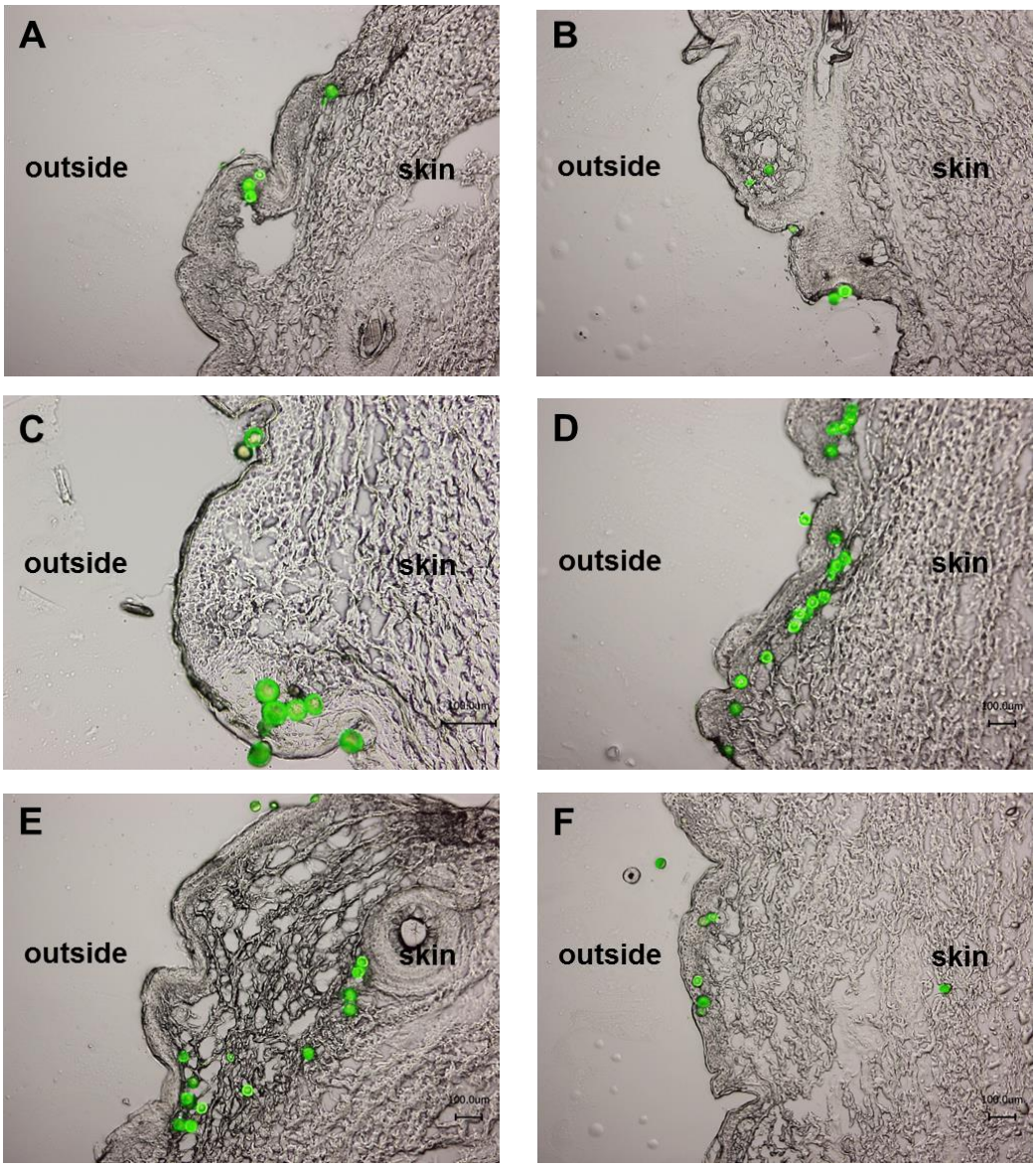

Figure 4.6.1: Overlay of particle penetration into the skin of German Landrace pigs during the *ex vivo* experiments. A -F B) overlay of 40 µm FITC labeled polystyrene particles in skin

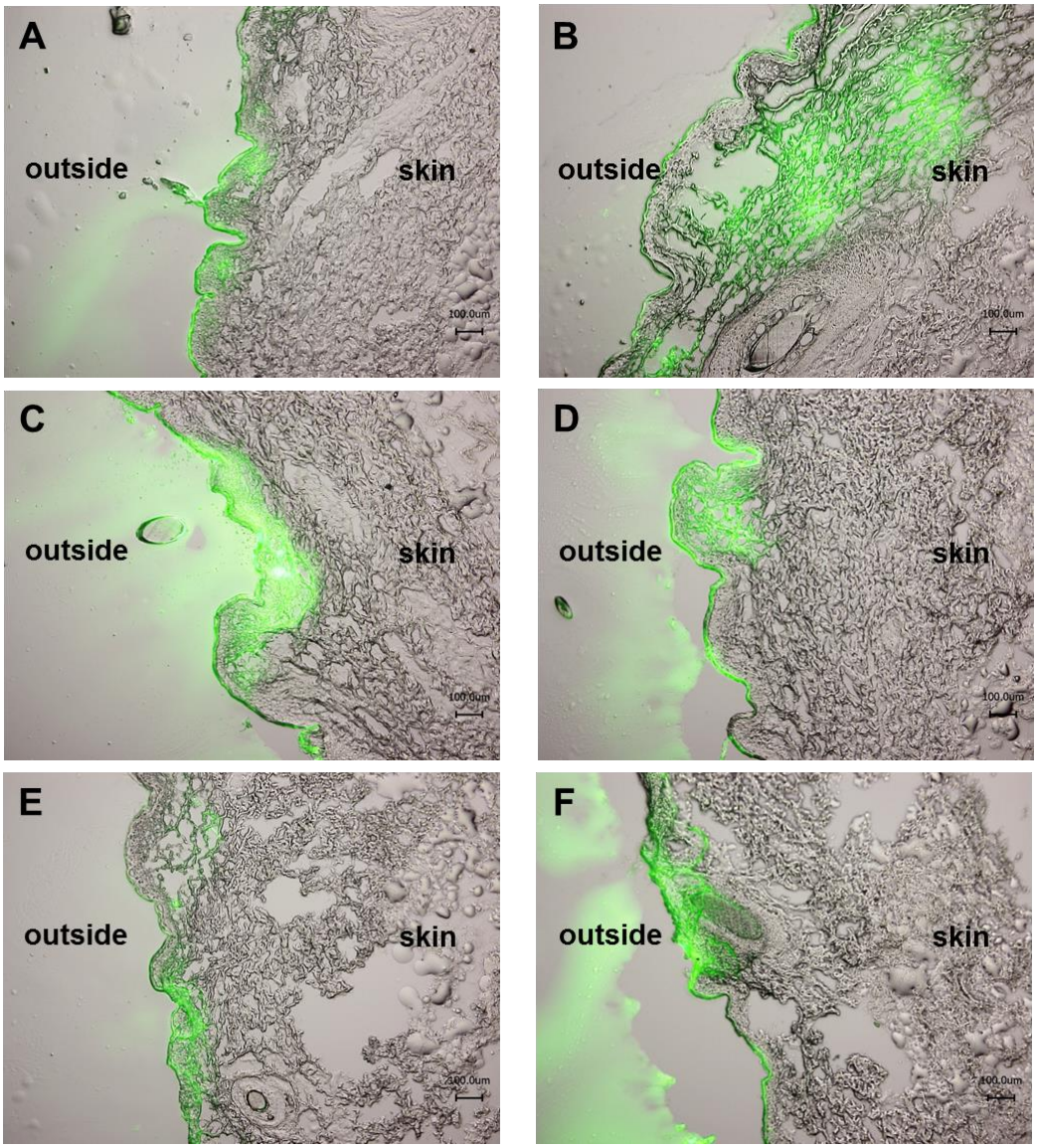

Figure 4.6.2: Overlay of 20 µm-80 µm FITC lyophilizate particles in skin; H) overview of the application site of 20 µm-80 µm FITC lyophilizate particles.

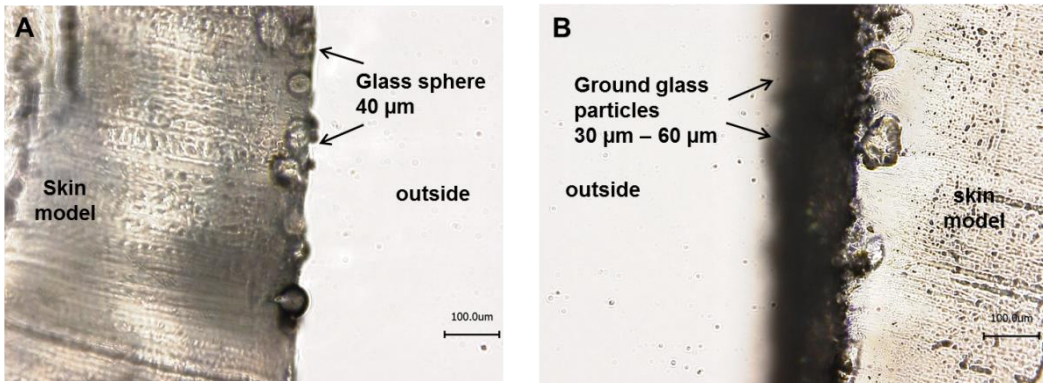

Figure 4.6.3: A) Administered glass spheres (40 µm) into a gelatin-skin model compared against B) ground glass particles administered into a gelatin skin model

4.7 References

1. Babiuk, S., et al., *Cutaneous vaccination: the skin as an immunologically active tissue and the challenge of antigen delivery.* Journal of Controlled Release, 2000. **66**(2-3): p. 199-214.

2. Lambert, L.E., J.S. Berling, and E.M. Kudlacz, *Characterization of the antigen-presenting cell and T cell requirements for induction of pulmonary eosinophilia in a murine model of asthma.* Clin Immunol Immunopathol, 1996. **81**(3): p. 307-11.

3. Hickling, J., et al., *Intradermal delivery of vaccines: potential benefits and current challenges.* Bull World Health Organ, 2011. **89**(3): p. 221-6.

4. Flacher, V., et al., *Targeting of epidermal Langerhans cells with antigenic proteins: attempts to harness their properties for immunotherapy*. Cancer Immunology, Immunotherapy, 2009. **58**(7): p. 1137-1147.

5. Romani, N., et al., *Targeting skin dendritic cells to improve intradermal vaccination.* Intradermal Immunization, 2011: p. 113-138.

6. Romani, N., et al., *Targeting of antigens to skin dendritic cells: possibilities to enhance vaccine efficacy.* Immunol Cell Biol, 2010. **88**(4): p. 424-430.

7. Hoffmann, K., et al., *Twenty MHz B-scan sonography for visualization and skin thickness measurement of human skin.* Journal of the European Academy of Dermatology and Venereology, 1994. **3**(3): p. 302-313.

8. Kendall, M., et al., *Effects of relative humidity and ambient temperature on the ballistic delivery of micro-particles to excised porcine skin.* J Invest Dermatol, 2004. **122**(3): p. 739-46.

9. Kendall, M., T. Mitchell, and P. Wrighton-Smith, *Intradermal ballistic delivery of micro-particles into excised human skin for pharmaceutical applications.* J Biomech, 2004. **37**(11): p. 1733-41.

10. Wagner, H., et al., *Drug distribution in human skin using two different in vitro test systems: comparison with in vivo data.* Pharmaceutical Research, 2000. **17**(12): p. 1475-1481.

11. Lambert, P.H. and P.E. Laurent, *Intradermal vaccine delivery: Will new delivery systems transform vaccine administration?* Vaccine, 2008. **26**(26): p. 3197-3208.

12. Kersten, G. and H. Hirschberg, *Needle-free vaccine delivery.* Expert Opin Drug Deliv, 2007. **4**(5): p. 459-74.

13. Thews, G., E. Mutschler, and P. Vaupel, *Anatomie, Physiologie, Pathophysiologie des Menschen*. Vol. 4. 1999: Wissenschaftliche Verlagsgesellschaft Stuttgart,, Germany.

14. Giudice, E.L. and J.D. Campbell, *Needle-free vaccine delivery.* Advanced Drug Delivery Reviews, 2006. **58**(1): p. 68-89.

15. Chen, D., et al., *Epidermal immunization by a needle-free powder delivery technology: immunogenicity of influenza vaccine and protection in mice.* Nature medicine, 2000. **6**(10): p. 1187-1190.

16. Chen, D., Y.F. Maa, and J.R. Haynes, *Needle-free epidermal powder immunization.* Expert Review of Vaccines, 2002. **1**(3): p. 265-276.

17. Deng, Y., G. Winter, and J. Myschik, *Preparation and validation of a skin model for the evaluation of intradermal powder injection devices.* European Journal of Pharmaceutics and Biopharmaceutics, 2012. **81**(2): p. 360-368.

18. Lell, P., *Needleless injection device with pyrotechnic drive*. 2007, Google Patents.

19. Barbero, A.M. and H.F. Frasch, *Pig and guinea pig skin as surrogates for human in vitro penetration studies: A quantitative review.* Toxicology in Vitro, 2009. **23**(1): p. 1-13.

20. Smalls, L.K., R. Randall Wickett, and M.O. Visscher, *Effect of dermal thickness, tissue composition, and body site on skin biomechanical properties.* Skin Research and Technology, 2006. **12**(1): p. 43-49.

21. Wu, K.S., W.W. van Osdol, and R.H. Dauskardt, *Mechanical properties of human stratum corneum: Effects of temperature, hydration, and chemical treatment.* Biomaterials, 2006. **27**(5): p. 785-795.

5. Chapter – Device development

The device development has been carried out by Dr. P. Lell, Mr. C. Fellner (Pyroglobe GmbH, Hettenshausen) and me as an assistant researcher. The project was co-supervised by Prof. G. Winter and Dr. Engert (Ludwig-Maximilians-University, Munich) and Dr. S. Henke (Innovative Injektionssysteme GmbH, Andernach).

The following Chapter contains a know-how reduced version of the full development report on file.

Major results of the development on the device are laid down in Patent application No.: EP 14 189 971.6 and EP 14 173 786.6, which will be published in May 2016.

5.1 Guiding principles of device design

This chapter will describe the development of the ballistic, particle acceleration device.

The guiding principles of the ballistic device were designing a particle accelerator with immobile parts, a no failure safety concept, providing a platform for easy assembly, and enabling a cost reduction. Of course, the device should provide sufficient acceleration to particles in order to penetrate into the upper layers of the skin (epidermis) and targeting the located antigen presenting cells (APCs) (Figure 5.1.1). After the penetration, the particles should dissolve and distribute to the immunocompetent cells. On the one hand, the vaccine matrix was composed of known and established ingredients in the pharmaceutical environment, the method of stabilization (collapse freeze-drying) demonstrated benefits in stability and the particles would dissolve almost instantly at the administration site due to the properties of a carbohydrate [1-7]. On the other hand, the matrixes of biodegradable carbohydrates led to low densities of approximately 1.0-1.5 g/cm^3 (after lyophilization) and irregular particle shapes induced by the production method of a collapse freeze-dry cycle and additional cryo-milling step [8]. These facts represented major challenges to put enough kinetic energy into the particles to breach through the stratum corneum and deliver the particles into the epidermis. The kinetic energy is composed of the acceleration and the accelerated mass. However, particles with a low density accumulate less kinetic energy compared to their volume, leading to a higher deceleration during the flight route of the particles between the detachments from the membrane to penetrating the skin. Due to the limitations of galenical density increase, higher accelerations are necessary to generate enough momentum in order to deliver the biodegradable carbohydrate particles into the epidermis. In preliminary tests, particle velocities of > 500 m/s were determined to breach the mechanical barrier (stratum corneum) and to accumulate still enough kinetic energy to target the APCs in a depth of 100-200 µm under the skin surface. In order to achieve this goal, the ballistic device had to be adapted to provide sufficient particle acceleration combined with a safe administration. Moreover, the environment of the vaccine powder should be serializable to provide a clean environment for the vaccine.

The device was composed of two functional parts (Figure 5.1.1). The pharmaceutical part was designed to provide a sterile/aseptic environment for the products (vaccine) while the pyrotechnical part supplied the energy source to deliver the particles to the targeted depth.

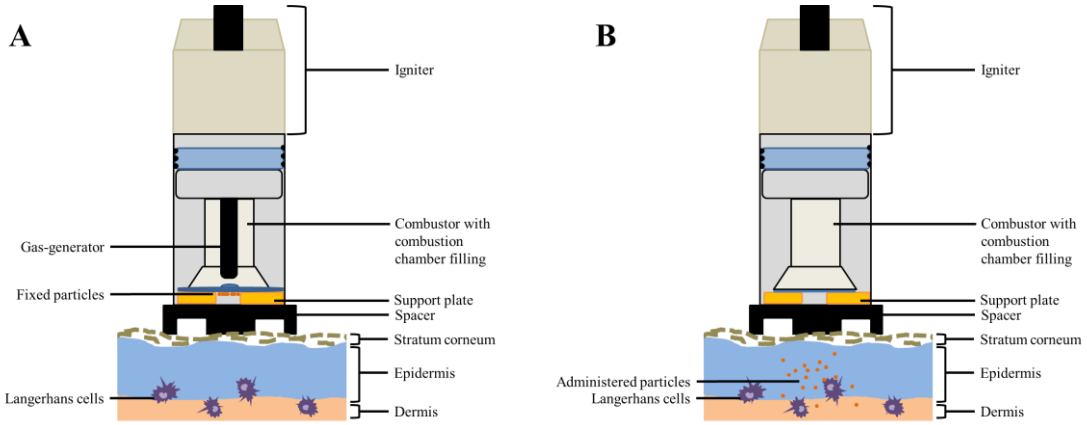

Figure 5.1.1: Particle administration through the stratum corneum into the epidermis to address the vaccine to the Langerhans cell using the ballistic particle applicator (BK01) A) fixed particles previous to administration; B) applied particles penetrated into the epidermis. Skin and device lengths not to scale.

In order to improve the final particle velocity and safety, different mechanical parts of the device were optimized. The development of the parts will be described in the following section (Figure 5.1.2).

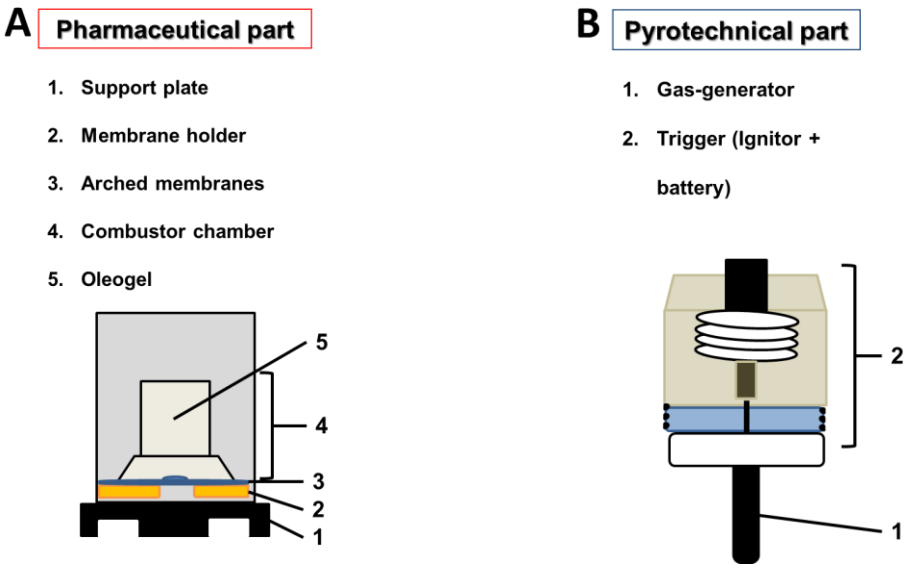

Figure 5.1.2: Experimental particle applicator, separated into the two functional parts A) pharmaceutical part, B) the pyrotechnical part.

5.2 Development of the combustor

While the combustor contains the blast of the gas-generator, it directs the pressure to the membrane in order to accelerate the particles towards the tissue. The amount and focus of the energy transmission highly depends on the design and the volume of the combustion chamber.

A limitation of the combustion chamber volume was given by the size of the gas-generator. A small volume of the combustion chamber would lead to a maximum of contained energy but would also increase the mechanical stress of the membrane disproportionately strong. This energy load could result in membrane damages and device failure. On the other hand, a large combustion chamber volume would decrease the particle velocity due to energy losses during the transmission through the chamber and would effect in insufficient particle acceleration. Fitting the gas-generator into the combustion chamber and thus creating safe but high particle acceleration was established with optimal choice of volume. Beside the optimized volume, the design of the chamber had a great impact to channelize the pressure to the membrane. A cylindrical form of the combustion chamber could not focus the energy adequately and resulted in unreproducible deformations of the membranes. A cone shape next to the membranes would transmit the pressure uniformly but would also increase the chamber volume. While a large cone resulted in decreased particle velocity and inchoate membrane deformations, a small cone increased reproducibly the final velocity.

The final design of a combustion chamber matched the requirements of high velocity and safe particle application due to better channelizing of the driving force through the gap between gas-generator and membranes.

5.3 Composition and development of combustion chamber filling

Optimal energy transmission to the membrane is crucial to accelerate the particles fast enough for sufficient tissue penetration while during the generation of pressure, large energies arise in form of heat, gas and pulse. The filling medium should possess certain properties such as lossless transmission of the pressure, prevention of gas expansion and scattering of gas-generator parts within the combustor, and sufficient viscosity and storage stability to facilitate handling operations. Moreover the filling should also be inert to avoid any interactions with the materials or be toxic. Furthermore, the combustion chamber filling should not evaporate to avoid an additional pressure increase within the combustion chamber. For example, water as a filling content would evaporate instantly during the gas-generation and would lead to an extreme pressure increase within the combustion chamber. Furthermore, storage stable and temperature independent fillings would open a large freedom of applicability of the device.

While air or lipophilic lubricants with high viscosity were poor energy transmitters which resulted in low particle velocities, fillings with low viscosities such as silicone oils (100 cSt, 500 cSt, and 1000 cSt) led to leakages and an oily layer on the membrane (pharmaceutical side) (Figure 5.3.1). Finally, silicone oil (100 cSt) mixed with 5% of a hydrophilic Aerosil® (type 200 pharma) resulted in a silicone oleogel 5% (w/w) with a sufficient viscosity for handling, being safe containing the explosion energy and particle scatter, and excellent transmission of the pressure to the membrane. The energy, which was focused by the combustor design and optimally transferred by the filling, accelerated the membrane and the particles fixed on the membrane.

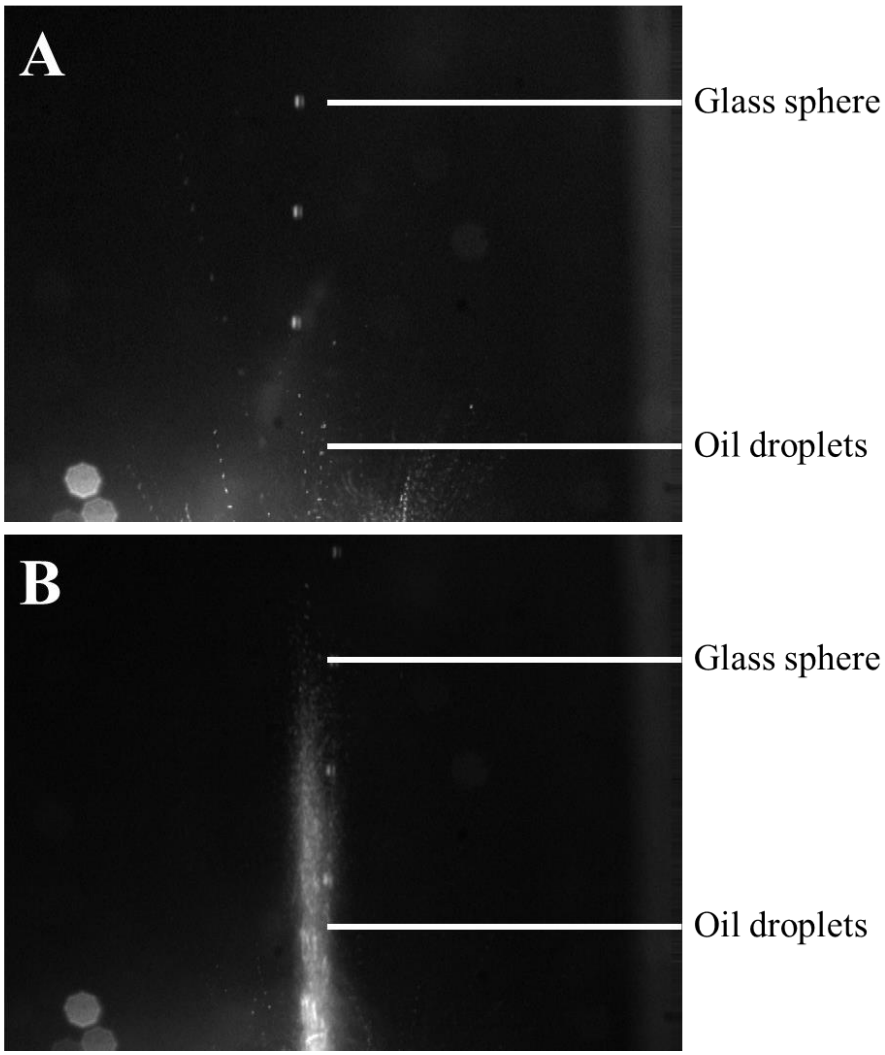

Figure 5.3.1: Photographic images of accelerated 500 µm glass sphere and oil droplets. Droplets occurred due to a thin layer of oil on the membrane prior to the ignition of the gas generator A) leaked out of the combustion chamber; B) coated with a swab on the membrane.

5.4 Choice of material and design of the membranes

Membranes function as the barrier between the pyrotechnical and the pharmaceutical part. Moreover, the membrane which is hit by the pressure should be stable enough to resist the load but at the same time flexible enough to acceleration movement (Figure 5.4.2). Apart from that, the material should possess a low friction force and a smooth surface to prevent irregular deformations during the membrane flipping or material split offs. Membranes consisting of stiff und hard materials are not able to deform fast enough. This delayed material response would lead to increased material stress and damages. On the other hand, materials which are too soft to contain the pulse melt or crack while hit by the pressure. The chosen membrane material demonstrated perfect compromises between hardness, flexibility, friction force, and surface properties. The membranes contained the energy within the combustor and were at the same time flexible enough to accelerate with the pressure and deform without damages. Beside the choice of material, the membrane design has strong impact of particle velocity. Preformed membranes demonstrated an improved acceleration compared to plane membranes (Figure 5.4.1). In order to ensure a maximum of safety in particle administration, a double layer of preformed membranes was established. Using this strategy, micro cracks of one membrane could be sealed by the other layer without any loss of particle velocity. After the particle detachments from the upper membrane (towards the tissue), subsequent membrane deformations occurred induced by the gas generation (Figure 5.4.2).

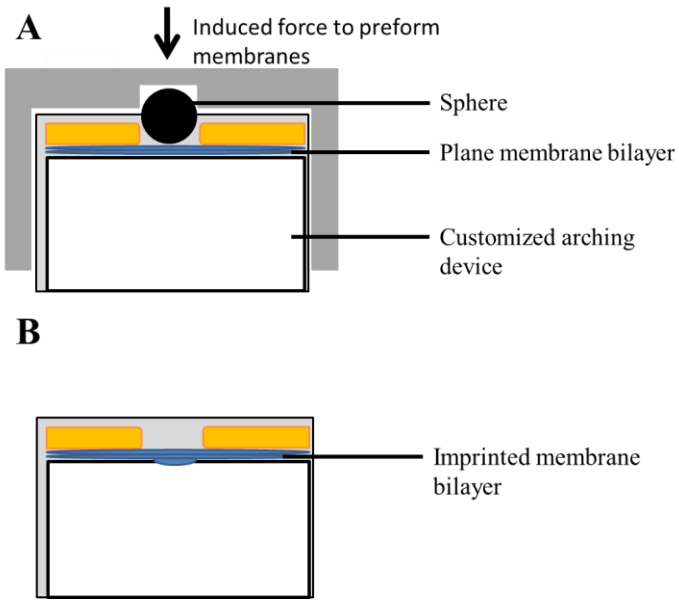

Figure 5.4.1: Schematic figure of membrane imprinting using a customized device. A) plane membrane with sphere to arch the membrane; B) imprinted membrane bilayer.

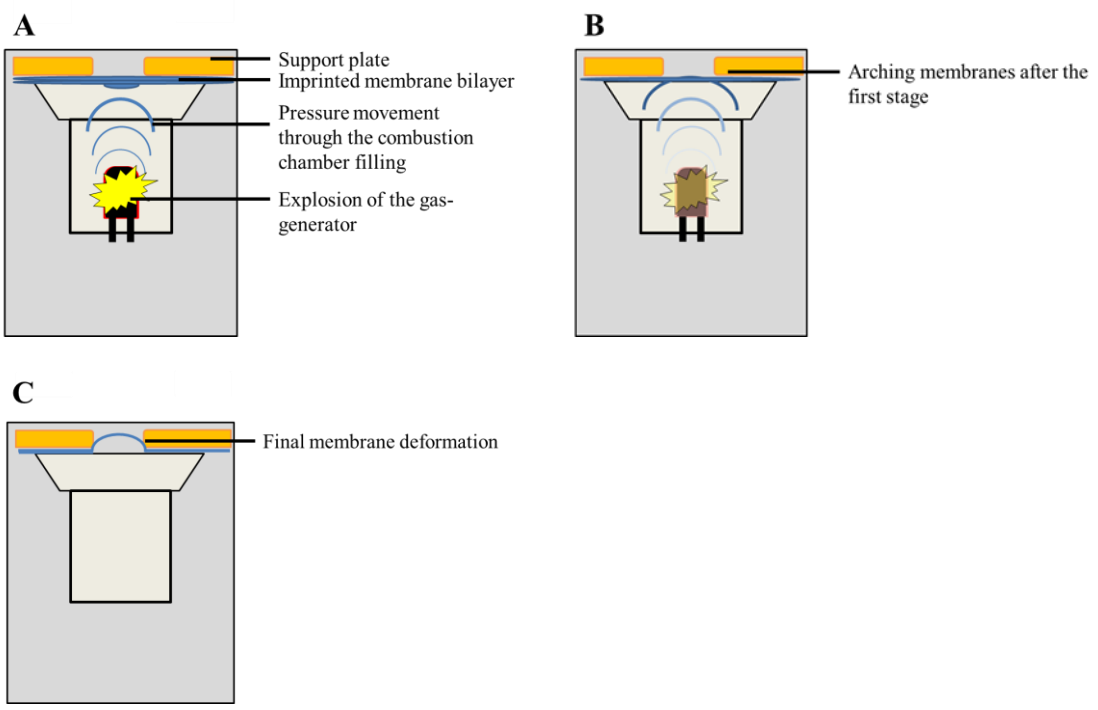

Figure 5.4.2: Flipping of membrane after gas generation A) Explosion of the gas-generator and direction of the pressure through the combustion chamber to the preformed arch; B) flipping of the membrane and C) final deformation of the membrane.

5.5 Design of support plate

The membranes should be fixed between the combustor and the support plate to transfer the momentum from pyrotechnical side of the membranes (induced by the gas-generator) to the particles fixed on the pharmaceutical site of the membranes. The design of the device should channel the deformation and support the membrane stability to resist the high driving forces of the gas generation (Figure 5.4.2).

A small nozzle diameter resulted in membrane damages due to high forces focused on small membrane areas which were forced to deform the membrane through a small nozzle. Furthermore, a smaller nozzle would be accompanied with a reduced loading capacity. On the other hand, a large nozzle diameter led to decrease particle velocity and caused membrane damages. Medium sized diameter stabilized the membrane while the driving force could accelerate the particles without any damages.

5.6 Choice of the gas-generator

The gas-generator as the energy source could be varied in order to optimize the particle acceleration. Variations of gas-generator charges were tested to determine resulting particle velocities and safety. Low gas-generator charges, let the particle velocity (500 µm glass sphere, $\varrho = 2.3\ g/cm^3$) drop drastically, while high charges could induce micro cracks in the membranes without any further velocity increase.

5.7 Conclusion

A gas-generator was established as the energy source and provided sufficient pulse in form of a sudden pressure which could sufficiently accelerate the membrane and the particles. Nonetheless, the pressure was channeled by the customized combustor to maximize the force of impact to the imprinted membrane bilayer. Moreover, transmission of the pulse through the combustor was improved using combustion chambers filling (silicon oleogel 5%) Finally, the pressure hit the membranes which flip from the preformed arch into the opposite direction (Figure 5.4.2). While the membranes deformed, the fixed particles accelerated and finally detached from the membrane with over 600 m/s.

5.8 References

1. Crowe, L.M., D.S. Reid, and J.H. Crowe, *Is trehalose special for preserving dry biomaterials?* Biophysical Journal, 1996. **71**(4): p. 2087-2093.

2. Johnson, R.E., C.F. Kirchhoff, and H.T. Gaud, *Mannitol–sucrose mixtures—versatile formulations for protein lyophilization.* Journal of pharmaceutical sciences, 2002. **91**(4): p. 914-922.

3. Schersch, K.B., *Effect of collapse on pharmaceutical protein lyophilizates*. 2009, Dissertation, Ludwig-Maximilians-University, Munich.

4. Schersch, K., et al., *Systematic investigation of the effect of lyophilizate collapse on pharmaceutically relevant proteins I: Stability after freeze-drying.* Journal of Pharmaceutical Sciences, 2010. **99**(5): p. 2256-2278.

5. Schersch, K., et al., *Systematic investigation of the effect of lyophilizate collapse on pharmaceutically relevant proteins, part 2: stability during storage at elevated temperatures.* Journal of Pharmaceutical Sciences, 2012. **101**(7): p. 2288-2306.

6. Kis, E., G. Winter, and J. Myschik, *Can Collapse Freeze Drying Provide High Density Protein Sugar Particles for Ballistic Powder Injection?* Scientia Pharmaceutica, 2010. **78**: p. 653.

7. Etzl, E.E., G. Winter, and J. Engert, *Toward intradermal vaccination: preparation of powder formulations by collapse freeze-drying.* Pharmaceutical Development and Technology, 2014. **19**(2): p. 213-222.

8. Kis, E.E., G. Winter, and J. Myschik, *Can Collapse Freeze Drying Provide High Density Protein Sugar Particles for Ballistic Powder Injection?* Scientia Pharmaceutica, 2010. **78**: p. 653.

6. Chapter – Proof of concept of intradermal ballistic vaccination in an animal model

6.1 Introduction

Upcoming immunization strategies are considering new vaccination routes such as oral, pulmonary or epidermal administration (described in **Chapter 1**). Especially the thin layer beneath the skin surface excels as a high potential target due to a high density of potent antigen presenting cells (APC, Langerhans cells and dendritic cells) which can generate a sufficiently protective immune response [1, 2]

Human studies would be the most accurate method to determine the effectiveness of intradermal vaccination but accessibility to human skin specimens is limited and suitable artificial skin models with mechanical properties comparable to human skin are lacking. Moreover immune response cannot be determined with artificial models or excised skin. Hence, *in vivo* experiments are inevitable to demonstrate the effectiveness of a new vaccination method. Animal studies are primarily used as a model for human vaccination and shall serve to assess the potential of the intradermal vaccination strategy proposed in this chapter.

A number of factors need to be considered for the selection of an animal model, in particular anatomical and physiological similarities to human skin structure and immune response [3]. Pig skin has been identified as a suitable model for human skin, as it shows comparable density of body hair, epidermis and stratum corneum (SC) thickness, and composition of the keratinous proteins and lipids [4-6]. Moreover, the overall structure of the skin demonstrates large similarities between humans and pigs, such as epidermal turnover time, orientation, and distribution of blood vessels in the dermis.

Intradermal needle injection of liquid vaccines requires intensive and time consuming training for health-care workers in order to pierce the needle through the stratum corneum and deliver the vaccine as a bolus to the APCs. This vaccination technique is difficult to perform and can cause high failure rates. This can be a problem in times of an epidemic, where vaccination programs needs to be performed quickly and effectively and particularly poorly developed health-care systems might have difficulties to implement and carry out extensive vaccination campaigns. [7, 8]. Moreover, antigen production capacities are limited and cannot be increased easily

according to demand. Cold chain storage and delivery can also contribute to shortcomings in vaccine supply. In our experiments we tried to address the above mentioned problems by preparing a powder vaccine product with better stability (demonstrated in **Chapters 2 and 3**) and no need for cold chain storage. The new concept of a ballistic intradermal powder applicator shall make vaccine application simple and painless and therefore speed up vaccination while increasing patient compliance at the same time.

In **Chapter 2 to 5** the preparation of a stable lyophilized influenza vaccine and the development of the new device for intradermal vaccination were described. The aims of the animal experiments presented in this chapter were finally to show whether intradermal application of lyophilized vaccine with the help of the new device was feasible and safe. For this purpose skin reactions and clinical parameters of the test animals before and after immunization were closely monitored. The second objective of the study was to find evidence for the immunogenic potential of intradermally applied HA-antigen (Pandemrix®, GlaxoSmithKline, Rixensart, Belgium). This was investigated by ELISA-assays of sera samples after intradermal vaccination in comparison to i.m. application of the commercial vaccine.

6.2 Material and Methods

6.2.1 Materials

Pandemrix®, H1N1 influenza vaccine, (GlaxoSmithKline, Rixensart, Belgium) was used as a model vaccine and was kindly provided by the Bavarian State Ministry of Environment and Public Health. The commercial product contains 15 µg/ml hemagglutinin formulated in a phosphate buffer with polysorbate 80, octoxynol 10 and thiomersal and an adjuvant (AS03) containing squalene, DL-α- tocopherol, and Polysorbate 80 in a phosphate buffer. The mixture of vaccine and adjuvant was used for the intra muscular **(i.m.) control group** in the experiments. The oily components of AS03 only (squalene, DL-α- tocopherol, and Polysorbate 80) were used to fix the vaccine lyophilizate particles on the device membrane in the verum group (**intradermal application with adjuvant**). Paraffin (Merck KGaA, Darmstadt, Germany) was also used for particle fixation (**intradermal application without adjuvant**) and served as a control to investigate the adjuvant effect. For buffer preparation, sodium hydrogen phosphate monohydrate was purchased from Gruessing (Gruessing, Filsum, Germany) and sodium dihydrogen phosphate dihydrate, sodium phosphate monobasic and dibasic, sodium hydroxide, and sodium chloride were obtained from Applichem (Applichem, Darmstadt, Germany).

Trehalose, used as lyoprotectant, was purchased from BDH Prolabo (VWR, Ismaning, Germany) and mannitol, used as bulking agent, was obtained from Boehringer Ingelheim (Ingelheim, Germany). For the Enzyme-linked Immunosorbent Assay (ELISA), di-sodium carbonate, potassium chloride, sodium hydrogen carbonate, and potassium dihydrogen phosphate were received from Merck KGaA (Darmstadt, Germany). Hematoxylin and eosin stain, 25% hydrochloric acid, 96% ethanol, and carbol-xylol were obtained from Merck (Darmstadt, Germany). Xylol was purchased from W.Gaeen GmbH&Co. (Munich, Germany). Eukitt solution was purchased from Vitro-Clud (Langenbrunck GmbH, Emmendingen, Germany). Tween 20, Bovine Serum Albumin (BSA), 3,3´,5,5´-Tetramethylbenzidine (TMB), stop reagent for TMB, Nunc maxisorb 96 well-plates, and anti-swine IgG (H+L)-peroxidase, produced in goat as secondary antibody, were obtained from Sigma-Aldrich (Taufkirchen, Germany). Endotoxin determinations were performed using an EndoSafe-PTS and

cartridges with a sensitivity of 0.5-0.005 EU/ml (Charles River Laboratories, L´Arbresle, France).

6.2.2 Methods

6.2.2.1 Concentration of vaccine by tangential flow filtration (TFF)

The concentration of influenza vaccine using a tangential flow filtration method was carried out under laminar air flow (LAF) (HeraSafe, (Thermo Fischer scientific, Rockford, USA) in order to ensure aseptic preparation. The vaccine was concentrated using a filtration cassette Minimate™ (PALL, Dreieich, Germany) with a cut-off pore size of 5 kDa. Prior to usage, the TFF cassette was sanitized with 0.5 M NaOH at 45°C for 45 min as recommended by the manufacturer. Subsequently, the TFF cassette was rinsed with highly purified water (Sartorius Arium Pro, Sartorius, Goettingen, Germany) until a neutral pH was measured, using a seveneasy® pH-meter (Mettler Toledo, Giessen, Germany) and until the endotoxin value was below the detection limit as described in section 6.2.2.15. The TFF cassette membrane was saturated with 60 ml of a circulating vaccine solution for 60 minutes. The concentration of the influenza vaccine was performed at a flow rate of 100 ml/min as recommended by the manufacturer using a peristaltic pump (Masterflex, Ponndorf, Germany). After a volume reduction of 96% (final concentration > 150 µg/ml), the concentrated vaccine solution was dialyzed against 10 mM phosphate buffer (0.22 µm filtered) (PALL life Sciences, Ann Arbor, USA). Finally, the concentration of the modified solution was adjusted to 150 µg/ml using RP-HPLC (as described below).

6.2.2.2 Adjusting of vaccine concentration

Hemagglutinin concentration was determined using RP-HPLC and was calculated as follows: area under the curve (AUC) of HA commercial product compared to AUC of modified vaccine solution. The hemagglutinin peak was recorded using a fluorescence detector (λ_{ex} 280 nm and λ_{em} 335 nm) and the AUC of the modified solution was

compared to the commercial product. Pandemrix has a declared hemagglutinin concentration by the manufacturer of 15 µg/ml.

6.2.2.3 Addition of lyoprotectants and bulking agents

A final concentration of 15% solid content with 3.75 µg/mg hemagglutinin was prepared by adding trehalose and mannitol (1:1) (w/w) to the modified vaccine solution. After gentle stirring at approximately 50 rpm (IGAMAG RCT, IKA®-Werke GmbH & Co. KG, Staufen, Germany), 0.22 µm filtration, and hemagglutinin concentration determination (RP-HPLC), the lyophilization mixture was ready for collapse freeze-drying.

6.2.2.4 Lyophilization processes

DIN 10R vials (Mglas AG, Muennerstadt, Germany) were heat sterilized (180°C/3 hours) in a Binder FED 53 (Binder GmbH, Tuttlingen, Germany) and filled with 2.625 ml of the final lyophilization mixture with a filling level of approximately 1 cm. Subsequently, the vials were semi-stoppered (Westar®RS.stoppers, Westpharma, Exton, USA) and transferred to the Martin Christ Epsilon 2-12D freeze-dryer equipped with a pirani pressure sensor (Martin Christ, Osterode, Germany).
The middle shelf was loaded with 84 vials filled with lyophilization mixture, 42 vials filled with 15% trehalose-mannitol (1:1) (w/w) solution in 10 mM phosphate buffer and surrounded by two rows of edge vials.
After the equilibration phase at 4°C for 1 hour, samples were frozen to -50°C within 1.5 hours and stabilized for a further hour. The temperature was increased to -40°C (ramp of 0.33°C/min) while the chamber pressure was reduced to 1.98 mbar. Subsequently, the shelf temperature was increased to 45°C (ramp of 0.71°C/min) and held at that temperature for further 24 hours. Secondary drying started with an additional pressure reduction to 0.3 mbar, and these conditions (0.3 mbar / 45°C) were maintained for further 20 hours. Finally, the temperature was reduced to the storage temperature of 4°C and the samples were stoppered at approximately 800 mbar with dry nitrogen gas atmosphere.

6.2.2.5 Cryo-milling and sieving

Previous to milling, the milling tools were placed in hot-air sterilizer (Binder GmbH, Tuttlingen, Germany) for heat sterilization and depyrogenation (180°C/3h) while the sieving equipment was sanitized in 80% ethanol for 48 hours. Afterwards, lyophilizates were transferred under a LAF into stainless steel milling jars with two stainless steel balls (Retsch Technology GmbH, Haan, Germany). After a precooling (liquid nitrogen) of ten minutes with a milling frequency of 5 Hz, the grinding was performed at 25 Hz for 15 sec. using a Retsch CryoMill (Retsch Technology GmbH, Haan, Germany). The equilibration of jars to ambient temperatures for 2 hours and classifying (20, 80, and 125 µm) was carried out under a LAF. Aliquots of particles (20-80 µm) were filled in DIN 10R vials and stoppered with Westar®RS.stoppers.

6.2.2.6 Reversed-Phase chromatography (RP-HPLC)

The hemagglutinin content in the samples was determined using a Dionex HPLC system equipped with a Dionex P680 HPLC Pump, ASI-100 automated sample injector, Dionex Column oven, Dionex RF-2000 Fluorescence Detector and a Dionex UVD170u UV/VIS-detector (Dionex, Idstein, Germany). Separation was performed using a Phenomenex Jupiter 5 µ, C18, 300 A column (250 x 4.6 mm) (Phenomenex, Aschaffenburg, Germany) at 60°C with a gradient elution over 30 min at a flow rate of 1.0 ml/min. Eluent A consisted of highly purified water with 0.1% trifluoric acid and eluent B comprised 75% 2-propanol, 25% acetonitrile and 0.1% trifluoric acid. Lyophilizated samples were dissolved in 2.625 ml highly purified water. The separation of a 25 µl sample solution was accomplished with the gradient starting at 20% eluent B, increasing to 36% within 10 min, a ramp to 95% (14.75%/min), plateau for further 4 min. and an abrupt drop to 20% for 12 min. Intrinsic fluorescence (λ_{ex} 280 nm and λ_{em} 335 nm) was used to determine hemagglutinin. Data acquisition was performed using the Chromeleon 6.80 software (Dionex, Idstein, Germany). Preparation of the oily part of AS03

The oily part of AS03, containing 10.69 g of squalene, 11.86 g DL-α-tocopherol, and 4.86 g Polysorbat 80 was mixed using a magnetic stirrer at approximately 50 rpm and then stored at 2-8°C until usage.

6.2.2.7 Preparing of 5% silicone oleogel as energy transmission medium

In order to transfer the energy from the gas-generator without any loss to the vaccine particles fixed on the membrane, a silicone oleogel was prepared (described in **Chapter 4 and 5**). Silicone oil (100 cSt) (Sigma-Aldrich, Taufkirchen, Germany) and 5% Aerosil R200 Pharma (Evonik Industries AG, Hanau-Wolfgang, Germany) (w/w) were mixed in 24 ml syringes (Norm-Ject, HenkeSassWolf, Tuttlingen, Germany) connected with a Luer adapter (Combifix Adapter, B.Braun, Melsungen, Germany) and depressurized to 10 mbar in a vacuum oven (Memmert, Schwabach, Germany) for 4 hours (Figure 6.2.1). Afterwards, silicone oil was pressed into Aerosil®, while the chamber was pressurized back to the atmospheric pressure (approximately 1 bar). After a final homogenization by mixing the oleogel within two connected syringes, the product was ready to use (Figure 6.2.1).

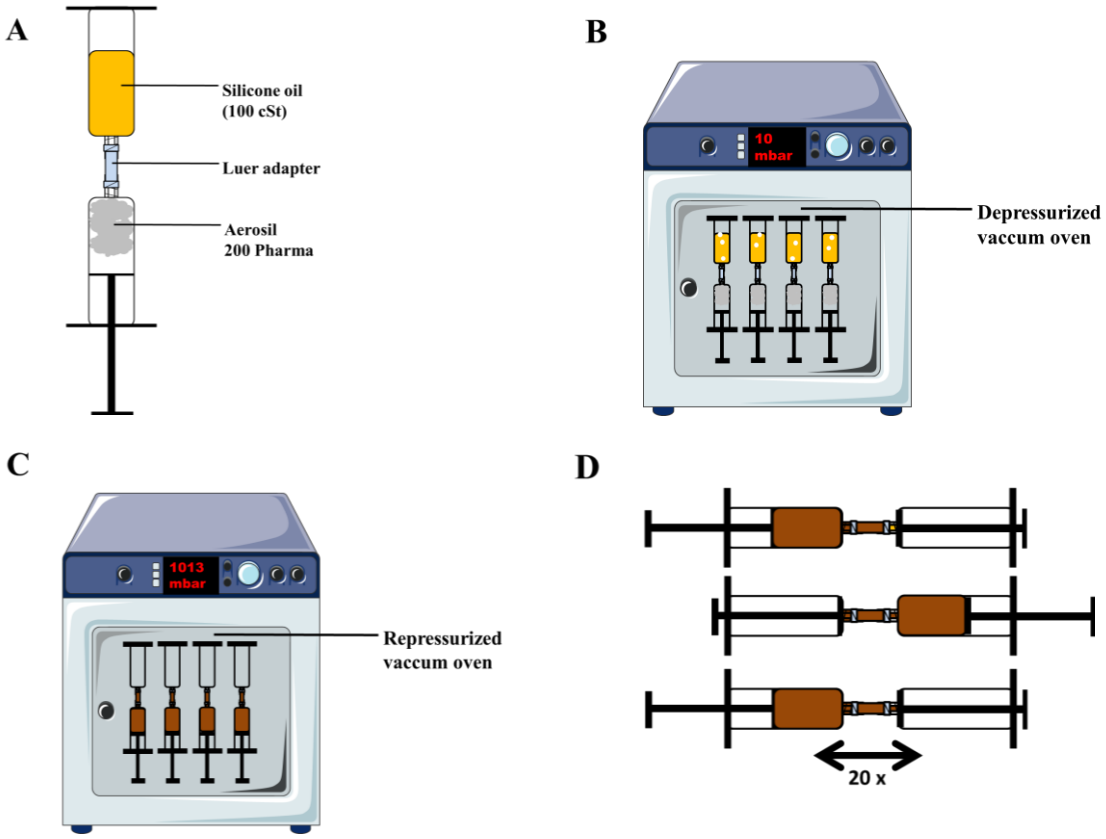

Figure 6.2.1: Schematic figure of air bubble free silicone oleogel 5% preparation. A) syringe with silicone oil and Aerosil 200 Pharma, B) depressurizing of Aerosil and silicone oil, C) silicone oil pressed into syringe with Aerosil, while pressurizing chamber, D) homogenization of oleogel

6.2.2.8 Device preparation and particle loading for animal experiments (Group A-C)

A more detailed description of the device can be found in **Chapter 4 and 5.** The device components of the pharmaceutical part with product contact (modified membranes and supporter plates) were cleaned with 70% 2-propanol and subsequently wrapped into aluminum foil (Carl Roth GmbH&Co KG, Karlsruhe, Germany) for heat sterilization and depyrogenation (180°C/3h) in a hot-air sterilizer (Binder GmbH, Tuttlingen, Germany). After the assembly of the pharmaceutical part on a clean bench, the membrane was coated with an oily component (paraffin or oily part of AS03) and loaded with prepared vaccine lyophilizate particles using a customized funnel which was gently put through the nozzle (Figure 6.2.2). The particles (placebo (trehalose-mannitol) particles or vaccine loaded particles) were

scattered through the funnel on the coated membrane until the membrane surface was overfilled (Figure 6.2.2). The device was inverted and the funnel was carefully taken out to avoid a swirling of the particles in the pharmaceutical part of the device. Subsequently the inverted particle applicator was tapped on the bench to detach loose particles (Figure 6.2.2). Finally, the pharmaceutical part was sealed with a customized foil (IIS, Andernach, Germany) to inhibit permeation of moisture and to keep the particle applicator clean and sterile until use.

Three groups of devices were prepared with particles fixed with an oily component on the membranes (Table 6.2.1). For the first group (**placebo without adjuvant, Group A**), only carbohydrate lyophilizate (15% trehalose-mannitol (1:1) (w/w) solution in 10 mM phosphate buffer) particles were fixed with paraffin on the membrane. Vaccine particles were fixed with paraffin in the second group (**verum without adjuvant, Group B**), while vaccine particles attached on the membrane using the oily part of AS03 in the third group (**verum with adjuvant, Group C**) (Table 6.2.1). About 0.35 mg±0.05 mg (n= 5) of the oily adjuvant mixture was coated onto the membrane which resulted in a particle amount of 1.81±0.19 mg (n= 5) (Figure 6.2.2) brought on the membranes after preparation. The amount of adjuvant loaded on the device was determined by the difference of weight of the membrane (before and after coating). The maximal particle loading capacity of the device was limited to 1.81 mg±0.19 mg (carbohydrate particles, 1.77 mg±0.07 mg for polystyrene particles 40 µm). The limitation was a result of the particle fixation area on the membrane of 3.14 cm^2 and the adhesion forces of the oily components to fix the particles on the membrane. The dose of 1 mg of vaccine particles was equivalent to 3.75 µg HA.

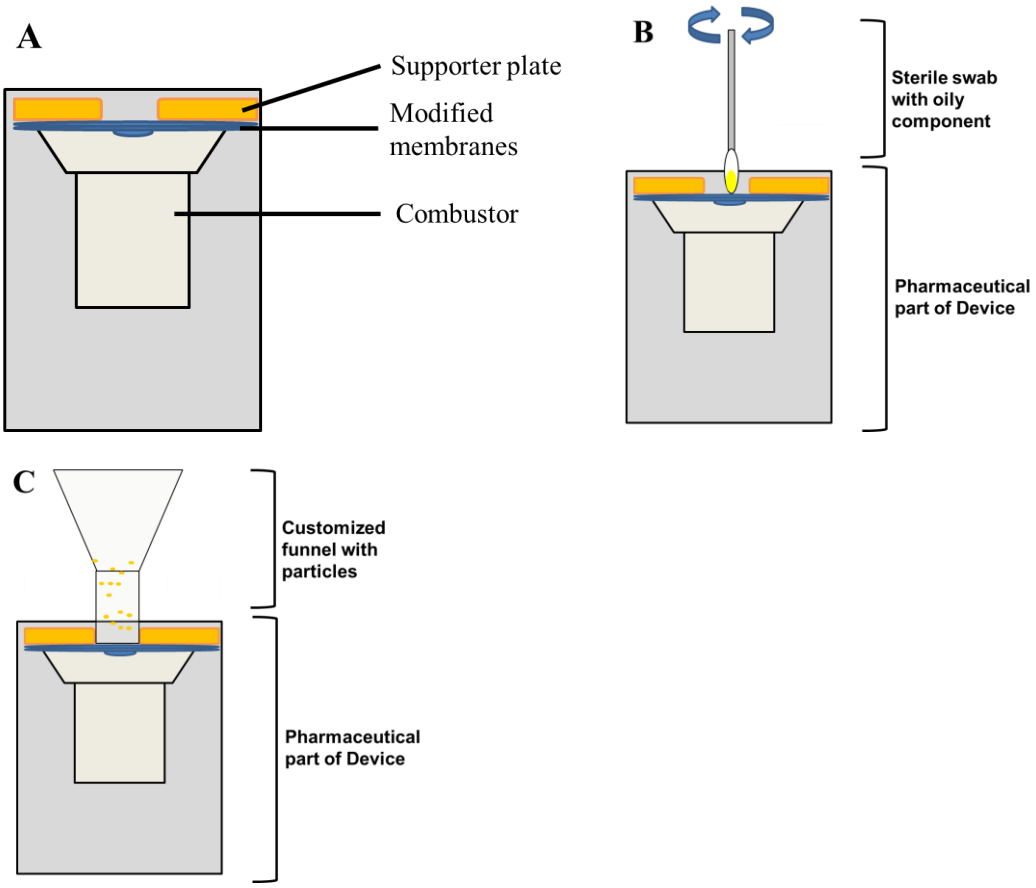

Figure 6.2.2: Preparation and particle loading on the membrane of the ballistic powder applicator A) the pharmaceutical part of the device, B) coating with oily component (paraffin or oily part of AS03 using a sterile swab, C) particle loading using customized funnel

6.2.2.9 Liquid vaccine preparation for intra muscular group (challenge group) (Group D)

Shortly before the animal experiments were conducted, the adjuvant (AS03) was transferred to the influenza vaccine vial using a syringe and carefully mixed as recommended by the manufacturer (GSK, Middlesex, United Kingdom) to prepare the injection. Doses of 0.5 ml of the mixture were stored in syringes at 2-8°C until use for intramuscular administration.

Table 6.2.1: List of administration groups, each group consisted of 7 pigs. The amount of adjuvant for intradermal administration was determined using three independent measurements (n=3).

Group	Particle	Fixation	Amount of adjuvant	Administration route
A	Placebo	Paraffin	No adjuvant	Intradermally
B	Vaccine	Paraffin	No adjuvant	Intradermally
C	Vaccine	Adjuvant (oily components of AS03)	0.35 mg±0.05 mg	Intradermally
D	Vaccine	Adjuvant (AS03)	0.25 ml	Intramuscularly

6.2.2.10 Animal keeping and immunization

From a farrowing to fattening farm 28 healthy, five weeks old, commercial cross-bred piglets (LWxPI) were transported to the Clinic for Swine (Oberschleissheim, Germany). Animals were randomly assigned to one of four groups (A-D) according to their weight. Each group was housed in pens of 2.5 m^2 x 4 m^2 on solid floor and straw. Water and food was available ad libitum. The general health status of each piglet was documented daily. After a two week adaptation phase, i.e. on study day d 0, piglets of groups A, B and C were fixed by one person, an anesthetic mask for dogs was put on the nose and anesthesia was introduced using 5 Vol% Isoflurane (Isoba® MAC 1,5 Vol% Essex Tierarznei) mixed with oxygen. After muscle relaxation induced by the anesthesia, the pig was placed on the right side. Inhalation anesthesia was maintained during particle application using the ballistic powder applicator. The administration sites for intradermal applications on day 0 were situated on the left of the mammilla complex approximately 15-20 cm cranial from the groin. The area was cleaned using tissues and the hog hairs were trimmed carefully to avoid any skin irritations. After the particle administration, the area application site was carefully marked with tattoo color. The animals of the placebo group (Group A) were vaccinated with carbohydrate lyophilizate particles fixed with paraffin, while Group B was vaccinated with vaccine particles (verum) fixed with also paraffin on the device. Vaccine particles fixed with the oily components of AS03 (squalene, DL-α-tocopherol, and Polysorbate 80) were applied to the animals of Group C. Particles which did not penetrate the skin could be rubbed of due to a lack of a coverage (e.g. adhesive plaster) on the administration site. The animals of Group D (positive control group) were fixed using a snear and received an intramuscular injection of 0.5 ml ready-made, commercial Pandemrix vaccine (see

section 6.2.2.9) into the left neck muscle (injection cannula 19 G) (B.Braun, Melsungen, Germany). After 14 days, all animals were boostered with their allocated group-vaccine preparation but on the right body side. Every single administration site was documented photographically and then covered using an adhesive plaster (Hansaplast, BSN medical GmbH, Hamburg, Germany).

A detailed clinical observation was performed daily from day 0 to day 28 and recorded according to a scoring system. (Results of clinical observations are described in section 6.3.2) Blood Samples (serum) were collected from the vena cava superior before and 1, 14, 21, and 28 days after the first application and stored at -80°C until examination. Additionally, the application sites were photographed on days 0 directly before and after application and after 5 minutes, 1, 2, and 14 days. On study day 28, all animals were euthanized using Pentobarbital (Release 500mg/ml, 45mg/kg i.v.) (WDT, Garbsen, Germany).

All procedures and the experimental protocol were officially approved by the Government Office of Upper Bavaria, Munich, Germany (authorization reference number 55.2.1.54-2532-87-12; 30.08.2012).

6.2.2.11 Skin preparation

On day 28 after euthanasia, the administration sites of the intradermal powder immunization were excised manually using a scalpel and stored on dry ice for transportation (detailed description in **Chapter 4**).

6.2.2.12 Hematoxylin and eosin stain (HE stain) of skin slices and microscopic examination

Specimens were dyed using a haematoxylin and eosin stain (HE stain). Skin slices were embedded in HE stain for 5 minutes and subsequently washed with tap water for further 5 minutes. Samples were shortly moved through a 0.5% hydrochloric acid-ethanol solution with an additional washing step afterwards. Thereafter, the samples were briefly put into a 1% eosin solution and subsequently washed again with water. The prepared slices were dried in ascending ethanol concentrations (50%, 70%, 80%,

96%, and 100%) for 1 minute per concentration. Finally, specimens were shortly covered with carbol-xylol and xylol. The slices were fixed with the Eukitt solution on microscope slides.
Specimens were microscopically examined using a BZ8100 Biozero Micrsocope (Keyence, Neu-Isenburg, Germany) (detailed description in **Chapter 4**).

6.2.2.13 Processing of blood samples (serum)

Blood samples were centrifuged at 15000 rpm/min for 45 minutes to separate sera from cellular components. Subsequently, these samples were stored at -80°C until further usage for specific anti-HA-antibody-titer determination using ELISA. A positive control was collected from H1N1 sera positive pigs and was kindly provided from the Friedrich-Loeffler-Institute (Riems, Germany).

6.2.2.14 Enzyme-linked Immunosorbent Assay (ELISA)

A carbonate-bicarbonate coating buffer pH 9.6 was prepared mixing di-sodium carbonate (0.318 g) and sodium hydrogen carbonate (0.586 g) with highly purified water (up to 200 ml). A 10x PBS (1.5 M) stock solution pH 7.4 resulted by mixing sodium chloride (80 g), di-sodium hydrogen phosphate (14.4 g), potassium di-hydrogen phosphate (2.0 g), potassium chloride (2.0 g) and highly purified water (1000 ml). A washing buffer (PBS-T) was prepared using 10% of the PBS-stock solution diluted with highly purified water (900 ml) and Tween 20 (500 µl). Blocking buffer and dilution buffer contained 5% (2.0 g/40 ml) or rather 1% (1 g/100 ml) BSA respectively and PBS-T was adjusted to pH 7.4. All solutions were adjusted using a seveneasy® pH-meter (Mettler Toledo, Giessen, Germany) and filtered through a 0.22 µm filter. Finally, a vaccine-coating solution was prepared using 200 µl of the commercial vaccine filled up to 20 ml with coating buffer. Sera samples were diluted 1:25 and the anti-swine IgG (H+L)-peroxidase conjugated secondary antibody 1:25000 with dilution buffer.

On the first day of the ELISA analysis, each well of a 96 well-plate was coated with 100 µl of vaccine-coating solution except row 8 (negative control row). After 12 hours incubation time at 2-8°C, the well-plates were washed with 600 µl/well PBS-T using a hydroflex plate washer (Tecan, Crailsheim, Germany). Subsequently, blocking buffer

(100 µl/well) incubated for 1 hour to minimize unspecific adsorptions. After a further washing cycle, 50 µl of dilution buffer was pipetted in each well and additionally 50 µl of serum sample in each well of the first column (two-fold determinations per animal). Subsequently, two-fold dilution steps were performed each with a transfer of 50 µl and incubated for 2 hours. Well-plates were washed again with PBS-T and 50 µl/well of secondary antibody was added and incubated for 1 hour. After the final washing cycle, 50 µl/well TMB was pipetted and developed for exact 10 min before the reactions were stopped using the Stop reagent (Figure 6.2.3). Intensity of the reaction was red out using a FLUOstar Omega (BMG-Labtech, Ortenberg, Germany). Data were collected with Omega Data Analysis (BMG-Labtech, Ortenberg, Germany). Statistical calculations were performed using SigmaPlot 12.5 (Systat Software GmbH, Erkrath, Germany).

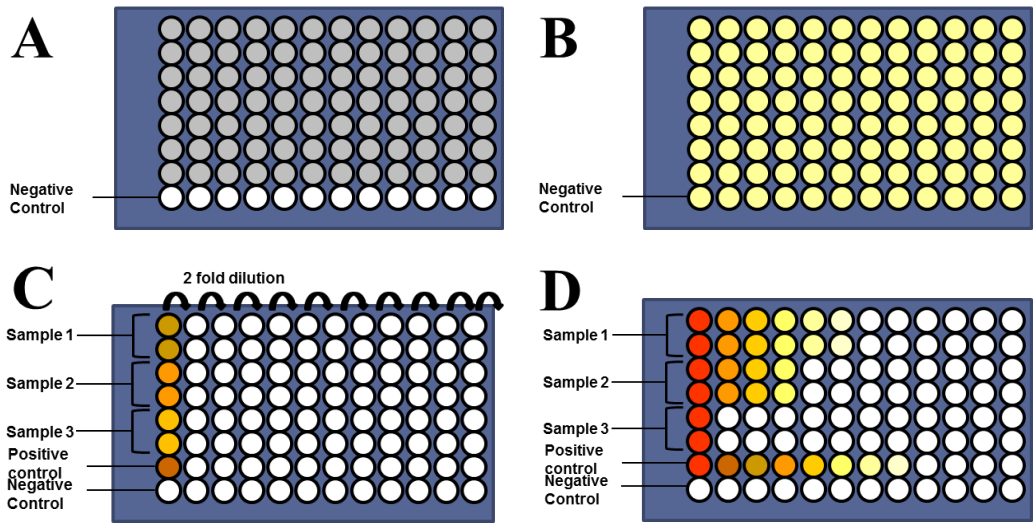

Figure 6.2.3: Schematic presentation of ELISA. A) coating with vaccine-coating solution on day 1, B) blocking to prevent unspecific reaction on day 2, C) 2-fold dilution of sera samples on day 2, D) TMB reaction and read out on day 2.

6.2.2.15 Endotoxin determination

EndoSafe- PTS and cartridges with a sensitivity of 0.5-0.005 EU/ml were inserted into the EndoSafe-PTS. After the equilibration, 200 µl of sample were carefully pipetted into the cartridge as recommended by the manufacturer. Finally, the endotoxin content was displayed by the device.

6.3 Results

6.3.1 RP-HPLC – Comparison of antigen concentration

The areas under the curves (AUC) of the samples were determined to calculate the amount of hemagglutinin in each specimen using a fluorescence detector (λex 280 nm and λem 335 nm). Therefore, the HA content of the commercial product was compared to collapse and cryo-milled lyophilized vaccines. The amount of HA was calculated as follows: AUC of commercial product (15 µg/ml) was directly compared to the AUC of lyophilized samples (adjusted to 15 µg/ml). All samples demonstrated an AUC of approximately 115.63 ± 2.71 mV*min (Figure 6.3.1). Neither the process of collapse lyophilization nor the cryo-milling had a detectable impact on hemagglutinin content and so a comparable dose of dried vaccine particle to the liquid dose could be administered to the animals.

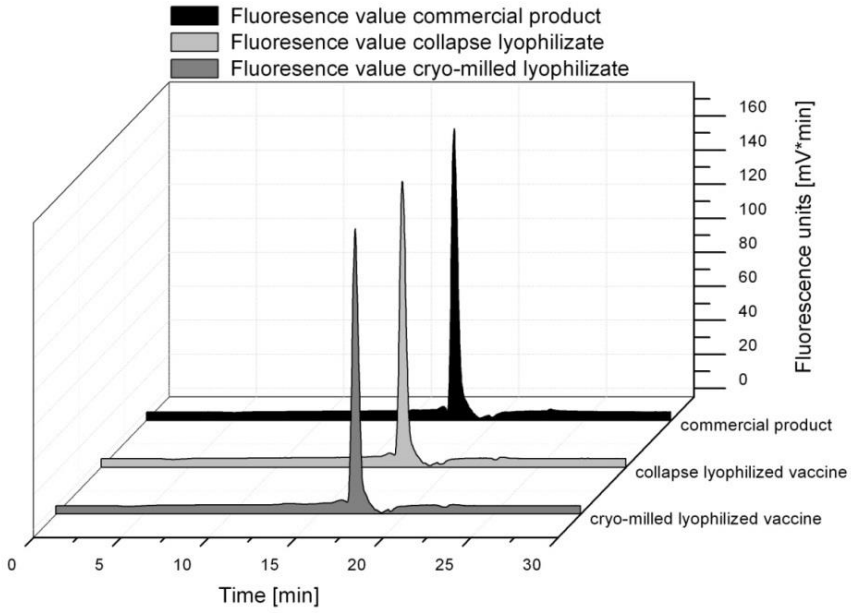

Figure 6.3.1: Fluorescence units of the commercially available product (15 µg/ml), stressed vaccine (15 µg/ml), and collapse lyophilized vaccine (15 µg/ml). Three independent measurements were performed (n=3).

6.3.2 Administration sites after intradermal powder immunization

The particles were administered within a marked administration site (marked with a permanent marker and tattoo dye) of 5 cm x 5 cm. A round imprint on the skin was observed on all administration sites after intradermal powder immunization. Circular particle residues were more distinct for the placebo group (Group A) compared to the two i.d. verum groups (Groups B and Group C). Redness up to slight bleedings and a discharge of tissue fluids were more pronounced in the verum groups (groups B and C) and developed within 5 minutes after immunization. The skin of the piglets felt soft which got firm over the time of four weeks. The bruises were consistent up to two days and vanished afterwards while the scab peeled from the skin without any traces (Figure 6.3.2, Figure 6.3.3, Figure 6.3.4 and Figure 6.3.5).

Day 0, group A, animal 1

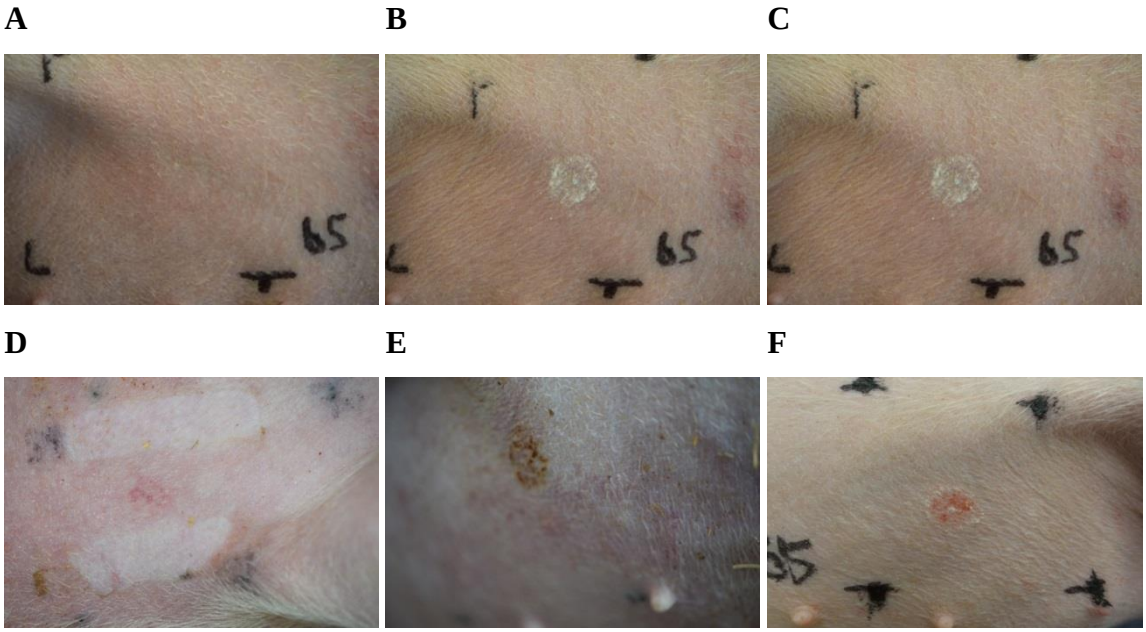

Figure 6.3.2: Group A (animal 1) i.d. application of placebo powder fixed with paraffin on ballistic device A) administration site before application; B) administration site directly after application; C) administration site after 5 min latency; D) administration site at day 1; E) administration site at day 2; F) administration site after boost application at day 14

Day 0, group A, animal 2

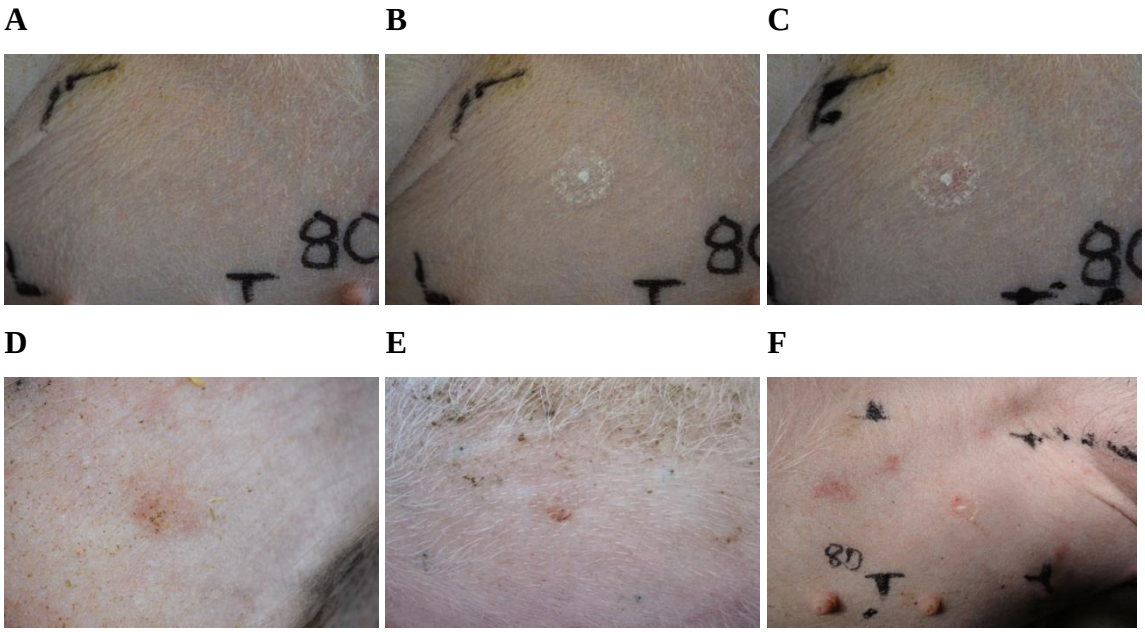

Day 0, group A, animal 3

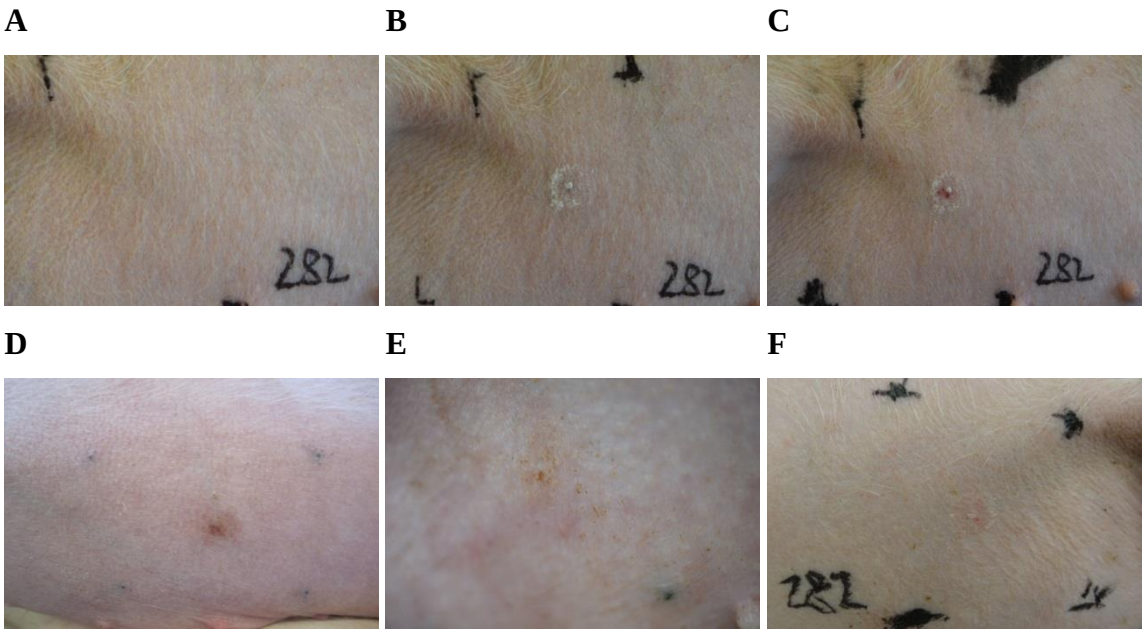

Figure 6.3.3: Group A (animal 2 and 3) i.d. application of placebo powder fixed with paraffin on ballistic device A) administration site before application; B) administration site directly after application; C) administration site after 5 min latency; D) administration site at day 1; E) administration site at day 2; F) administration site after boost application at day 14

Day 0, group A, animal 4

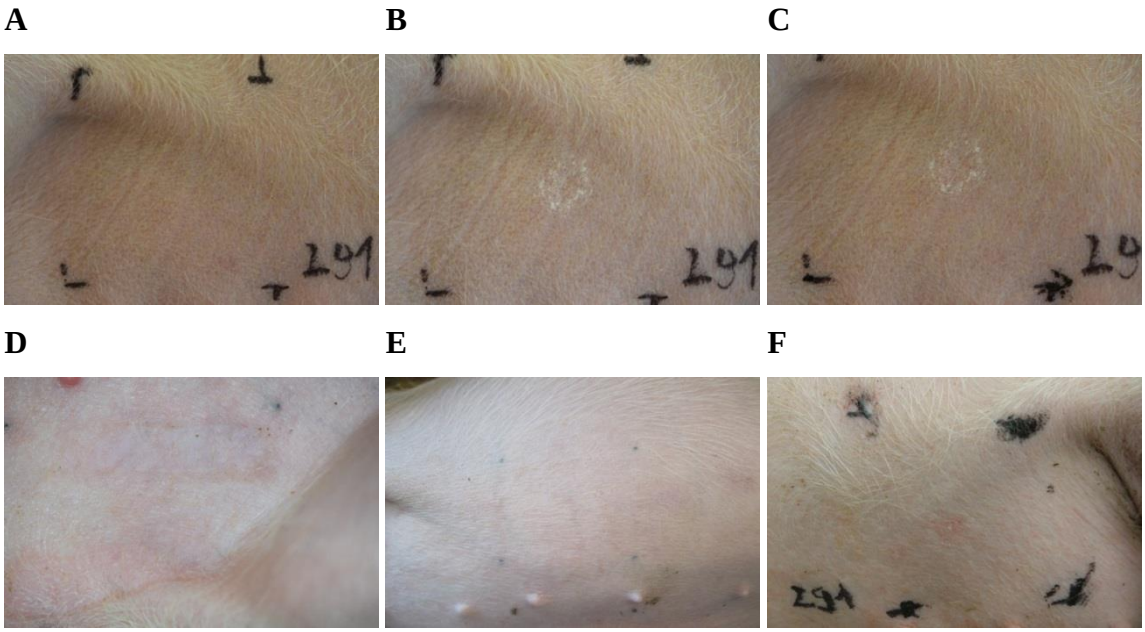

Day 0, group A, animal 5

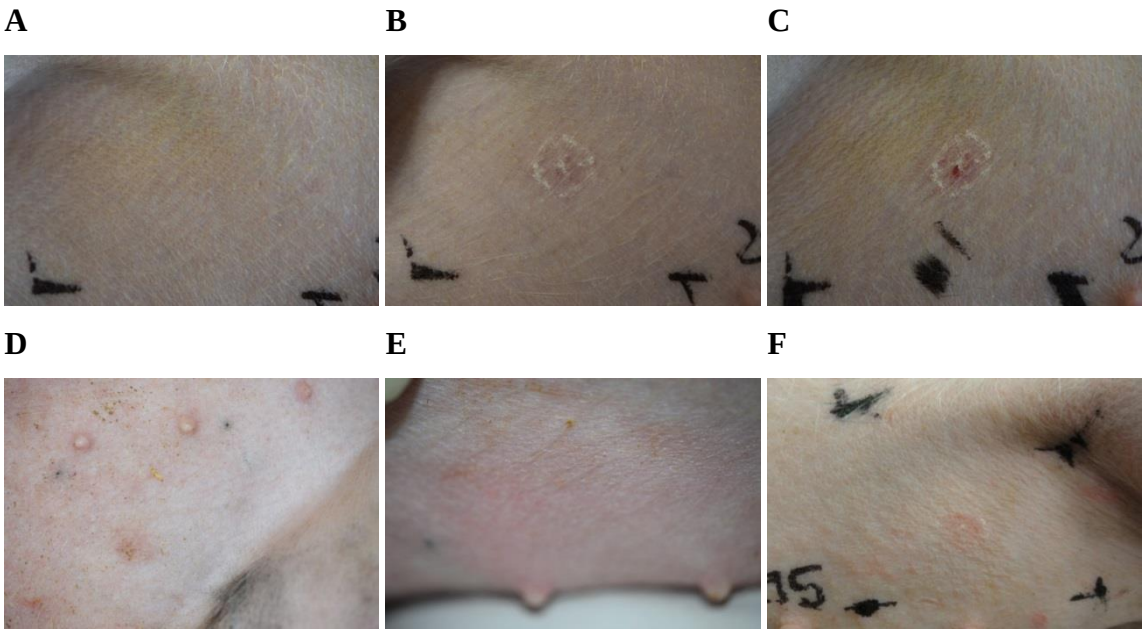

Figure 6.3.4: Group A (animal 4 and 5) i.d. application of placebo powder fixed with paraffin on ballistic device A) administration site before application; B) administration site directly after application; C) administration site after 5 min latency; D) administration site at day 1; E) administration site at day 2; F) administration site after boost application at day 14

Day 0, group A, animal 6

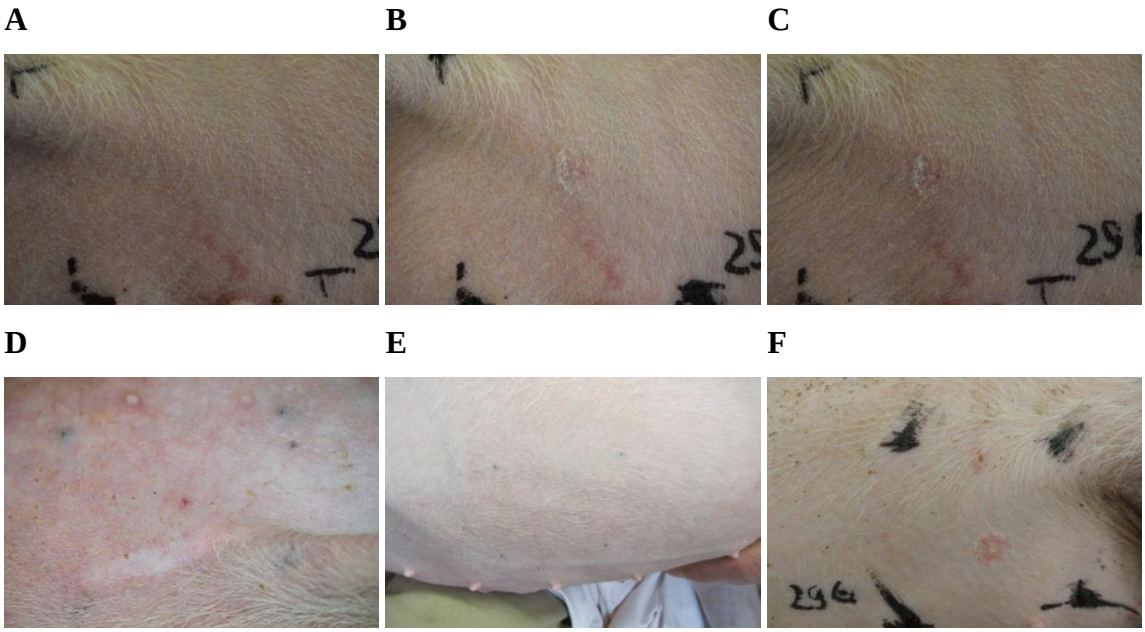

Day 0, group A, animal 7

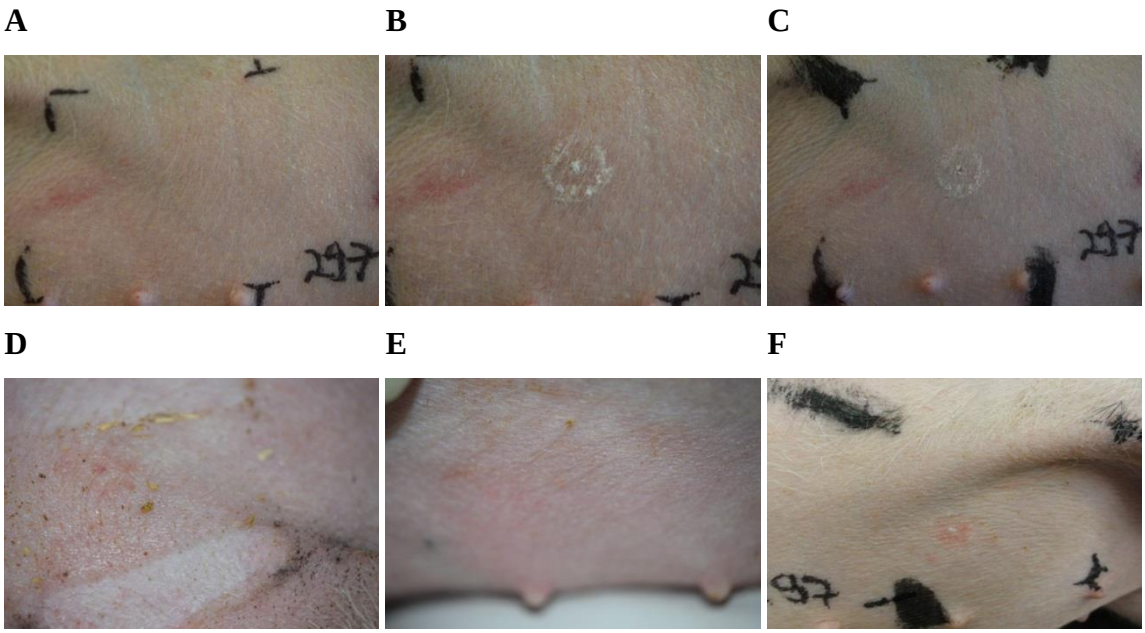

Figure 6.3.5: Group A (animal 6 and 7) i.d. application of placebo powder fixed with paraffin on ballistic device A) administration site before application; B) administration site directly after application; C) administration site after 5 min latency; D) administration site at day 1; E) administration site at day 2; F) administration site after boost application at day 14

The skin irritations of the intradermal powder immunization did not distinctly extend to the surrounding tissues after the application. However, the second immunization (day 14) left less distinct marks at the administration sites compared to the first particle application (day 0) due to firm skin of maturated piglets. The powder immunization of the verum groups (Group B and Group C) resulted in a slightly stronger irritation on the skin while the administration sites of Group A were barely visible. Nevertheless, bleedings or discharges of tissue fluids were not observed and all application marks healed until the next day (Figure 6.3.6, Figure 6.3.7, Figure 6.3.8 and Figure 6.3.9).

Day 0, group B, animal 8

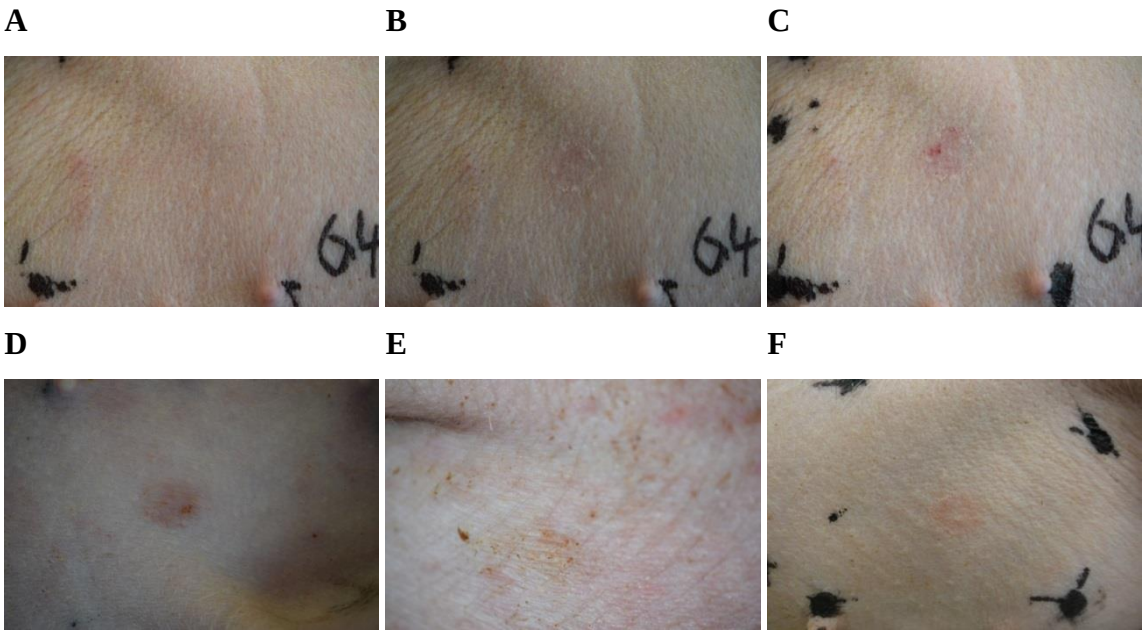

Figure 6.3.6: Group B (animal 8) i.d. application of vaccine powder fixed with paraffin on ballistic device A) administration site before application; B) administration site directly after application; C) administration site after 5 min latency; D) administration site at day 1; E) administration site at day 2; F) administration site after boost application at day 14

Day 0, group B, animal 9

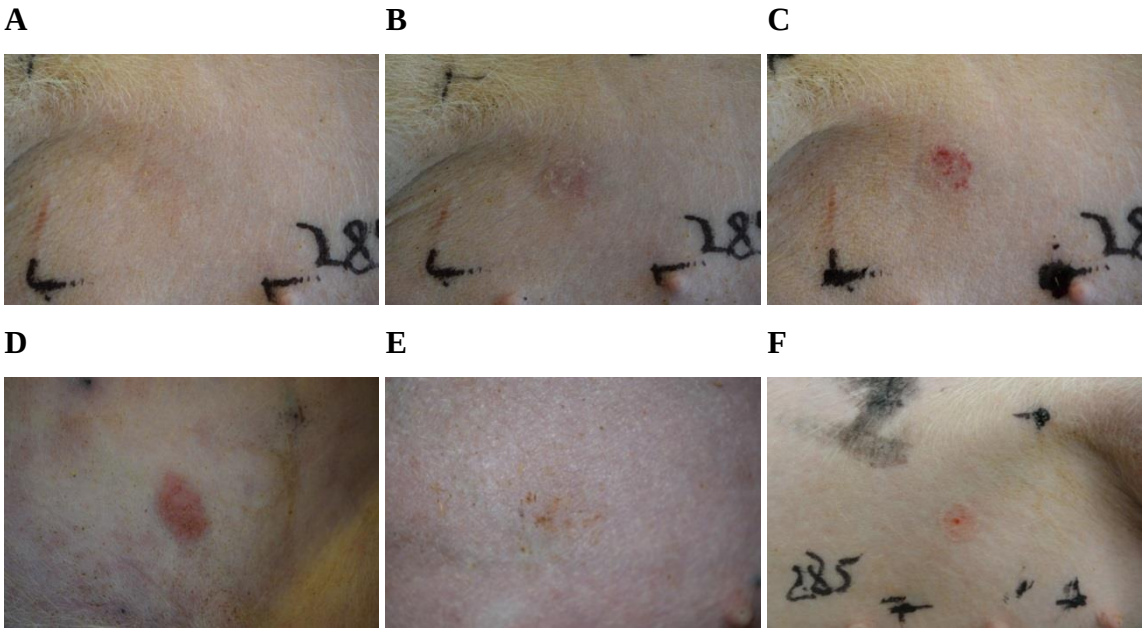

Day 0, group B, animal 10

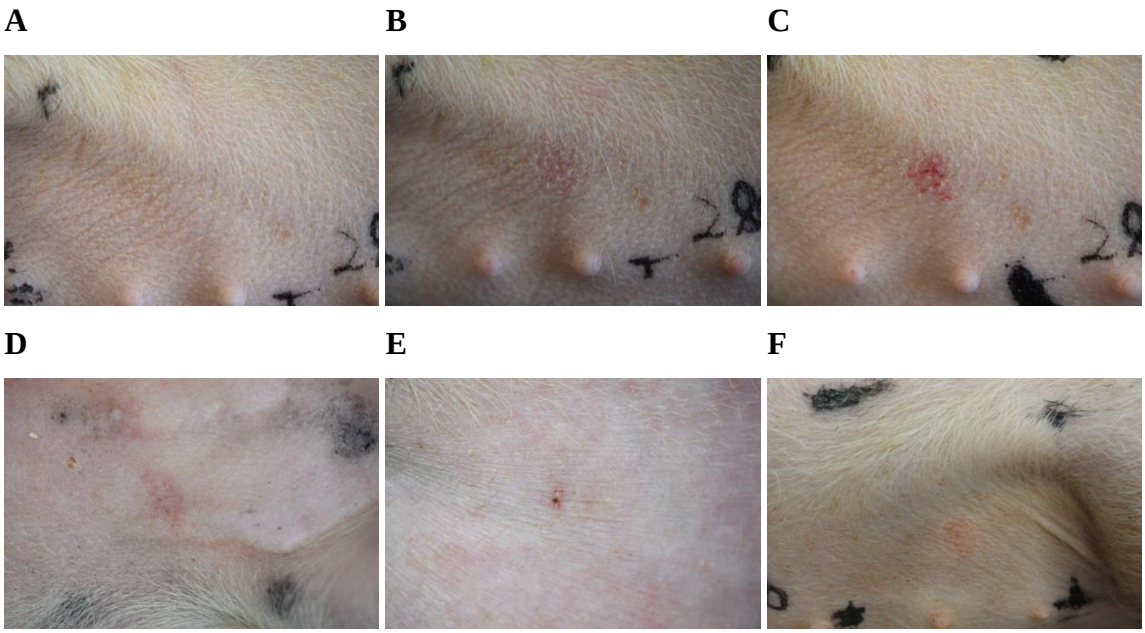

Figure 6.3.7: Group B (animal 9 and 10) i.d. application of vaccine powder fixed with paraffin on ballistic device A) administration site before application; B) administration site directly after application; C) administration site after 5 min latency; D) administration site at day 1; E) administration site at day 2; F) administration site after boost application at day 14

Day 0, group B, animal 11

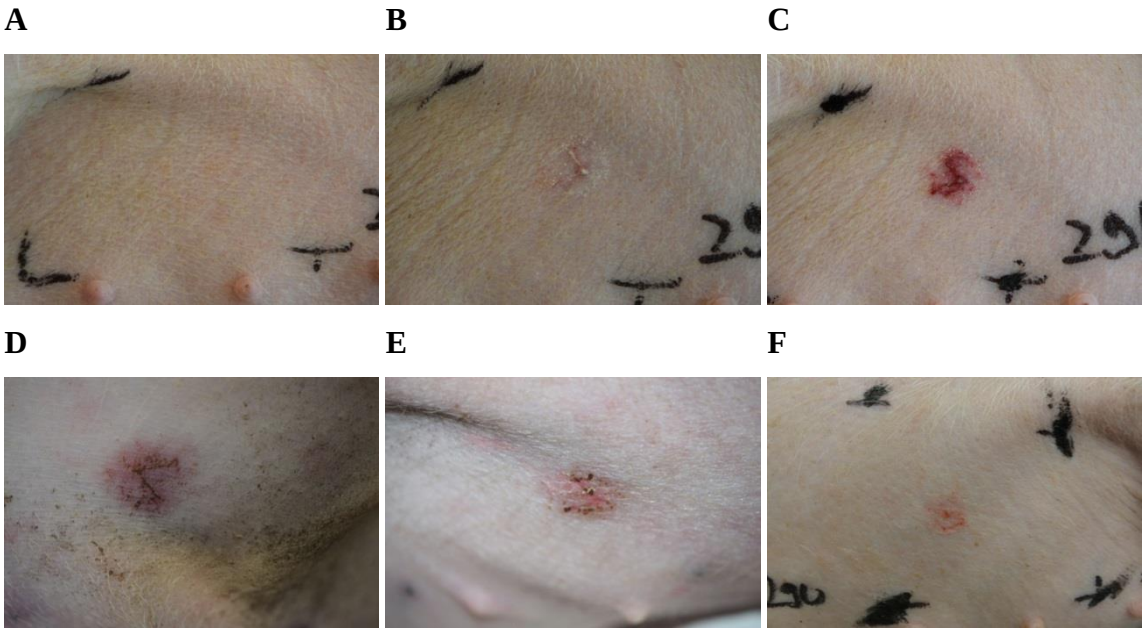

Day 0, group B, animal 12

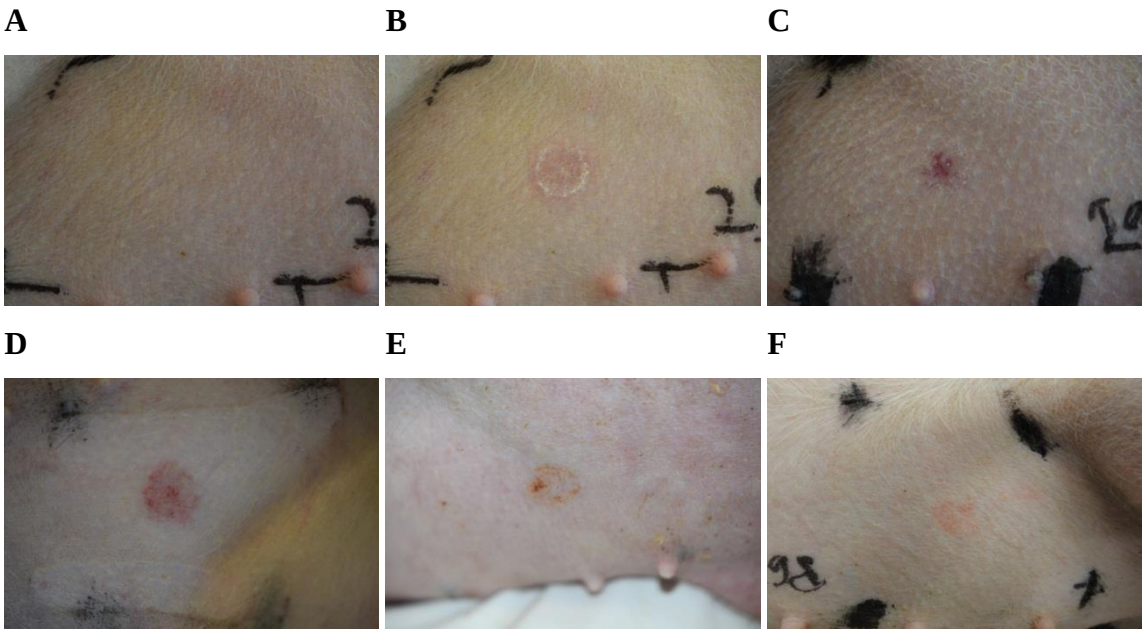

Figure 6.3.8: Group B (animal 11 and 12) i.d. application of vaccine powder fixed with paraffin on ballistic device A) administration site before application; B) administration site directly after application; C) administration site after 5 min latency; D) administration site at day 1; E) administration site at day 2; F) administration site after boost application at day 14

Day 0, group B, animal 13

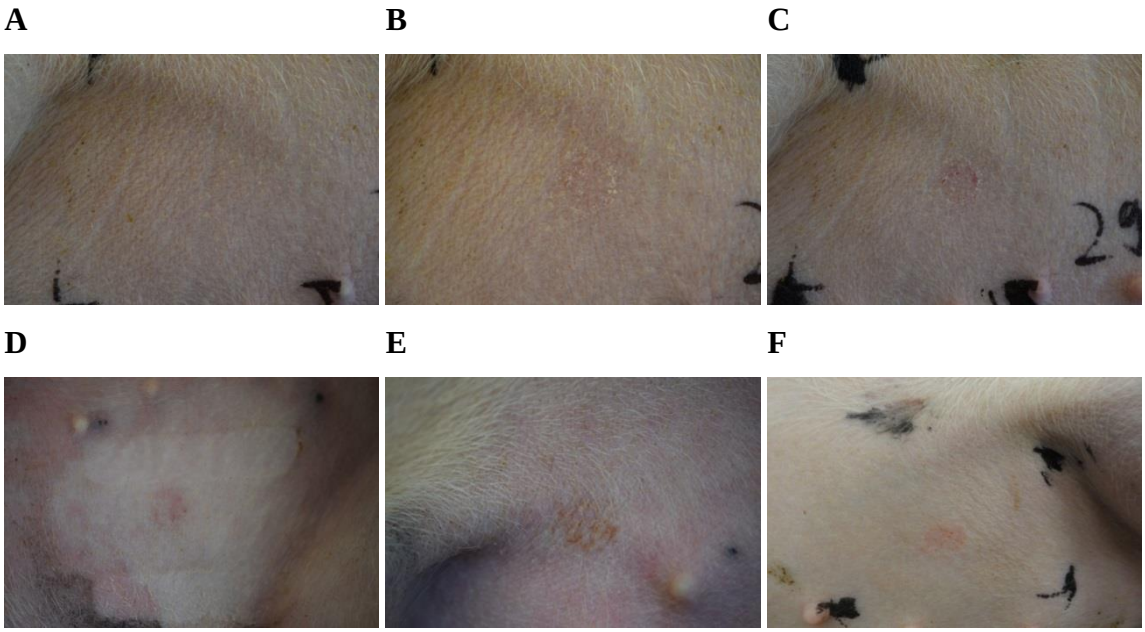

Day 0, group B, animal 14

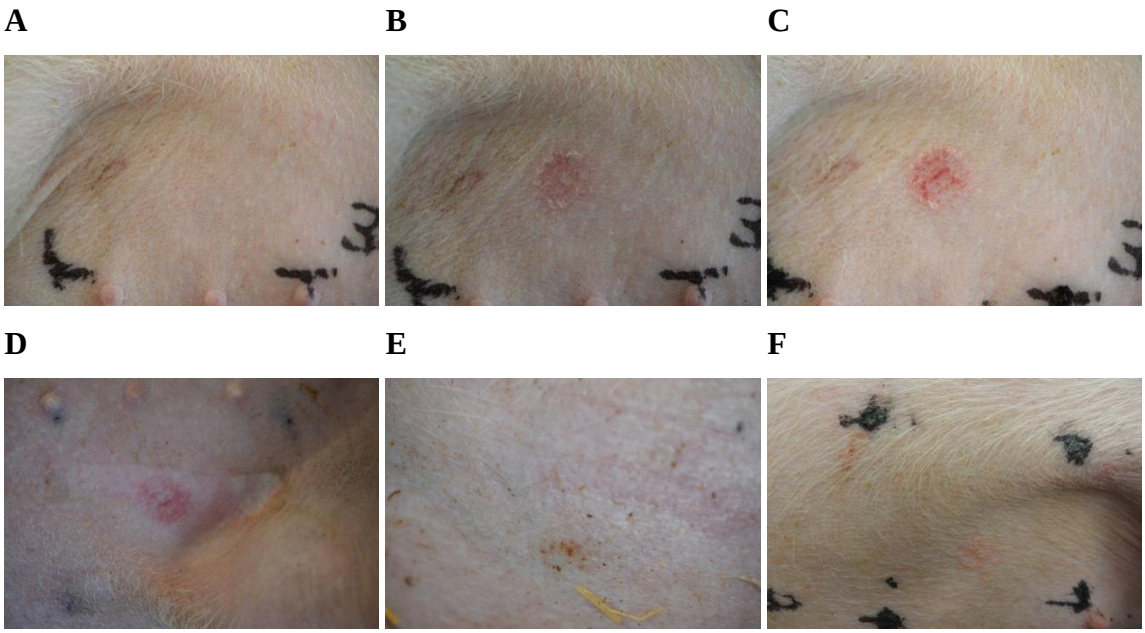

Figure 6.3.9: Group B (animal 13 and 14) i.d. application of vaccine powder fixed with paraffin on ballistic device A) administration site before application; B) administration site directly after application; C) administration site after 5 min latency; D) administration site at day 1; E) administration site at day 2; F) administration site after boost application at day 14

After the immunization, the bruises and bleedings of the verum groups were different in each animal despite the comparable skin region of the administration sites 15-20 cm cranial from the groin. While the administered vaccine powder fixed with oily components of AS03 (Group C) induced stronger discharge of tissue fluids, Group B resulted in more distinct bruises and slight bleedings (Figure 6.3.10, Figure 6.3.11, Figure 6.3.12 and Figure 6.3.13).

All animals well tolerated the immunizations; however one animal of Group B showed side effects of the influenza vaccination such as fever and fatigue on day 1. This animal was treated with analgesic and antipyretic drugs. To prevent a superinfection, an additional treatment with antibiotics was performed.

Day 0, group C, animal 15

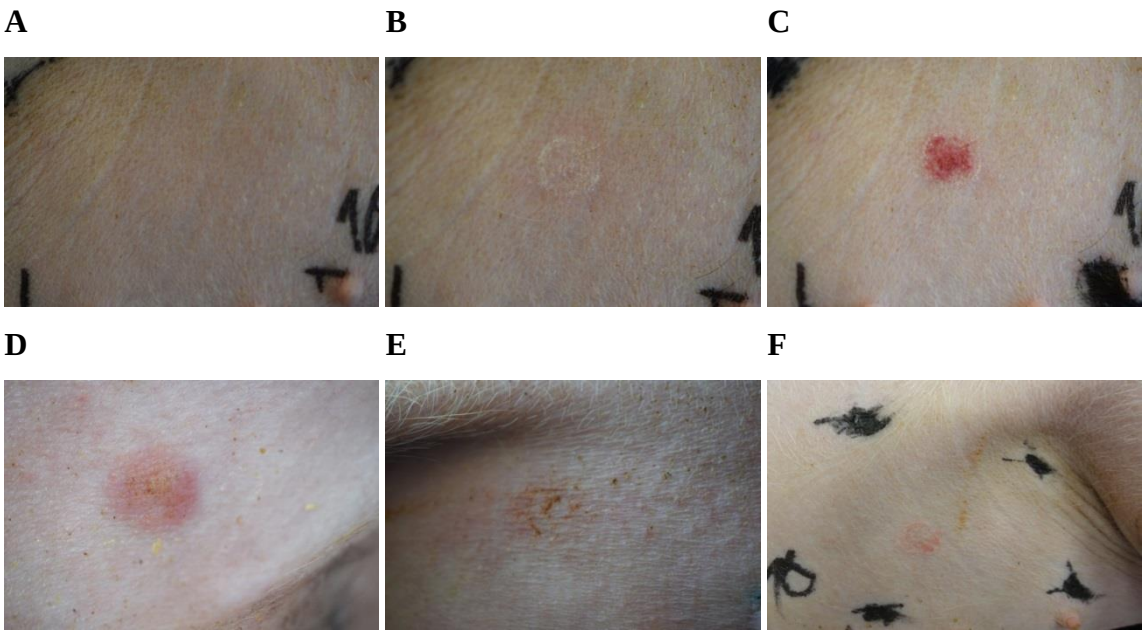

Figure 6.3.10: Group C (animal 15) i.d. application of vaccine powder fixed with oily part of AS03 on ballistic device A) administration site before application; B) administration site directly after application; C) administration site after 5 min latency; D) administration site at day 1; E) administration site at day 2; F) administration site after boost application at day 14

Day 0, group C, animal 16

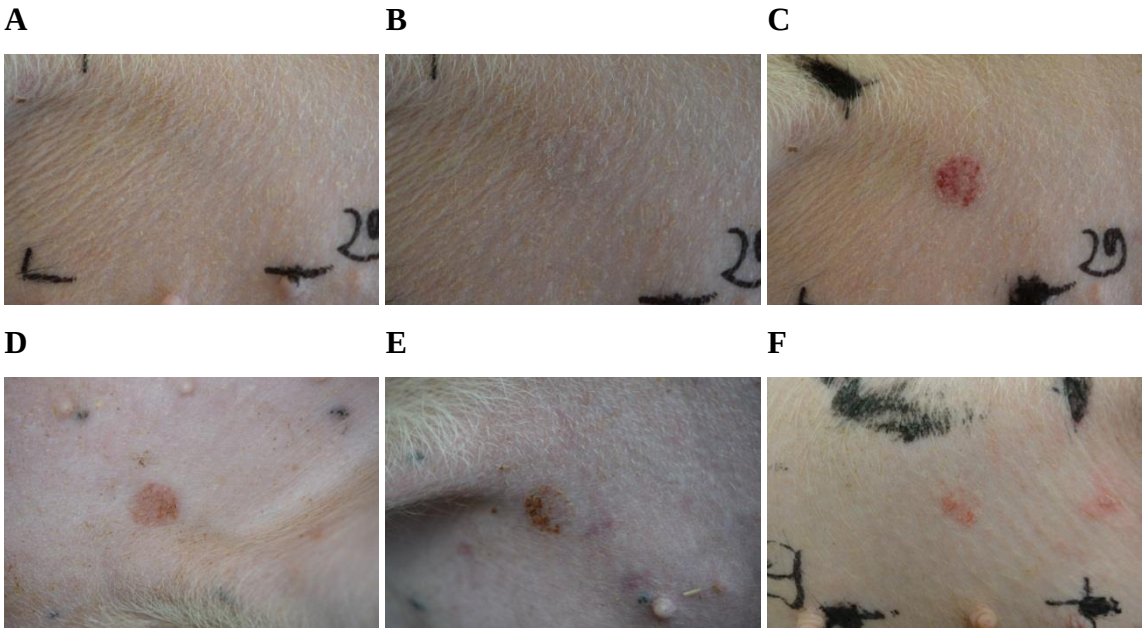

Day 0, group C, animal 17

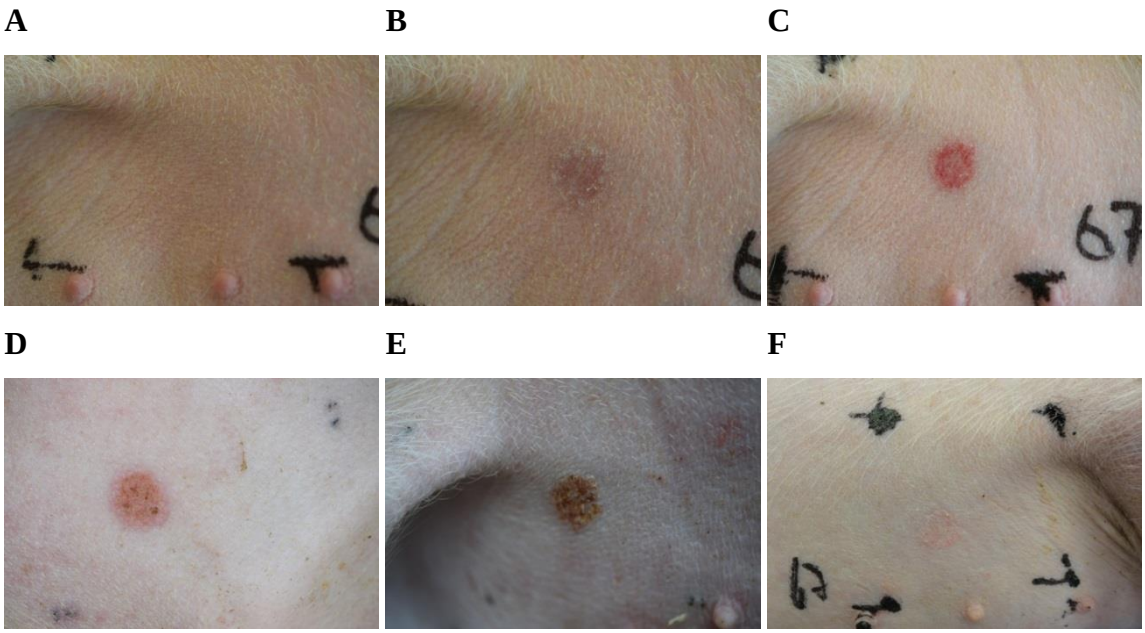

Figure 6.3.11: Group C (animal 16 and 17) i.d. application of vaccine powder fixed with oily part of AS03 on ballistic device A) administration site before application; B) administration site directly after application; C) administration site after 5 min latency; D) administration site at day 1; E) administration site at day 2; F) administration site after boost application at day 14

Day 0, group C, animal 18

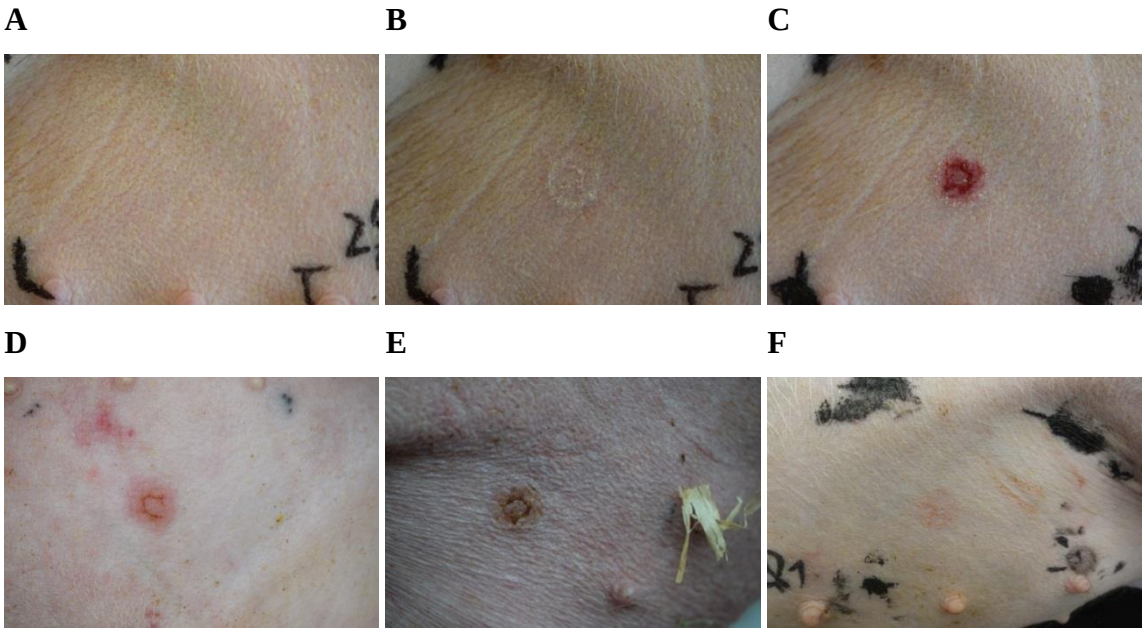

Day 0, group C, animal 19

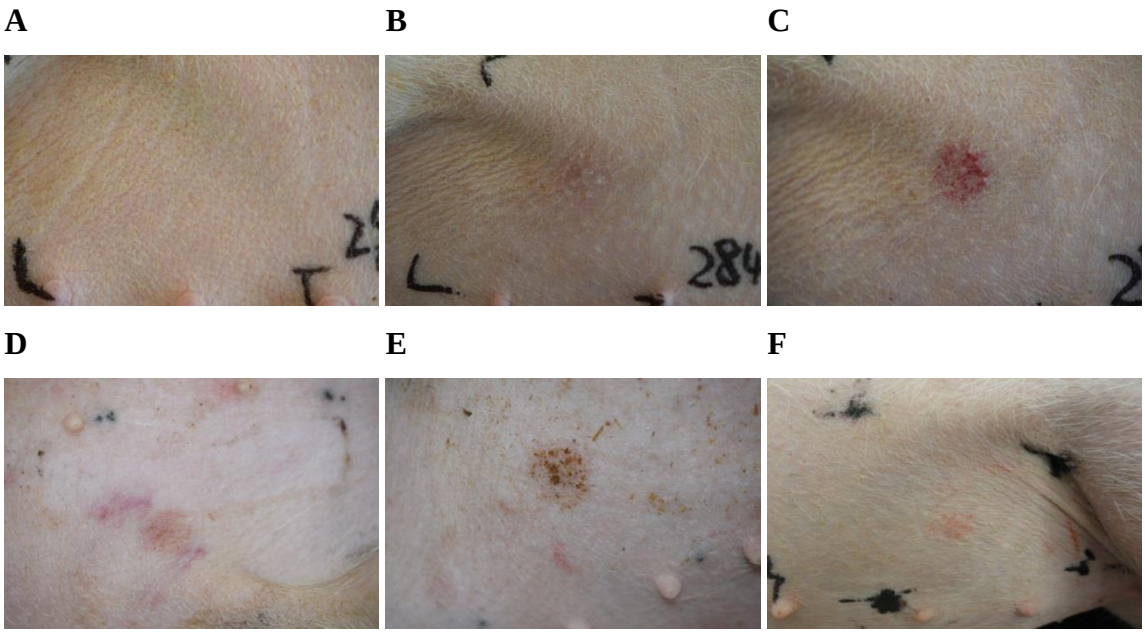

Figure 6.3.12: Group C (animal 18 and 19) i.d. application of vaccine powder fixed with oily part of AS03 on ballistic device A) administration site before application; B) administration site directly after application; C) administration site after 5 min latency; D) administration site at day 1; E) administration site at day 2; F) administration site after boost application at day 14

Day 0, group C, animal 20

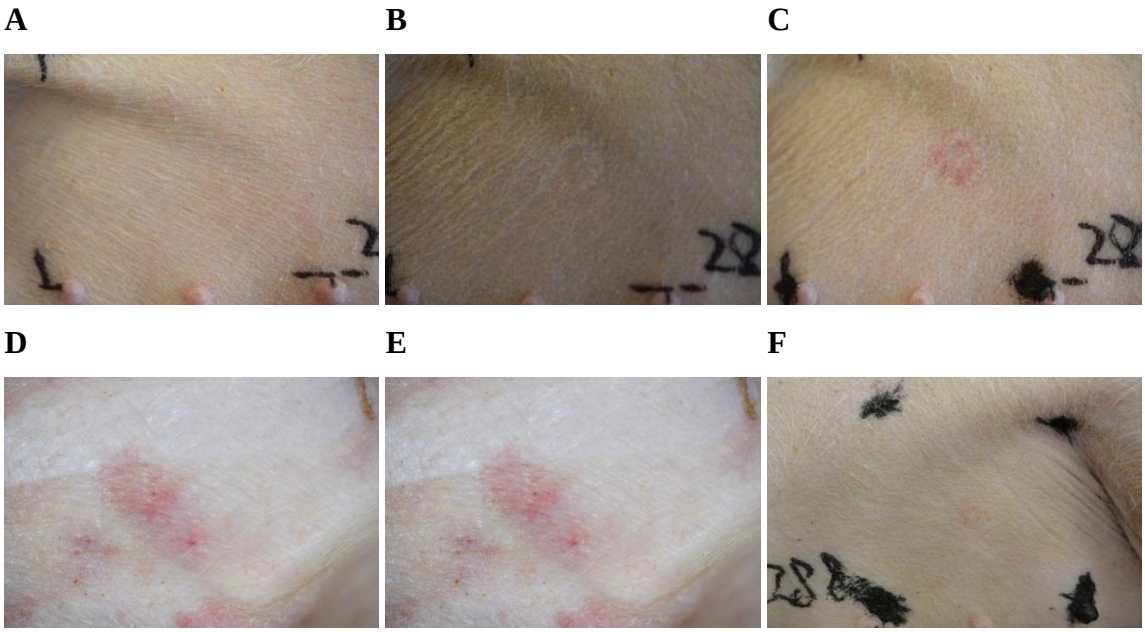

Day 0, group C, animal 21

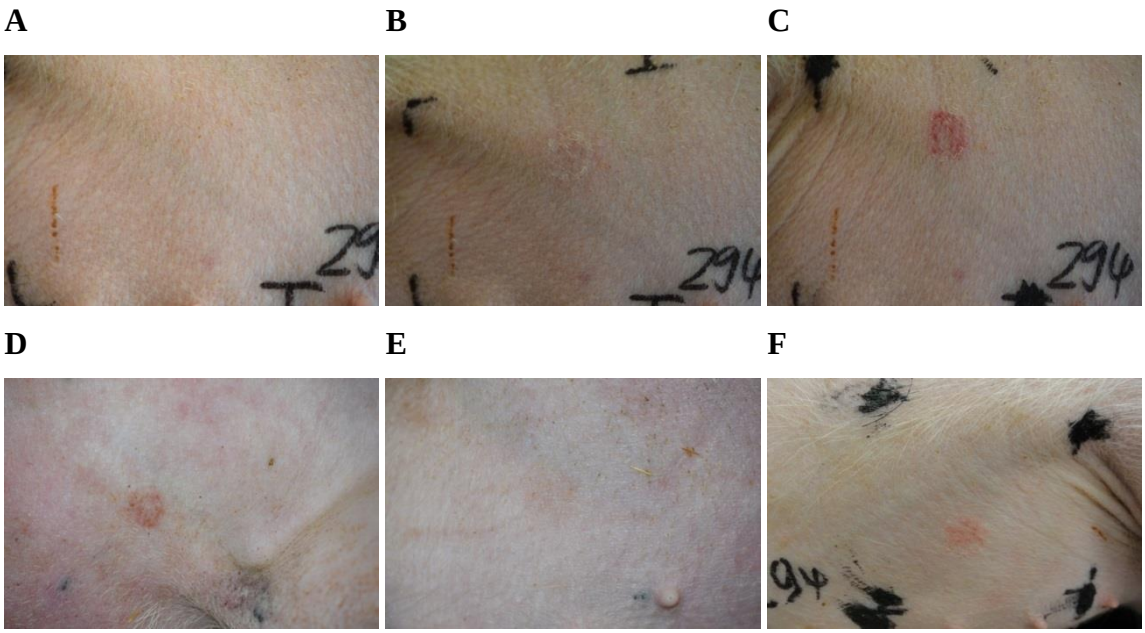

Figure 6.3.13: Group C (animal 20 and 21) i.d. application of vaccine powder fixed with oily part of AS03 on ballistic device A) administration site before application; B) administration site directly after application; C) administration site after 5 min latency; D) administration site at day 1; E) administration site at day 2; F) administration site after boost application at day 14

6.3.3 Histological characterization of administration site

The excised and stained skin was microscopically characterized to determine any tissue changes after intradermal vaccine deposition using the ballistic powder applicator. Skin samples from the administration sites were taken after the euthanasia of the animals. Therefore, the tissue could heal 28 or 14 days after the administration. It should be kept in mind if the particles would damage parts of the viable skin (below stratum basale), this could lead to tissue scarring. The results of the skin samples demonstrated an unchanged tissue independently of the healing time (28 days or 14 days after administration) and particle/coating compared to an unprocessed control side. No scarring or tissue changes could be detected (Figure 6.3.14).

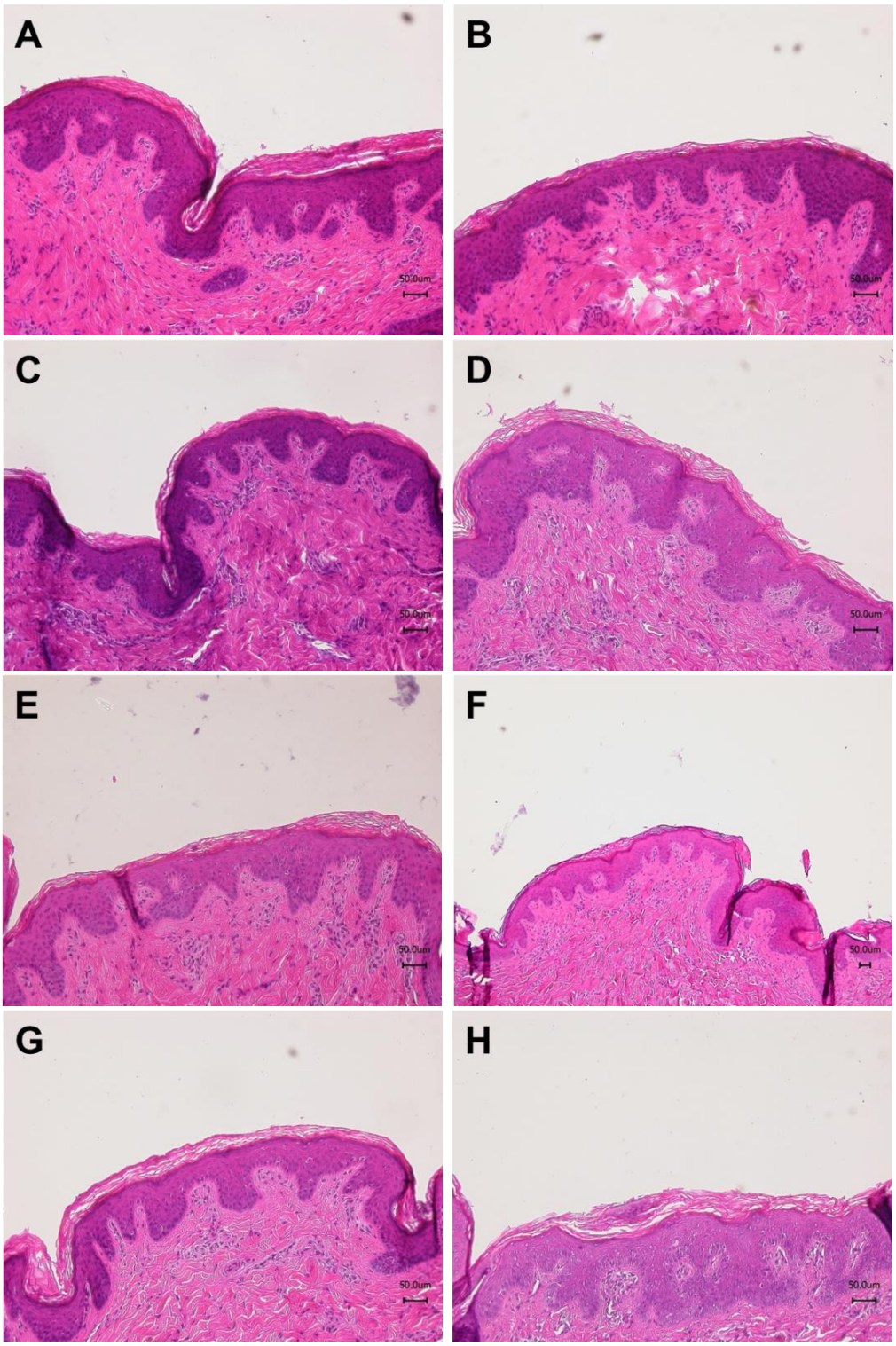

Figure 6.3.14: Images of histological HE stained skin slices taken at day 28 of administration sites after ballistic powder deposition. A) placebo particles coated with paraffin administered on day 0; B) placebo particles coated with paraffin administered on day 14; C) vaccine particles coated with paraffin administered on day 0; D) vaccine particles coated with paraffin administered on day 14; E) vaccine particles coated with oily components of AS03 administered on day 0; F) vaccine particles coated with oily components of AS03 administered on day 14; G and H) control sites without any particle deposition

6.3.4 Determination of endotoxin content in samples

Endotoxins (pyrogens) can influence immune response and therefore interfere with immunogenicity of HA. [134, 135]. Low endotoxin content has to be warranted, when the genuine specific immune response triggered only by the antigen (hemagglutinin) is under investigation. While highly purified water demonstrated endotoxin content below the detection limit, the measurement of the commercial product resulted in approximately 0.71 Endotoxin Units (EU)/dose (Figure 6.3.15). The placebo formulation, composed of the buffer components (10 mM phosphate buffer) and carbohydrates (trehalose and mannitol), was measured with approximately 0.34 EU/dose. The concentration of the vaccine using TFF and dialyzed against 10 mM phosphate buffer resulted in an endotoxin level of about 1.1 EU/dose, while the addition of a bulking agent, cryo-protectant (trehalose and mannitol), collapse lyophilization and cryo milling increased the content only up to approximately 2 EU/dose. Endotoxins levels < 2 EU/dose were sufficiently low to match the requirements of the European Pharmacopoeia (< 100 EU/dose) for influenza subunit vaccines (Pharm. Eur. 2.6.14). Using the EndoSafe-PTS system with cartridges, the recovery of the test may vary between 50% and 200% as described by the manufacturer. Keeping this in mind, recoveries from 76% to 109% of additionally spiked endotoxins into the samples were perfectly in range of the assay.

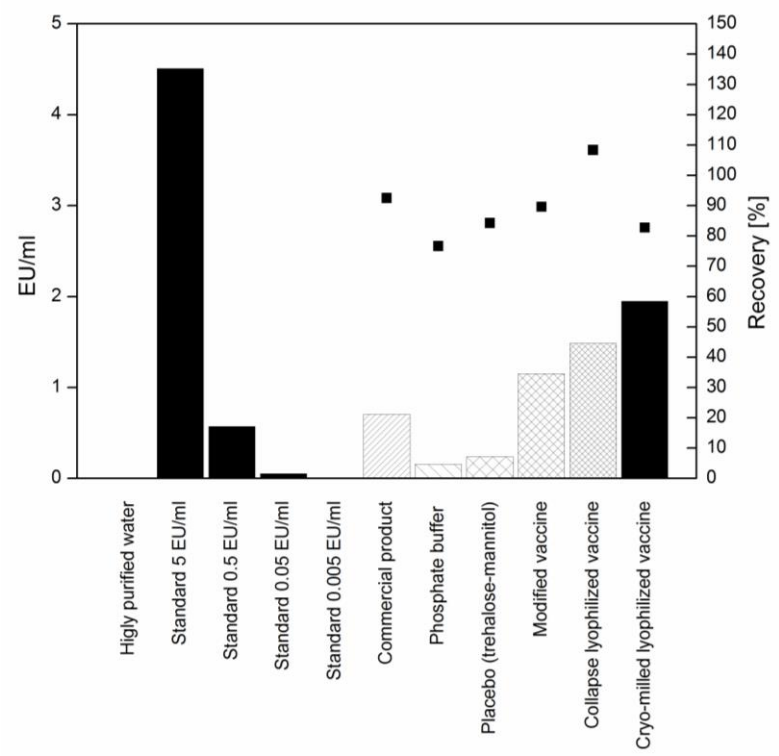

Figure 6.3.15: Content in EU/ml of commercially available product, collapse lyophilized vaccine and cryo-milled lyophilized vaccine.

6.3.5 Blood samples and IgG immune response determined using ELISA

All sera samples from the i.d. and i.m. vaccination were successfully tested using the enzyme-linked immunosorbent assay (ELISA) (Figure 6.3.16). The results of the assay demonstrated a consistent H1N1-specific antibody titer of Group A (placebo group) over the whole period of 28 days. Intradermal application of vaccine powder (verum groups B and C) resulted in higher antibody titers compared to the placebo group regardless of an adjuvant usage while the immunization (Group D) strongly increased the specific antibody titer significantly. The intradermal vaccine administration independently of adjuvant usage induced in four of seven animals a significant immune response compared to the placebo group. The booster immunization on day 14 only improved the immune response in the positive control group D leading to higher titers while only slight titer increases were observed for Group B and C within the period from day 14 to 28.

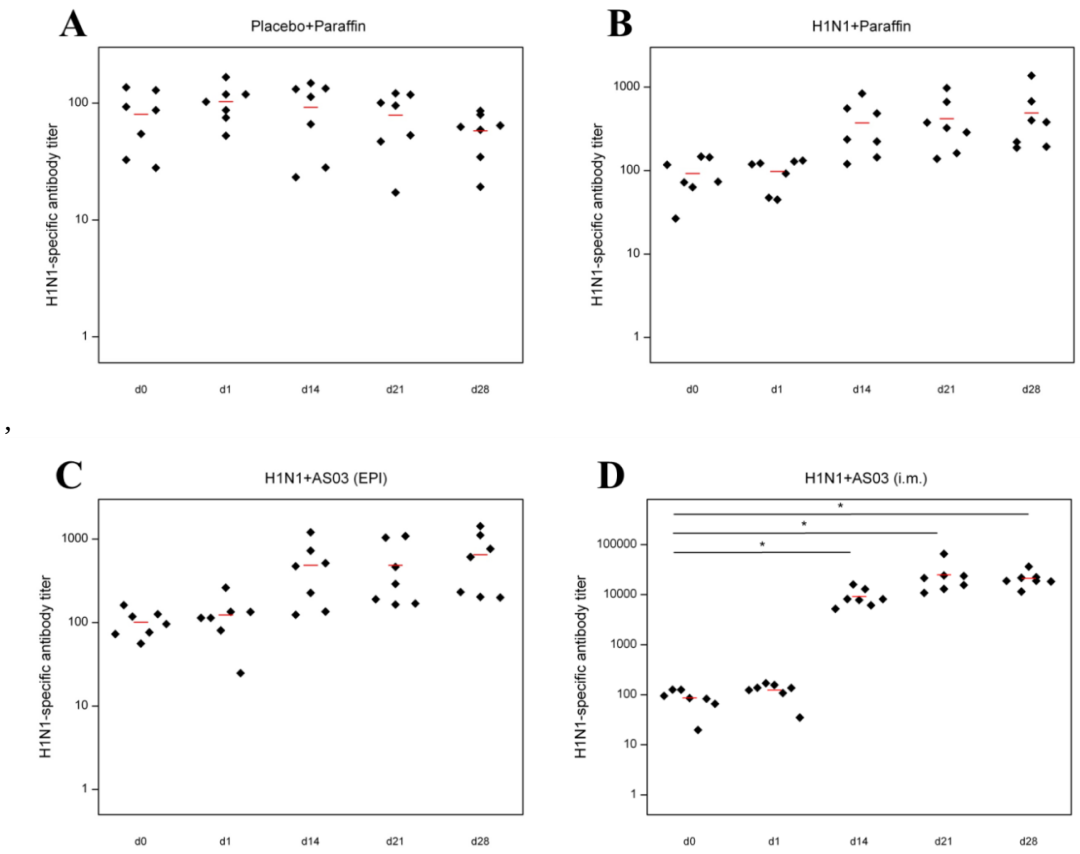

Figure 6.3.16: ELISA results of specific anti-hemagglutinin-antibody measurements. A) i.d. placebo group; B) i.d. vaccine particles without oily adjuvant (paraffin); C) i.d. vaccine particles with oily adjuvant (AS03); D) i.m. commercial vaccine injection with adjuvant (AS03). Red line marks the mean value of the titer, * with black bar marks the significance P= 0.005

The comparable anti-HA-specific antibody titers of all four groups demonstrated a similar starting titer at day 0. A value unequal zero can be induced due to unspecific surface/protein adsorptions or randomly matching antibodies against the antigen. Due to the lag time of the immune response, the titers were still unchanged at day 1 after the immunization. While the i.m. immunization modified the titer significantly at day 14, both intradermal verum groups resulted in observable but not significant antibody titer increase compared to the placebo group due to the broader deviation. These trends continued after the boost administration (day 14) at days 21 and 28. However, the development of the intradermal verum powder group titers was not high enough for significance compared to Group 1. Additionally no significance could be calculated between titers of the intradermal groups and the i.m. group.

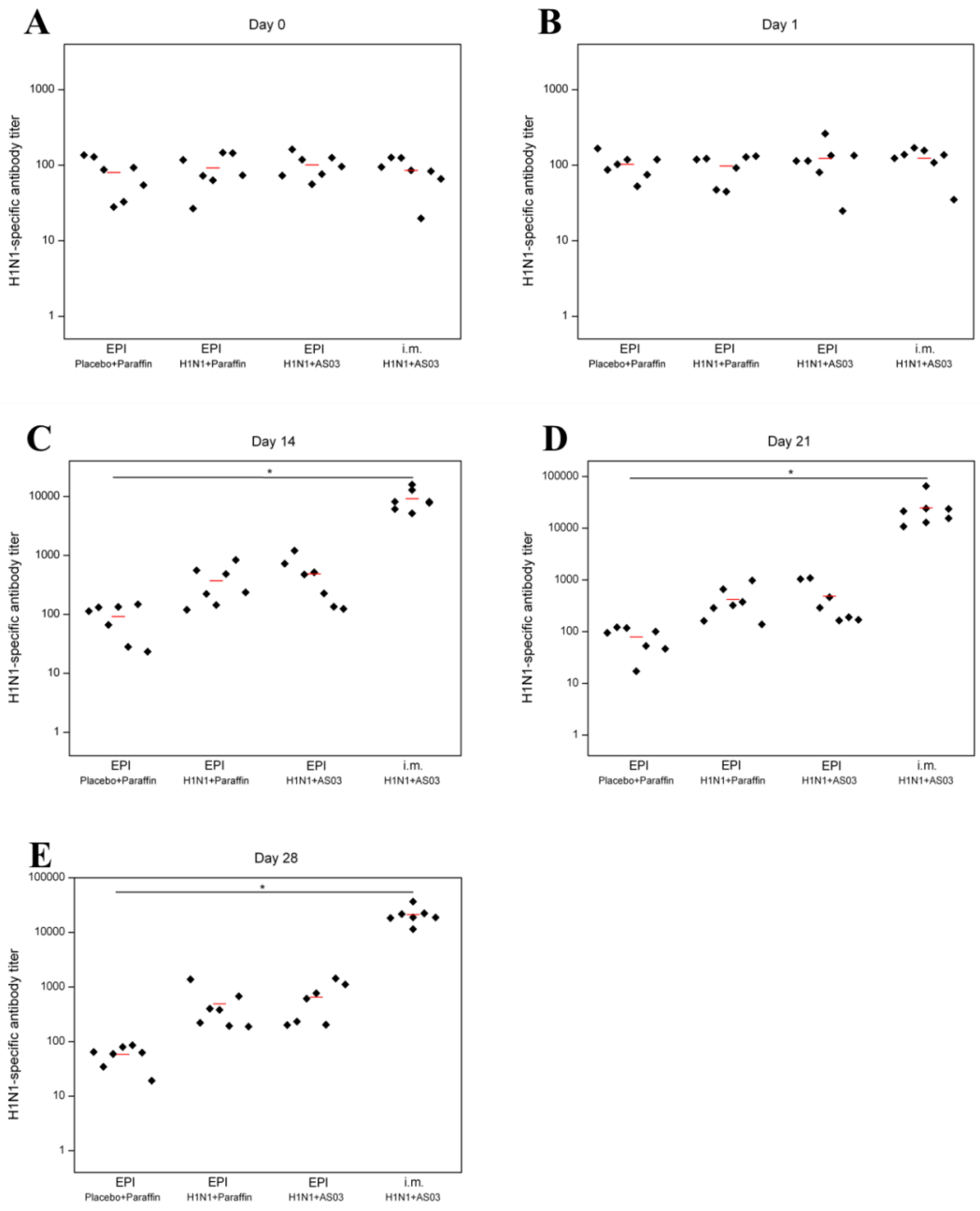

Figure 6.3.17: Comparison of ELISA results of specific anti-hemagglutinin-antibody measurements. IgG levels of A) Day 0; B) Day 1; C) Day 14; D) Day 21; E) Day 28. Red line marks the mean value of the titer, * with black bar marks the significance P= 0.005

The broad titer value distribution of the EPI groups resulted in a lack of significance between the control and the EPI group (Table 2.4.1). While the titers of the control group showed a narrow distribution about 58±23 titer value the titers of the EPI groups were distributed in a range of 490±426 titer value (H1N1 + paraffin) or 650±486 titer value, respectively. The larger range of the titer values of the i.m. group

(21078±7615 titer value) resulted in a lack of significance to the EPI groups while demonstrating significance against the control group (Figure 6.3.17 and Table 6.3.1).

Table 6.3.1: Titer values of each animal at day 28 after immunization

	EPI (placebo + paraffin)	**EPI (H1N1 + paraffin)**	**EPI (H1N1 + AS03**	**i.m. (H1N1 + AS03)**
Titer animal 1/group	79.64	380.36	764.82	22269.95
Titer animal 2/group	59.13	400.31	610.93	18795.83
Titer animal 3/group	85.90	193.27	202.98	11463.83
Titer animal 4/group	34.59	219.95	231.82	18270.88
Titer animal 5/group	62.61	675.03	1430.16	18761.72
Titer animal 6/group	64.32	1375.70	200.01	21560.94
Titer animal 7/group	19.24	188.28	1113.95	36420.27

6.4 Discussion

The application of both the intramuscular administration of the commercial liquid vaccine and the intradermally deposited lyophilized vaccine led to a detectable increase of IgG antibody titer. The latter (for each intradermal application group) however was not statistically significant. The HA content for each delivery route (i.d. or i.m) was determined and confirmed using RP-HPLC measurements with fluorescence detection. While the complete dose of 3.75 µg of HA and the whole amount of 27.41 mg of adjuvant (squalene 10.69 mg, DL-α-tocopherol 11.86 mg, and Polysorbate 80 4.86 mg) mixed in 0.25 ml emulsion was injected intramuscularly to animals of the positive control group, the actual available dose of the intradermal application in the verum groups was significantly lower. As described in **Chapter 4.3.2** ca. 93% of HA and adjuvant could be ejected from the device. Only a fraction (about 25%) of the ejected dose actually could penetrate the stratum corneum and could reach the immune cells located in the epidermis. The device was loaded with 1.81±0.19 mg and each mg of the particles was equivalent to 3.75 µg of the vaccine. Thus the amount of vaccine particles that was delivered to the immune cells in the epidermis amounted to 0.4-0.5 mg. This led to an intradermally applied vaccine dose of 1.5-1.875 µg and would result in 40-50% of the i.m. dose. Regarding the adjuvant (oily components) amount 27.41 mg (in 0.25 ml emulsion) were injected with a single commercial vaccine dose intramuscularly but only 1.28% ± 0.74% thereof were used to fix the particles on the device membrane. The H1N1 specific IgG titer of all laboratory animals of Group D (i.m. vaccine injection) was indicative of a strong immune response and resulted in titers that elicited more than two orders of magnitude after the vaccination while the i.d. verum groups B and C developed an increase of approximately one order of magnitude. A more differentiated view revealed that within each intradermally vaccinated group (groups B and C) four of seven animals showed a significant increase while the other three animals responded with a poor immune reaction. This titer deviation of both sub groups limited the intradermal vaccination success. The immune-stimulating effect of the oily components of AS03 (group C) was comparable to paraffin. The immune-stimulating effect of oily components could be increased, if an emulsification within the administration site could occur as described in the literature [136]. Additionally, it can be excluded that

the minimal increase of endotoxins (from 0.71 EU/dose for the commercial i.m. vaccine to 2 E markedly below the requirements of the Ph. Eur. (< 100 EU/dose; Pharm. Eur. 2.6.14) and thus unlikely to contribute to the specific immune response [12, 13].

After boost administration at day 14 IgG titers increased further in the i.m. group whereas both i.d. groups barely changed. The lack of a boost effect could be caused by a poorer particle penetration into the epidermis. After the first intradermal powder administration (day 0), the skin of all laboratory animals showed reactions to the procedure (bruising or discharge of fluids) but poorer skin responses were observed after the boost powder application (day 14). This effect may be attributed to changed mechanical skin properties as a result of weight gain and aging of the laboratory animals which demonstrate the requirement of human studies.

Further phenomena were observed considering the skin reactions, which could be summarized as particle and/or fixation type induced effects. The first observation was that the skin responded differently to placebo and verum powder. Intradermal powder application with verum particles induced distinct bruises, minimal bleedings and a discharge of tissue fluids, while placebo particles induced primarily erythema. More intense redness could be a result of higher proportion of larger particles within the range of 20-80 µm of the verum particles compared to the placebo particles which may be induced by different milling properties (incorporated protein). Larger particles would result in higher momentum and higher impact forces into the skin. The second observation was that applied verum particles attached with paraffin resulted in bruises and bleedings while verum particle fixed with the oily components of AS03 demonstrated a trend to stronger tissue fluid outflow. However, the observed effect could be caused by the different wetting characteristics of the oils used for particle fixation. Nonetheless, all i.d. administration sites healed within 2-3 days after the epidermal powder immunization (day 0 and day 14) without any visible tissue lesions or scaring (see **Attachments** Figure 6.6.1 to Figure 6.6.5).

6.5 Conclusion

We were able to demonstrate a successful and safe intradermal powder immunization using a new ballistic device. Vaccine preparation and device loading could be performed under aseptic conditions. After i.d. immunization, the H1N1 specific IgG titer was lower compared to the benchmark i.m. vaccination. However, the administered dose using the EPI was only 50% compared to the i.m dose due to incomplete administration or penetration of the vaccine particles into the skin, respectively. The particle penetration hardly depends on particle momentum and mechanical properties of the skin. While the particle momentum should be comparable between the two application time points, the skin of the laboratory animals could be changed drastically due to ageing and weight gain.

Moreover, the amount of adjuvant in the EPI group was limited by the coated membrane area and the coating thickness and resulted in only 1.28% ± 0.74% of the recommended amount for the i.m. application. Therefore, the contribution to an immune-stimulating effect in order to induce a sufficient immune response was limited due to the low delivered quantity. Despite all these facts, the intradermal powder immunization induced an observable H1N1 specific IgG titer increase.

Intradermal powder immunization using the new ballistic device is a safe and fast technique. The stable, lyophilized vaccines and easy handling promise advantages such as a cost reduction for health-care staff training and a minimization of cold chain maintenance. The potential of dose-reduction as described by Romani et al. could be achieved if a sufficient vaccine dose and adjuvant could be delivered into the skin

Furthermore, the minimal invasive route of the vaccine application may prevent pain during the vaccination and demonstrated healed administration sites within 2-3 days without any tissue lesions and scars. In times of vaccine shortage and distribution problems, this new epidermal powder immunization technique could provide a method to face the vaccination challenges. In addition, the alleviating fear of needles and the reduction of needle-stick injuries (more than 500 000 deaths per year) could increase the patient compliance and improve worldwide accessibility to vaccination, especially in times of a pandemic outbreak [14]. The ballistics powder applicator could provide a

technology for epidermal powder immunization for a minimal invasive, painless, and simple vaccination.

6.6 Attachments

Verum particles fixed with paraffin

A **B** **C**

D **E**

Verum particles fixed with paraffin

A **B** **C**

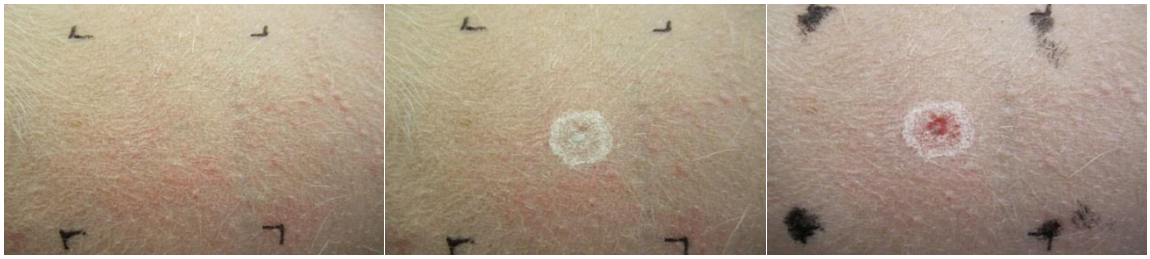

D **E**

Figure 6.6.1: Administration site of i.d. application of verum powder fixed with paraffin on ballistic device A) administration site before application; B) administration site directly after application; C) administration site after 5 min latency; D) administration site at day 1; E) administration site at day 2

Verum particles fixed with paraffin

A **B** **C**

D **E**

Verum particles fixed with paraffin

A **B** **C**

D **E**

Figure 6.6.2: Administration site of i.d. application of verum powder fixed with paraffin on ballistic device A) administration site before application; B) administration site directly after application; C) administration site after 5 min latency; D) administration site at day 1; E) administration site at day 2

Verum particles fixed with AS03

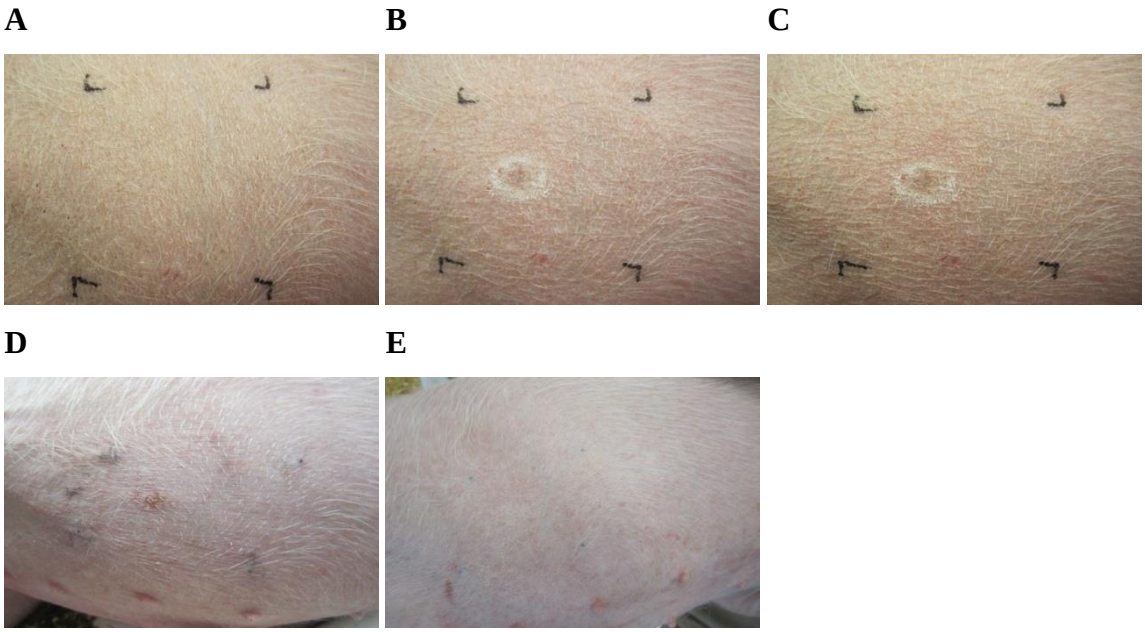

Verum particles fixed with AS03

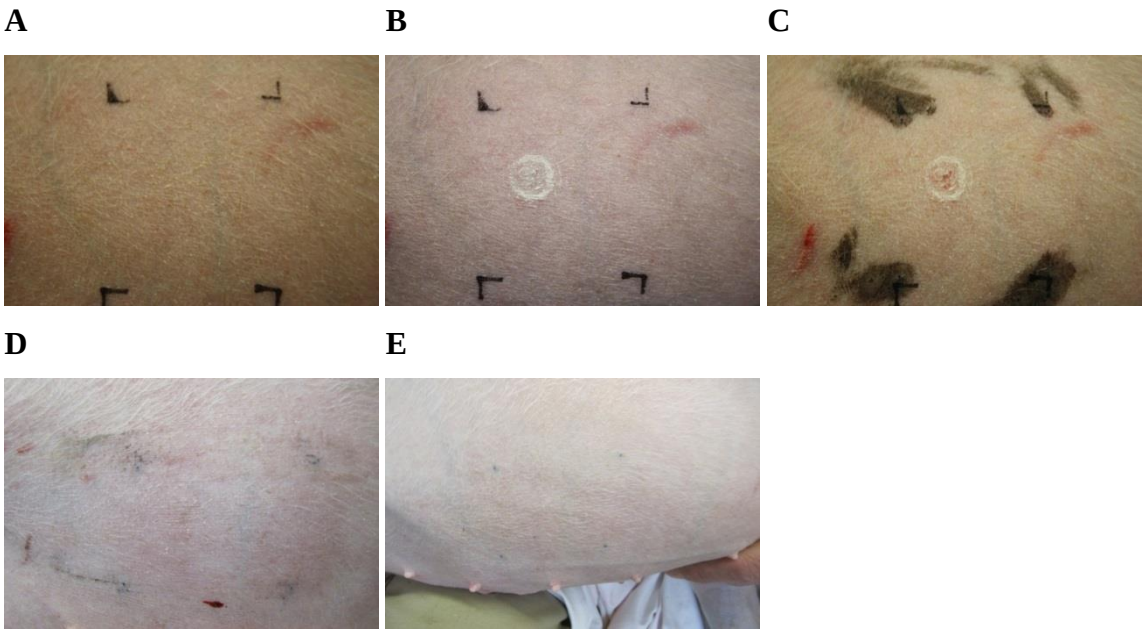

Figure 6.6.3: Administration site of i.d. application of verum powder fixed with AS03 on ballistic device A) administration site before application; B) administration site directly after application; C) administration site after 5 min latency; D) administration site at day 1; E) administration site at day 2

Verum particles fixed with AS03

A **B** **C**

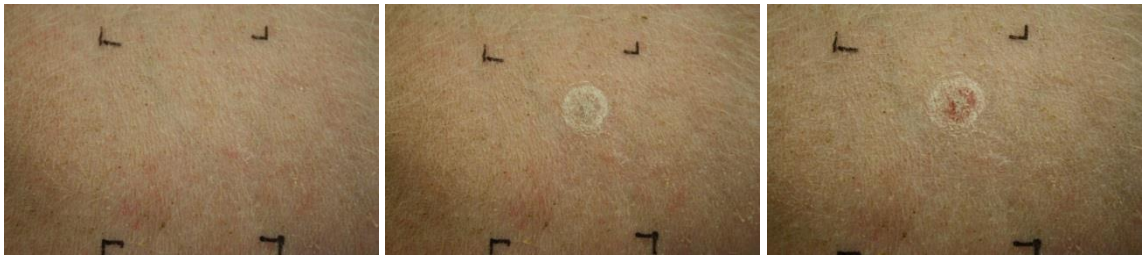

D **E**

Verum particles fixed with AS03

A **B** **C**

D **E**

Figure 6.6.4: Administration site of i.d. application of verum powder fixed with AS03 on ballistic device A) administration site before application; B) administration site directly after application; C) administration site after 5 min latency; D) administration site at day 1; E) administration site at day 2

Placebo versus verum particles fixed with paraffin

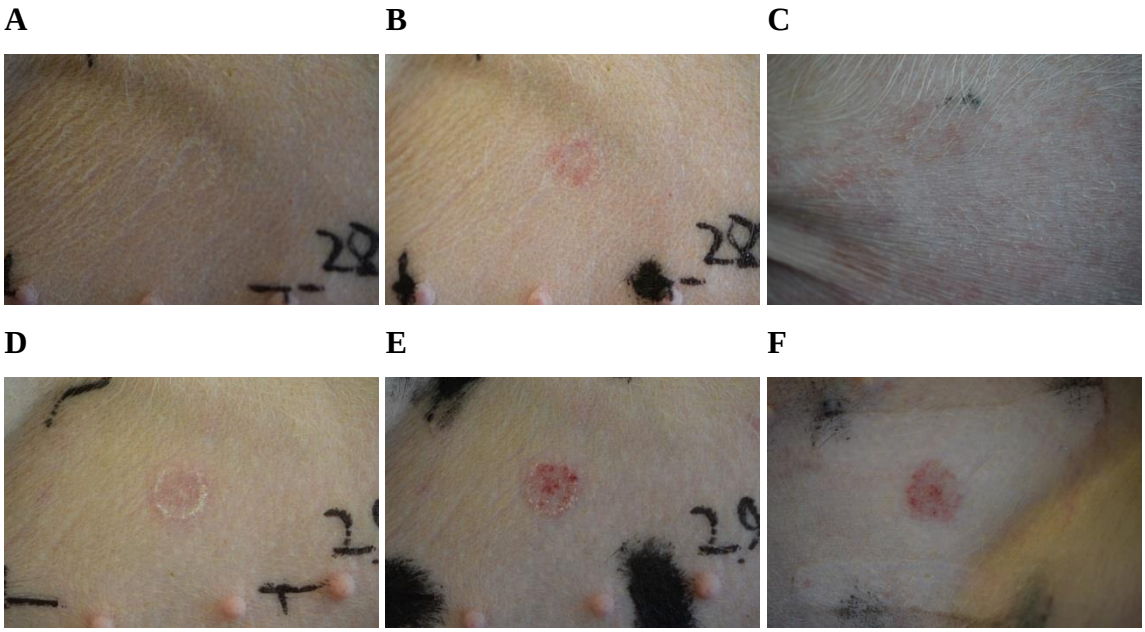

Placebo versus verum particles fixed with paraffin

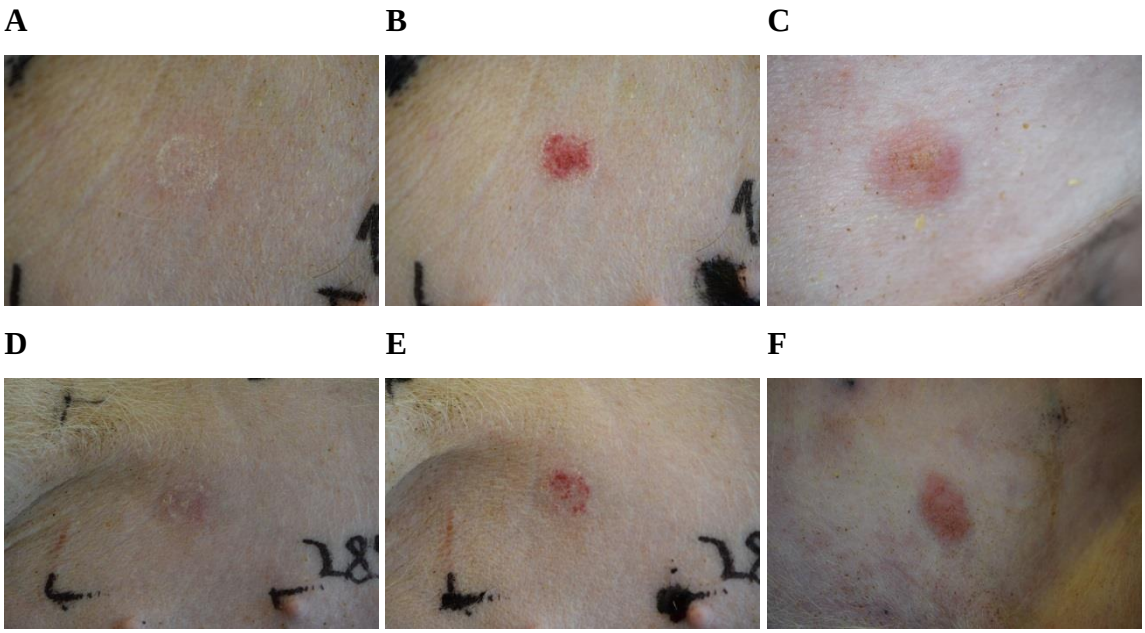

Figure 6.6.5: Administration site of i.d. application of placebo and verum powder fixed with paraffin on ballistic device A) administration site directly after application of placebo; B) administration site after 5 min latency of placebo administration; C) administration site 2 days after placebo administration; D) administration site directly after application of verum; E) administration site after 5 min latency of verum administration; F) administration site 2 days after verum administration

6.7 References

1. Marquet, F., et al., *Characterization of Dendritic Cells Subpopulations in Skin and Afferent Lymph in the Swine Model.* PLoS One, 2011. **6**(1): p. e16320.

2. Kupper, T.S. and R.C. Fuhlbrigge, *Immune surveillance in the skin: mechanisms and clinical consequences.* Nature Reviews Immunology, 2004. **4**(3): p. 211-222.

3. Rothkötter, H.J., E. Sowa, and R. Pabst, *The pig as a model of developmental immunology.* Human & Experimental Toxicology, 2002. **21**(9-10): p. 533-536.

4. Bronaugh, R.L., R.F. Stewart, and E.R. Congdon, *Methods for in vitro percutaneous absorption studies II. Animal models for human skin.* Toxicology and Applied Pharmacology, 1982. **62**(3): p. 481-488.

5. Bronaugh, R.L., R.F. Stewart, and M. Simon, *Methods for in vitro percutaneous absorption studies VII: Use of excised human skin.* Journal of Pharmaceutical Sciences, 1986. **75**(11): p. 1094-1097.

6. Sullivan, T.P., et al., *The pig as a model for human wound healing.* Wound Repair and Regeneration, 2001. **9**(2): p. 66-76.

7. Palache, B., *New vaccine approaches for seasonal and pandemic influenza.* Vaccine, 2008. **26**(49): p. 6232-6236.

8. Lambert, P.H. and P.E. Laurent, *Intradermal vaccine delivery: Will new delivery systems transform vaccine administration?* Vaccine, 2008. **26**(26): p. 3197-3208.

9. Jones, J.M. and P.D. Kind, *Enhancing effect of bacterial endotoxins on bone marrow cells in the immune response to SRBC.* The Journal of Immunology, 1972. **108**(5): p. 1453-1455.

10. David, C.M. and J. Ryan, *Bacterial endotoxins and host immune responses.* Adv. Immunol, 1979. **28**: p. 293-450.

11. Morel, S., et al., *Adjuvant System AS03 containing α-tocopherol modulates innate immune response and leads to improved adaptive immunity.* Vaccine, 2011. **29**(13): p. 2461-2473.

12. Wood, J.M., *Selection of influenza vaccine strains and developing pandemic vaccines.* Vaccine, 2002. **20, Supplement 5**(0): p. B40-B44.

13. Wallin, R.P.A., et al., *Heat-shock proteins as activators of the innate immune system.* Trends in Immunology, 2002. **23**(3): p. 130-135.

14. Mitragotri, S., *Immunization without needles.* Nature Reviews Immunology, 2005. **5**(12): p. 905-916.

7. Chapter - Final summary of the thesis

7.1 Basis of the thesis

Vaccination is one of the most effective medical interventions to prevent infections [1]. Generally, vaccines are administered intramuscularly (i.m.) via syringe and needle while few can also be delivered orally or intradermally [2, 3]. Though intramuscularly application is the mainly used administration, several major drawbacks have to be taken into consideration. First of all, for a successful liquid vaccine administration into the muscle intensive training of health care staff is mandatory [4-6]. Moreover, the deposition into a tissue (muscle) in which the circulation of immune cells is low can result in delayed and reduced immune response [7, 8]. In addition, the humoral immune response is limited to systemic antibodies (e.g. to IgM, IgG, IgD) due to the application site deep in the tissue and may result in a lack of IgA secreted into the mucosa. The invasive application can induce pain, tissue damage, and bleedings which open possibilities to transmit blood-borne diseases after needle-stick injuries or needle reuses [9]. Beside the administration drawbacks, the storage stability of the liquid vaccine calls for special handling in a small temperature range (2-8°C) to prevent a temperature induced degradation [10, 11].

Keeping this in mind, a project on epidermal powder immunization (EPI) was conducted to provide a minimally invasive administration route which could improve immunogenicity and patient compliance and additionally to design a vaccine vehicle which can improve the product storage stability.

The skin excels as a multifunctional tissue. Beside the physiological support to control body temperature and moisture, the skin also forms a physical barrier to the environment and has built in the first line of immunogenic defense against pathogens [12]. Furthermore, the skin stands out as an easily accessible application site. The target area in 100-200 µm depths in the epidermis, where the immunocompetent cells (APCs) are located, can induce an improved immune response while a lack of blood vessels and free nerve endings would bypass pain induction and bleedings. Moreover, a dose reduction can be envisaged due to the effective antigen presentation and escalation of immune response [13]. After an antigen contact or immunization, APCs from the epidermis migrate to the draining lymph nodes to present the fragments of scavenged pathogens and provoke an intensified immune response. This mechanism results in a sufficient systemic immunogenicity and additional mucosal protection by

secreted IgA from specific immune cells (B-plasma cells) which can prevent the entry of pathogens into the host [5].

In order to take full advantage of the benefits of intradermal immunization (i.d.) it is vital to design an appropriate administration technology. The most known i.d. vaccination technologies are i.d. injections, liquid jets, micro-needle systems, and the PowderJect®-technology [6]. Up to date, the introduced platform technologies could not fully convince their suitability as a cost-effective and competent vaccination system. The i.d. injection (known as the Mantoux technique), needs intensive and specialized training of health-care staff and, thus, result in comparatively high error rates [14]. The liquid jet technology deposits the vaccine into the whole skin, from the epidermis down to the subcutaneous tissue. Consequently higher vaccine doses are applied and pain and bleedings can result from this technique because of the higher administered volume. Both platforms (i.d. injection and liquid jets) can utilize the existing liquid vaccines without intensive galenical developments but the handling is limited to the strict storage temperature range of 2-8°C. The PowderJect® administration aimed specifically in this direction by stabilizing the temperature sensitive vaccine in a dry vehicle to improve the storage stability [15, 16]. The spray (freeze) dried powder particles were accelerated using pressurized helium gas to penetrate the skin. The cost-intensive technology limited the field of application, particularly in developing countries. However, vaccine stabilization using a dry carbohydrate matrix was a step in the right direction due to improved storage stability, low ingredient costs, known material properties, and biocompatibility. Moreover, a carbohydrate matrix would dissolve instantly after particle deposition into the skin which would result in largely distributed vaccine in the tissue. A large immunized area would address a high number of APCs that would induce an exceled immune response.

Consequently, a concept of intradermal powder application was conducted using a new platform of vaccine stabilization, particle preparation, and vaccine powder application into the skin. Primarily, collapse freeze-drying was performed to stabilize the vaccine, a new pyrotechnical ballistic device was designed to transfer the powder particles into the skin and finally, the innovative concept were confirmed in provoking an immune response in an animal experiment.

In **Chapters 2 and 3** the stabilization of an influenza vaccine in a carbohydrate matrix using collapse freeze-drying, preparation of vaccine particles using cryo-milling, and the characterization of the product stored at 2-8°C, 25°C, and 40°C over a time period of 12 months was described. The galenical stabilization was necessary because the liquid vaccine loses activity after approximately 24 hours when stored outside the approved temperature range of 2-8°C. In order to optimize the energy and time consuming process of lyophilization, the model vaccine was stabilized in a faster and more aggressive collapse freeze-drying cycle above the glass transition temperature of the carbohydrate matrix. In addition, the process of collapse freeze-drying was selected to reduce the specific surface area (SSA) to obtain harder lyophilizates which would prevent a shattering on the skin surface of the particles during the impact. The potential of SSA reduction was previously demonstrated in the work by E. Etzl et al [17]. The influence of the more aggressive collapse-freeze-drying cycle to the product was monitored using the thermo-sensitive influenza vaccine which was incorporated into a carbohydrate matrix. A large set of analytical tools was established to characterize the stability and activity of the influenza vaccine during preparation, collapse-freeze-drying, and storage under different conditions (2-8°C, 25°C, and 40°C) over a time period of 12 months. Beside a successful freeze-drying cycle a particle preparation at the desired size range of 20 µm-80 µm could also be confirmed by scanning electron micrographs (SEM). Consistent vaccine content and structural integrity of lyophilizates and vaccine particles were determined using RP-HPLC. However, results of the chromatographical method did not correlate with an alteration in activity of the protein (hemagglutinin). In order to fill this gap, the samples were characterized using the hemagglutination inhibition assay (HAI). The membrane affinity and cross-linking property of hemagglutinin (HA) was determined in a red blood cell suspension and resulted in unchanged biological activity despite certain degradation detectable in the electrophoretic assays. Unexpected was the clearly visible formation of agglomerates in the electrophoretic assays (SDS-Page and westernblot). The distinct alteration, particularly observed in cryo-milled samples stored at 40°C/12 months, resulted in modified protein migration through the SDS-Page gels and ended in faded bands (SDS-Page) and a lack of bands in westernblot analytics. The formation of aggregates was further investigated using light obscuration (sub-visible particle counts) and turbidity measurements. While the results showed

consistently low counts for lyophilizates the particle counts increased 5-8 folds for cryo-milled samples stored at high storage temperatures. At the same time, slightly higher turbidity results but an additional tendency to increasing turbidity values under higher storage temperature conditions of cryo-milled samples demonstrated a less unambiguous impact of cryo-milling to the storage samples. Beside the stability of the incorporated vaccine, the integrity of the lyophilizate was determined using Karl-Fisher measurement. While the values for the unprocessed lyophilizates were plateaued at < 1.5% the residual moisture of cryo-milled samples increased after cryo-milling but leveled out at / or below 3.5%. The successful collapse lyophilization and vaccine stabilization in the carbohydrate vehicle at up to 25°C/12 months was the first major step for this work.

Some liquid vaccines, as the model influenza vaccine, are delivered in association with an adjuvant (e.g.:AS03) to boost the immune response. The adjuvant can improve the immune response, so that e.g. the WHO recommended amount of hemagglutinin of 15 µg/dose could be reduced to 3.75 µg/dose in an influenza vaccination. In order to utilize the benefits offered by adjuvants (e.g. AS03) the powdered vaccine stability in presence of adjuvants was investigated. The usage of freeze-dried vaccines limited the choice of adjuvants to oily components to prevent a premature dissolution of the matrix. In this work, the lyophilized vaccine was not stored in presence of the oily components. In order to compare the stability and biological activity of the freeze-dried vaccine and the liquid vaccine (commercial product), both samples were mixed with the adjuvant prior to analytical testing. The characterization of the vaccine stability in presence of oily components was limited. Therefore, the tests focused on biological activity using HAI while vaccine content and integrity was determined using RP-HPLC. The biological activity determination failed due to the unexpected strong influence of the oily components. While the vaccine samples dissolved in the aqueous phase (HAI), hemolysis of the red-blood cells prevented a successful read-out of the assay and meaningful data could not be collected. The vaccine stability could only be characterized using the chromatographic assay. In future works, vaccine activity could be determined in immunization studies of laboratory animals as an alternative to tested assay (HPLC, gel electrophoresis etc.).

This work could demonstrate a successful particle preparation and sufficient stabilization of the thermo-sensitive influenza vaccine as a freeze-dried product over a

time period of 12 months and particle preparation of the cryo-milled samples were storage stable at 2-8°C and 25°C for up to 12 months.

In **Chapters 4 and 5**, the detailed device development, velocity determination, and penetration tests into excised pig skin as a model for human skin were described. The device design put the accent on two crucial conceptions. The first aspect was to accelerate particles using a pyrotechnical energy source and secondly an independent preparation of a sterile pharmaceutical part from the pyrotechnical part to load the stabilized vaccine particles. Due to the low density of the carbohydrate particle matrix (1.3 g/cm^3) only particles sizes of (20-80 µm) could store enough momentum to breach through the mechanical barrier (stratum corneum) of the skin and deposit the vaccine into the epidermis [18]. Therefore, gas-generator excelled as the energy source to generate enough impulse to accelerate the particles at a sufficient rate. A maximum of safety for both caregiver and patient, possible sterilization of the pharmaceutical part, reproducible particle velocity and particle distribution were continuously considered during the design and optimization of all device components (combustor, support plate, customized membranes, silicone oleogel and membrane holder). While the combustor concealed the generated high pressure, it also directed the impulse towards the particles fixed on a customized membrane. In order to reduce the energy losses and prevent impacts of gas-generator fragments the combustor was filled with a viscous silicone oleogel which transferred the pressure more efficiently compared to other fillings (air, water, hydrogels etc.). When the load hit the customized membrane, the surface with the fixed particles was accelerated to velocities larger 550 m/s. During the acceleration, the customized membrane flipped instantly and formed a curvature which improved the particle velocity due to the stored material tension.

Velocity, trajectory, the flight characteristics, penetration behavior into skin of model particles (glass sphere 500 µm for velocity determination and polystyrene particles 20 µm, 40 µm, and 60 µm for penetration test) were compared against the lyophilizate particles. The particle penetration behavior and depths was investigated in excised pig skin to ensure the highest possible degree of comparability with the mechanical properties of human skin. The penetration depths of the particles in skin samples were histologically examined and an administration into the desired depths of 100-200 µm was successfully demonstrated. The device was modified for the animal experiments using the data of the particle penetration tests in excised pig skin. Particles applied in

in vivo skin of the laboratory animals demonstrated that the skin healed completely after two days (macroscopic images) (**Chapter 6**). In addition, a lack of tissue damages and scarring was shown in the histological skin samples after the completion of the animal experiment. Moreover, the dissolving and distribution of the carbohydrate matrix could also be shown which was requested to address as much APCs as possible with one epidermal powder immunization.

Chapter 6 describes the proof of concept of the new epidermal powder immunization technology by depositing the stabilized influenza vaccine particles into the skin *in vivo* with the pyrotechnical powder applicator. The study was performed on pigs as laboratory animals due to the close similarity of mechanical properties between human and pig skin. During the animal experiment the i.d. powder application was challenged against the conventional i.m. liquid vaccine injection. Additionally, the adjuvant effect of the oily components of the adjuvant AS03 used in one EPI-group as well as AS03 in the i.m. group (commercial product) was analyzed. Three groups of i.d. applications were tested against one i.m. injection: (A) EPI negative control group (placebo particles + paraffin); (B) EPI group (vaccine particles + paraffin); (C) EPI challenge group (vaccine particles + oily components of an adjuvant); (D) i.m. positive control group (liquid vaccine + AS03). The specific antibody titer of the control group remained low while all other groups demonstrated a titer increase during the four weeks of the immunization study. On day 14, the ELISA assay revealed comparably elevated titer of both i.d. groups (groups B and C) and a one magnitude higher immune response of the positive control group (group D). The anti-HA-antibody titer of the i.m. positive control group increased further while the i.d. verum groups only changed minimally after the observed 28 days. The particle deposition into the skin was not complete. Using the micro flow imaging system the deposition of vaccine particles into the skin could be determined which revealed an approximately 50% lower dose (1.875 µg/dose) in the EPI groups compared to the i.m. positive control group (3.75 µg/dose). Beside the lower vaccine dose, the weak titer increase of the challenge group (group C) could be explained by the low amount of adjuvant which was transferred with the vaccine. The surface area to fix the powdered vaccine with the oily components of AS03 was limited to 3.14 cm^2 which resulted in an amount of only 1.5-1.1875 µg compared to 27.41 mg (in 0.25 ml emulsion). The low amount only 1.28% ± 0.74% of the oily components of the adjuvants and the lower deposited

vaccine dose was not enough to provoke a comparably strong immune response to i.m. vaccination.

It should be kept in mind that the WHO recommends 15 µg/dose if no adjuvant is administered. The intradermal deposited vaccine was only 1/10 of the recommended dose. Therefore, it was a remarkable success of the new vaccination strategy that a titer increase was still observable in spite of a lack of adjuvant boosting effects and low deposited vaccine dose.

7.2 Final summary and outlook

In summary, the present study demonstrated a successful immunization of laboratory animals using a newly developed and built pyrotechnical powder applicator which deposited stabilized influenza vaccine particles into the skin. The new concept of vaccine stabilization using an economic collapse freeze-drying resulted in storable vaccine lyophilizates and vaccine particles at up to 25°C over a time period of 12 months. Moreover, a sufficient acceleration of the vaccine particles using the newly designed powder applicator was demonstrated in histological examined skin samples in which the particles were deposited into the desired penetration depths to deliver the vaccine directly to the APCs. The concept of instantly dissolving vaccine particles in the tissue to address as many APCs as possible could also be shown. Future studies could further optimize the powder applicator to generate higher particle velocities or prepare particles with higher density to store more momentum into the particles to deposit higher amounts of particles into the skin. However, it should be kept in mind that the impact energy of the particles should be limited to prevent skin lesions, pain and bleedings induced by deeply penetrated or shattering particles. Beside the modification of particle administration, a higher vaccine load (using a model protein) into the vehicle successfully were investigated in preliminary tests to optimize the intradermal vaccine deposition. Despite the small amount of deposited vaccine and adjuvant into the skin, an observable titer increase could be detected which demonstrated potential of this new strategy of epidermal powder immunization. The feasibility of ballistic intradermal vaccination has to be tested for each vaccine but the concept of stabilized freeze-dried vaccine and pyrotechnical powder administration opens a new possibility to safe, ease-of-use and effective vaccination.

7.3 References

1. Scuffham, P.A. and P.A. West, Economic evaluation of strategies for the control and management of influenza in Europe. Vaccine, 2002. 20(19–20): p. 2562-2578.

2. Andre, F., et al., Vaccination greatly reduces disease, disability, death and inequity worldwide. Bulletin of the World Health Organization, 2008. 86(2): p. 140-146.

3. Bloom, D.E., D. Canning, and M. Weston, The value of vaccination. World Economics, 2005. 6(3): p. 15-39.

4. Romani, N., et al., Targeting skin dendritic cells to improve intradermal vaccination. Intradermal Immunization, 2011: p. 113-138.

5. DeBenedictis, C., et al., Immune functions of the skin. Clinics in Dermatology, 2001. 19(5): p. 573-585.

6. Mitragotri, S., Immunization without needles. Nature Reviews Immunology, 2005. 5(12): p. 905-916.

7. Mackay, I. and I.M. Roitt, The immune system. N Engl J Med, 2000. 343(1): p. 37-49.

8. Mackay, I. and I. Roitt, The immune system: second of two parts. New England Journal of Medicine, 2000. 343(2): p. 108-117.

9. Moingeon, P., C. de Taisne, and J. Almond, Delivery technologies for human vaccines. British Medical Bulletin, 2002. 62(1): p. 29-49.

10. Hickling, J., et al., Intradermal delivery of vaccines: potential benefits and current challenges. Bull World Health Organ, 2011. 89(3): p. 221-6.

11. Chen, D., Y.F. Maa, and J.R. Haynes, Needle-free epidermal powder immunization. Expert Review of Vaccines, 2002. 1(3): p. 265-276.

12. Thews, G., E. Mutschler, and P. Vaupel, Anatomie, Physiologie, Pathophysiologie des Menschen. Vol. 4. 1999: Wissenschaftliche Verlagsgesellschaft Stuttgart,, Germany.

13. Kenney, R.T., et al., Dose sparing with intradermal injection of influenza vaccine. New England Journal of Medicine, 2004. 351(22): p. 2295-2301.

14. Mahomed, H., et al., Comparison of Mantoux skin test with three generations of a whole blood IFN-γ assay for tuberculosis infection. The International Journal of Tuberculosis and Lung Disease, 2006. 10(3): p. 310-316.

15. Amorij, J.-P., et al., Needle-free influenza vaccination. The Lancet Infectious Diseases, 2010. 10(10): p. 699-711.

16. Amorij, J.P., et al., Development of Stable Influenza Vaccine Powder Formulations: C*hallenges and Possibilities. Pharmaceutical Research, 2008. 25(6): p. 1256-1273.*

17. Etzl, E.E., G. Winter, and J. Engert, Toward intradermal vaccination: preparation of powder formulations by collapse freeze-drying. Pharmaceutical Development and Technology, 2014. 19(2): p. 213-222.

18. Chen, D., Y.F. Maa, and J.R. Haynes, *Needle-free epidermal powder immunization.* Expert Review of Vaccines, 2002. **1**(3): p. 265-276.

Publications associated with this Thesis

Anamur, Cihad, Gerhard Winter, and Julia Engert. Stability of collapse lyophilized influenza vaccine formulations. International journal of pharmaceutics 483.1 (2015): 131-141.

Nadellose Injektionsvorrichtung aufweisend ein Gel und eine Membran. Patent application No.: EP 14 189 971.6 and EP 14 173 786.6 will be published in May 2016.

Poster presentation

Cihad Anamur, Gerhard Winter, Julia Engert. Stabilization of a model flu vaccine by collapse freeze drying. 7th Vaccine and ISV Annual Congress 2013, Sitges, Barcelona, Spain, October 2013